γ-Secretase mediated proteolytic processing of the triggering receptor expressed on myeloid cells-2 – functional implications for intracellular signaling

DISSERTATION

zur

Erlangung des Doktorgrades (Dr. rer. nat.)

der

Mathematisch-Naturwissenschaftlichen-Fakultät

der

Rheinischen Friedrich-Wilhelms-Universität Bonn

vorgelegt von

Dipl. Biochem. Patrick Wunderlich

aus

Brühl

Bonn, 21.12.2010

Angefertigt mit Genehmigung der Mathematisch-Naturwissenschaftlichen Fakultät
der Rheinischen Friedrich-Wilhelms-Universität Bonn

1. Gutachter: Prof. Dr. rer. nat. Jochen Walter

2. Gutachter: Prof. Dr. rer. nat. Sven Burgdorf

Tag der Abgabe: 21.12.2010

Tag der Promotion: 06.04.2011

Erscheinungsjahr: 2011

An Eides statt versichere ich, dass ich die Dissertation "γ-Secretase mediated proteolytic processing of the triggering receptor expressed on myeloid cells-2 – functional implications for intracellular signaling" selbst und ohne jede unerlaubte Hilfe angefertigt habe und dass diese oder eine ähnliche Arbeit noch an keiner anderen Stelle als Dissertation eingereicht worden ist.

Promotionsordnung vom 7. Januar 2004 _____

Patrick Wunderlich

CONTENTS

LIST OF FIGURES

LIST OF TABLES

ABBREVIATIONS

aa	Amino acid
Ab	Antibody
ACE	Angiotensin converting enzyme
AD	Alzheimer´s disease
ADAM	A disintegrin and metalloprotease
AICD	APP intracellular domain
APH-1	Anterior pharynx defective-1
APLP	Amyloid precursor like protein
APP	Amyloid precursor protein
APS	Ammonium persulfate
Aβ	β-Amyloid
BACE	β-Site APP cleaving enzyme
BBB	Blood brain barrier
BSA	Bovine serum albumin
Cdk5	Cyclin dependent kinase 5
CK-1	Casein kinase-1
CNS	Central nervous system
co-IP	Co-immunoprecipitation
CR3	Complement receptor-3
CS	Cover slip
CT	C-terminus
CTF	C-terminal fragment
DAMPs	Damage associated molecular pattern molecules
DAP12	DNAX activating protein of 12 kDa
DAPT	*N*-[(3,5-Difluorophenyl)acetyl]-L-alanyl-2-phenyl]glycine-1,1-dimethylethyl ester
DC	Dendritic cell
dko	Double knock-out
DMEM	Dulbecco´s Modified Eagle´s Medium
DMSO	Dimethyl sulfoxide
DN	Dominant negative
DOC	Deoxycholic acid
DR-6	Death receptor-6
DTT	Dithiothreitol
ECD	Extra cellular domain
ECE	Endothelin converting enzyme
ECL	Enhanced chemiluminescence

EDTA	Ethylenediaminetetraacetic acid
EEA1	Early endosome antigen 1
EGTA	Ethylene glycol tetra acetic acid
EOAD	Early-onset AD
ESdM	Embryonic stem (ES) cell derived microglia
EtOH	Ethanol
FAD	Familial Alzheimers' disease
FAM	Amine-reactive succinimidyl ester of carboxyfluorescein
FcR	Fc receptor
FCS	Fetal calf serum
FL	Full-length
GFP	Green fluorescent protein
GGA	Golgi associated, gamma adaptin ear containing, ARF binding protein
GSAP	γ-Secretase activating protein
GSH	Glutathione
GSK3β	Glycogen synthase kinase 3β
GSM	γ-Secretase modulator
GST	Glutathione S-transferase
gt	Goat
HA	Hemagglutinin tag
HBSS	Hank´s balanced salt solution
HEK	Human embryonic kidney cells
HEPES	4-(2-hydroxyethyl)-1-piperazineethanesulfonic acid
HRP	Horse radish peroxidase
HSP60	Heat shock protein 60
ICC	Immunocytochemistry
ICD	Intracellular domain
IDE	Insulin degrading enzyme
IL	Interleukin
iNOS	Inducible nitric oxide-synthase
IP	Immunoprecipitation
IPTG	Isopropyl β-D-1-thiogalactopyranoside
ITAM	Immunoreceptor tyrosine-based activation motif
ITIM	Immunomodulatory tyrosine inhibitory motif
LB medium	Lauria-Bertani medium
LDL	Low density lipoprotein
LOAD	Late-onset AD
LPS	Lipopolysaccharide

LRP	Low density lipid protein receptor related protein
MAPK	Mitogen activated protein kinase
MAPKKK	Mitogen activated protein kinase kinase kinase
MCP	Monocyte chemo attractant protein
MDL-1	Myeloid DAP12-associated lectin
MIP1α	Macrophage inflammatory protein-1α
MMP9	Matrix metalloprotease-9
ms	Mouse
Mut. Pr.	Mutation primer
mycHis	Myc-histidine tag
MyD88	Myeloid differentiation primary response gene 88
NEP	Neprilysin
NEXT	Notch extracellular truncation
NK cells	Natural killer cells
NMDA	N-methyl-D-aspartic acid
NO	Nitric oxide
NP-40	Nonidet P-40
NPC	Neural progenitor cell
NSAIDs	Non steroidal anti inflammatory drugs
OD	Optical density
PAMPs	Pathogen associated molecular pattern molecules
PBS	Phosphate buffered saline
PCR	Polymerase chain reaction
PDBu	Phorbol 12,13-dibutyrate
PEN-2	Presenilin enhancer-2
PenStrep	Penicillin/Streptomycin solution
PFA	Paraformaldehyde
PHF	Paired helical filaments
PI3K	Phosphatidylinositol-3 kinase
PKC	Protein kinase C
PLC	Phospholipase C
PLOSL	Polycystic lipomembraneous osteodysplasia with sclerosing leukoencephalopathy
PS	Presenilin
PtdIns	Phosphatidylinositol
RAGE	Receptor for advanced glycosylated end products
RAP	Receptor-associated protein
rb	Rabbit
RIP	Regulated intramembrane proteolysis

ROS	Reactive oxygen species
RT	Room temperature
S2P	Site-2 protease
SAP	Shrimp alkaline phosphatase
sAPP	Soluble amyloid precursor protein
SDS	Sodium dodecyl sulfate
SH2	Src homology-2
SHP	Src homology region-2 domain-containing phosphatase
SICC	Surface immunocytochemistry
SIRPβ	Signal regulatory protein-β
SOC medium	Super optimal broth with catabolite repression
SPP	Signal peptide peptidase
SPPL	Signal peptide peptidase like protein
SREBP	Sterol regulatory element binding protein
sTREM	Soluble TREM
Syk	Spleen tyrosine kinase
TBS	Tris buffered saline
TCA	Trichloroacetic acid
TEMED	N,N,N´,N´-tetramethylethylenediamine
TFB	Transformation buffer
TGN	Trans Golgi network
TICD	TREM2 intracellular domain
TLR	Toll-like receptor
tm	Trans membrane
TNFα	Tumor necrosis factor-α
TREM	Triggering receptor expressed on myeloid cells
VEGF	Vascular endothelial growth factor
WB	Western immunoblot
WT	Wild-type

Amino acid	3-letter code	1-letter code
Alanine	Ala	A
Arginine	Arg	R
Asparagine	Asn	N
Aspartic acid	Asp	D
Cysteine	Cys	C
Glutamic acid	Glu	E
Glutamine	Gln	Q
Glycine	Gly	G
Histidine	His	H
Isoleucine	Ile	I
Leucine	Leu	L
Lysine	Lys	K
Methionine	Met	M
Phenylalanine	Phe	F
Proline	Pro	P
Serine	Ser	S
Threonine	Thr	T
Tryptophan	Trp	W
Tyrosine	Tyr	Y
Valine	Val	V

1 INTRODUCTION

1.1 Alzheimer's disease (AD)

Alzheimer's disease (AD) is a neurodegenerative disorder, characterized by a progressive cognitive decline. According to recent studies, more than 35 million people worldwide (Wimo & Prince 2010) or rather more than 800.000 people in Germany suffer from AD (Bickel 2010). Because of an increased life expectancy in western industrial countries the number of dementia cases is estimated to double every 20 years (Wimo & Prince 2010). AD is the most common form of dementia diagnosed in mid-to-late life, affecting 7–10 % of all individuals over 65 years of age and approximately 40 % of all persons over 80 years of age (Sisodia 1999; Prince & Jackson 2009). In the beginning of the disease, affected people show an impairment of short term memory, language and cognitive functions. Further they have paranoia, delusions and show a loss of social appropriateness. Later all these hallmarks become intensified and additional problems with motor and sensory functions become manifested. AD is a terminal disease, but the most frequent cause of death are pneumonia and myocardial infarction and not the disease itself (Forstl & Kurz 1999). The symptoms are attributed to alterations or loss of neurons in several brain areas or neural systems including the cortex, hippocampus, amygdala, anterior thalamus, basal forebrain and several brainstem regions (Sisodia 1999; Wenk 2003; Jalbert et al., 2008).

More than 100 years after the first description of AD by the german psychiatrist Alois Alzheimer, this severe form of dementia is still not fully understood. However, there is evidence that besides age also high cholesterol levels and diabetes are risk factors for AD (Tan et al., 2003; Akomolafe et al., 2006). AD cases can be classified into the so-called early onset forms and the late onset forms. Only about 5 % of all AD cases account for early-onset AD (EOAD) in which genetic mutations either in the amyloid precursor protein (APP) or in presenilins 1 and 2 (PS1, PS2) are associated with an age-of-onset below 65 years, with some really severe mutations already between 20-40 (Selkoe 2001).

In contrast, cases of late-onset AD (LOAD) which are also called sporadic AD are not linked to mutations in APP or PS, but genetic determinations like ApoE4 are known to increase the risk for developing AD.

1.1.1 Neuropathological hallmarks of AD

Both the sporadic and the familiar forms exhibit the same histopathological characteristics: neurofibrillary tangles and β-amyloid plaques, appearing mostly in the neocortex, hippocampus and in the limbic system (Braak & Braak 1996). There are several hypotheses how these hallmarks can account for the very complex pathology of AD and how they could be linked.

1.1.1.1 Neurofibrillary tangles

Neurofibrillary tangles (see fig. 1) are intraneuronal accumulations of hyperphosphorylated forms of the tau protein. Under physiological conditions tau is associated with microtubules in axonal compartments, forming and stabilizing their structure (Grundke-Iqbal et al., 1986a; Goedert et al., 1988; Friedhoff et al., 2000). Aside this, tau might have additional functions due to its interaction with the plasma membrane (Brandt et al., 1995; Maas et al., 2000) and the actin cytoskeleton (Fulga et al., 2007). Furthermore, a recent paper also highlights a localization and function of tau in dendritic compartments without association to microtubules (Ittner et al., 2010). The association of tau with microtubules is regulated by phosphorylation (Drewes et al., 1995). Several kinases including the glycogen synthase kinase 3β (GSK3β) also known as tau kinase 1, the cyclin dependent kinase 5 (Cdk5) and the mitogen activated proteinkinase (MAPK) are known to phosphorylate tau (Ishiguro et al., 1993; Chung 2009). Under conditions present in AD, tau becomes hyperphosphorylated. The hyperphosphorylated tau loses its binding capacity to the microtubules, thereby destabilizing their structure. Additionally, the hyperphosphorylation enables tau to aggregate into so-called paired helical filaments (PHFs) (Alonso et al., 2001). Continuous aggregation of PHFs finally forms the neurofibrillary tangles in the soma of neurons. The combination of the loss of function, compromising axonal transport through changes of microtubules dynamics and the toxic gain of function forming intracellular protein aggregates results finally in cell death of the affected neurons (Grundke-Iqbal et al., 1986b; Ishiguro et al., 1993; Li et al., 2006; Li & Paudel 2006; Ballatore et al., 2007). Thus, the intracellular neurofibrillary tangles become detectable in the extracellular environment (Bondareff et al., 1994).

There is strong evidence that the activity of protein phosphatase 2A, responsible for the dephosphorylation of tau, is reduced in the brain of AD patients (Gong et al., 1994; Tian & Wang 2002; Chung 2009). However, to date it is not clear whether the hyperphosphorylation of tau is connected with decreased dephosphorylation, hyperactivity of the tau related kinases or both (Mandelkow & Mandelkow 1998).

In the tau hypothesis neuronal loss as a consequence of the accumulation of neurofibrillary tangles was described as the initial events in the development of AD. However, there are some findings that challenge this. The presence of hyperphosphorylated tau and tangles is not limited to AD (Joachim & Selkoe 1992; Morris et al., 2001). Other neurodegenerative diseases characterized by the aggregation of tau are classified as tauopathies. Important members of this group are the frontotemporal dementia (Dickson 2009). Moreover, there is no way known in which tau could cause amyloid plaques. However, it was shown that tau is mediating Aβ induced cognitive impairments and excitotoxicity. The reduction of endogenous tau in APP transgenic mice prevents behavioral deficits without affecting Aβ levels by blocking Aβ- and excitotoxin-induced neuronal dysfunction (Roberson et al., 2007). Although the exact mechanism for the rescue is unclear, it might be linked to the prevention of Aβ-induced axonal transport defects (Vossel et al., 2010). While incubation of primary hippocampal neurons with oligomeric Aβ rapidly inhibited axonal transport of mitochondria and the neutrotrophin receptor TrkA, these transport defects were rescued in primary neurons of tau $^{-/-}$ and tau $^{+/-}$ mice (Vossel et al., 2010). Another recent study suggests a link by which tau could facilitate Aβ toxicity to synapses. Dendritic localized tau supports the recruitment of the Src-family kinase Fyn to NMDA (N-methyl-D-aspartic acid) receptors on postsynaptic membranes. The resulting phosphorylation of NMDA receptors by Fyn renders them more susceptible to Aβ (Ittner et al., 2010).

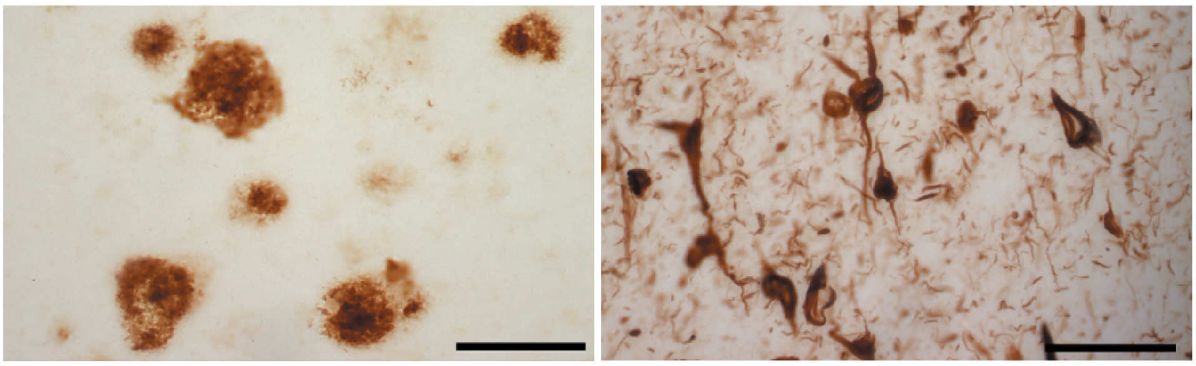

Figure 1: Neuropathological hallmarks of AD.

Representative photographs of amyloid plaques (left picture) and neurofibrillary tangles (right picture) in an AD brain. Scale bar: 62.5 μM. Adopted from "Alzheimer's disease: Aβ, tau and synaptic dysfunction." (LaFerla & Oddo 2005).

1.1.1.2 β-amyloid plaques

In contrast to neurofibrillary tangles, amyloid plaques (fig. 1) are extracellular deposits that are also detectable in the basement membranes of cerebral vessels. One main component of β-amyloid plaques is the small hydrophobic β-amyloid peptide (Aβ) which is derived from the amyloid precursor protein (APP), as explained in 1.1.3. Plaques can be microscopically subclassified into neuritic, also called senile plaques, and diffuse plaques. Neuritic plaques are spherical multicellular lesions, consisting of Aβ fibrils intermixed with non fibrillar variants of the peptide as well as degenerated axons and neurites (Braak & Braak 1996). These compact structures also contain a variable number of activated microglia within and near the fibrillar core. Furthermore, the plaques are often surrounded by reactive astrocytes (Mattiace et al., 1990; Pike et al., 1994; Jefferies et al., 1996; Stalder et al., 1999).

Diffuse plaques appear mainly in the cerebellum (Yamaguchi et al., 1989). They are mainly composed of non-fibrillar Aβ (Tagliavini et al., 1988; Yamaguchi et al., 1988), thereby representing most likely initial stages of the plaque pathology in AD (Tagliavini et al., 1988; Giaccone et al., 1989). In contrast to neuritic plaques which are only found in brains of AD patients, diffuse plaques are also present in brains of healthy older people (Hardy & Selkoe 2002). Although plaques are strong characteristics of AD their density and distribution pattern turned out to be of limited significance for differentiation of neuropathological stages (Braak & Braak 1991).

According to the amyloid-cascade hypothesis, Aβ is the triggering factor of a severe pathological cascade. The accumulation of Aβ leads to neuronal dysfunction, followed by inflammatory processes. The resulting progressive synaptic and neuritic injury entails impaired neuronal homeostasis, thereby altering the activity of several kinases and phosphatases leading to hyperphosphorylation of tau and favoring the generation of neurofibrillary tangles. Aβ plaques and neurofibrillary tangles together cause widespread neuronal deficits which end up in dementia (Hardy & Selkoe 2002). There are a lot of *in vitro* findings supporting this Aβ cascade hypothesis: the impairment of synaptic activity in hippocampal slice cultures through treatment with naturally secreted Aβ oligomers (Lambert et al., 1998; Walsh et al., 2002) and Aβ oligomeric species extracted from human brains (Shankar et al., 2008) as well as the loss of memory and cognitive functions of mice and rats injected with natural Aβ oligomers (Cleary et al., 2005; Lesne et al., 2006; Shankar et al., 2008). There are also some *in vitro* evidences that Aβ can modulate the activity of tau phosphorylating kinases (Hooper et al., 2008; Magdesian et al., 2008; De Felice et al., 2009; Lee et al., 2009). However, these findings could not be confirmed in animal models. No APP single transgenic or APP/PS1 double transgenic animal model which develop plaque

pathology is known to exhibit neurofibrillary tangles (Wong et al., 2002). Only triple transgenic models, harboring $PS1_{M146V}$, APP_{swe} and tau_{P301L} transgenes progressively develop amyloid plaques, neurofibrillary tangles and synaptic dysfunctions (Oddo et al., 2003a; Oddo et al., 2003b). Also the neuronal loss strongly differs in all AD mouse models (Duyckaerts et al., 2008). Moreover, pharmacological reduction of Aβ load, like immunization fail to delay AD progression (Small & Duff 2008).

Keeping all pros and cons of both hypothesis in mind, Small & Duff proposed a dual pathway model in which overriding factors like ApoE4 and GSK3β act in parallel on Aβ- and tau pathology, triggering amyloid plaques as well as neurofibrillary tangles and finally result in synaptic and cell loss (Small & Duff 2008). Such a dual pathway model would further explain the importance of ApoE4 as the major genetic risk factor for sporadic AD.

1.1.2 Genetic factors involved in AD

1.1.2.1 Late onset or sporadic AD

Most of all AD cases belong to the so-called sporadic form of the disease. Little is known about genetic factors underlying this type of AD pathogenesis. Only the *ApoE* gene was confirmed as risk factor for sporadic AD. The *ApoE* gene exists as three polymorphic alleles ε2, ε3 and ε4. Individuals bearing one ε4 allele of the *ApoE* gene were found to develop AD after the age of 65 with a three to four times higher risk compared to individuals carrying no ε4 allele (Corder et al., 1993; Strittmatter et al., 1993; Bertram & Tanzi 2008). In contrast, the ε2 allele was found to be protective against sporadic AD (Corder et al., 1993).

ApoE is a 34 kDa protein which appears, corresponding to three alleles, in three different isoforms ApoE2, ApoE3 and ApoE4. These isoforms differ only in one or two amino acids (Mahley 1988). ApoE4 is the major lipoprotein in the CNS. In the brain it is predominantly produced by astrocytes and to some extent also by microglia (Pitas et al., 1987; Uchihara et al., 1995). The uptake into neurons is mediated by a group of receptors known as the LDL receptors (Herz & Bock 2002; Herz & Chen 2006).

The mechanisms underlying the increased risk of ApoE4 are poorly understood. However, it is suggested that ApoE4 could promote the Aβ aggregation or could be responsible for an impaired Aβ clearance via receptor mediated endocytosis (Bu 2009; Kim et al., 2009). Indeed, a decreased binding capacity of ApoE4 to Aβ was found compared to ApoE3 (LaDu et al., 1994).

Besides ApoE, recent genome wide association studies identified variants of CLU and PICALM to be associated with AD risk (Harold et al., 2009; Corneveaux et al., 2010; Kamboh et al., 2010). Nevertheless, all of them have much lower significance compared to ApoE.

1.1.2.2 Early onset or familiar AD

About 5 % of all AD cases are linked to mutations in AD relevant genes. Since these forms appear before the age of 65, they are often referred as EOAD (Selkoe 2001). All known mutations linked with EOAD are located in the genes coding for APP or presenilin 1 and 2 and are mainly associated with increased $A\beta_{42}/A\beta_{40}$ ratio and/or alteration of the Aβ aggregation (Goate et al., 1991; Citron et al., 1992; Cai et al., 1993; Borchelt et al., 1996). All mutations in APP are located within or nearby the Aβ domain (Wolfe 2007). A well analyzed mutation, which belongs to this group is the swedish double mutation. This mutation was initially found in a swedish family with EOAD (Mullan et al., 1992). The mutations K595N/M596L in APP increases the affinity of BACE-1 to its substrate APP (Citron et al., 1992; Cai et al., 1993; Vassar et al., 1999). Thus, APP bearing this mutation is cleaved earlier and more efficiently in the secretory pathway by BACE-1 than APP WT (Haass et al., 1995; Thinakaran et al., 1996). Other mutations in APP near the γ-secretase cleavage site lead to increased production of the more aggregation-prone $A\beta_{42}$ relative to $A\beta_{40}$. Mutations in the Aβ region itself alter the biophysical properties of the peptide, thereby changing its aggregation and degradation behavior (Wolfe 2007).

So far, more than 160 mutations were identified in the genes encoding PS1 and 2. Most of them are simple missense mutations resulting in the exchange of one amino acid in PS1, but there are also more complex ones, for example small deletions or insertions. The most severe mutation is a splice mutation leading to the deletion of exon 9 (Δexon9) (De Strooper 2007). Such AD causing mutations in PS1 lead both to increased $A\beta_{42}/A\beta_{40}$ ratios (Goate et al., 1991; Citron et al., 1992; Cai et al., 1993; Borchelt et al., 1996) and partial loss of γ-secretase function (Song et al., 1999; Bentahir et al., 2006; Tamboli et al., 2008). To explain this apparent paradox at least two different cleavage sites of γ-secretase in APP were assumed. Cleavage at the so-called ε-site produces the C-terminus of Aβ and releases the AICD. Afterwards the cleavage at the γ-site releases Aβ. This cleavage site can vary in its position, leading to the various Aβ-species ($A\beta_{40}$ and $A\beta_{42}$). Longer forms of Aβ (e.g. $A\beta_{42}$) are thought to be retained in the active site of the γ-secretase because of their larger hydrophobic tm-domain. Shorter variants (e.g. $A\beta_{40}$) in contrast are more likely to be released. A less active γ-secretase would thereby allow more time for the release of the longer, more hydrophobic $A\beta_{42}$ (Qi-Takahara et al., 2005; Wolfe 2007).

1.1.3 Characteristics of the β-amyloid precursor protein (APP)

As mentioned above, Aβ originates from a sequential processing of APP, a large type I transmembrane protein, expressed in several human tissues. APP and its homologues APLP-1 and APLP-2 (amyloid precursor like protein-1 and -2) form a small family of proteins of 100-140 kDa in size, which are ubiquitously expressed throughout mammalians as well as *Caenorhabditis elegans* and *Drosophila melanogaster* (Goldgaber et al., 1987; Rosen et al., 1989; Luo et al., 1990; Daigle & Li 1993; Zheng & Koo 2006). Additional heterogeneity is caused on the one hand by alternative splicing (Weidemann et al., 1989; Oltersdorf et al., 1990; Hung & Selkoe 1994), producing several isoforms of which APP 695, 751 and 770 are the most abundant in the brain (Wertkin et al., 1993). On the other hand a couple of posttranslational modifications as O- and N-glycosylation (Tomita et al., 1998), sulfation as well as phosphorylation (Hung & Selkoe 1994; Walter et al., 1997) raises the heterogeneity of this group of proteins. APP can be divided in three main parts (see fig. 2), a 47 aa long C-terminal cytoplasmic domain, a 24 aa long transmembrane domain (tm-domain) and a N-terminal extracellular domain, varying in size between the different isoforms.

There are several physiological functions discussed for APP, including modulation of cell-cell interaction, cell adhesion, signal transduction and neurite outgrowth (Milward et al., 1992; Nishimoto et al., 1993; Koo 2002). Cell-cell contacts and cell adhesion could be mediated by the E1 domain of the extracellular part by which APP is able to form homodimers or heterodimers with its homologues APLP-1 and -2 (Soba et al., 2005).

While single gene knock out mice for APP, APLP-1 or APLP-2 show only mild phenotypes, double knockout models (APP/APLP-2; APLP-1/APLP-2) are lethal, showing that the APP protein family plays important physiological roles, that are partly redundant (Zheng et al., 1995; von Koch et al., 1997; Heber et al., 2000). Particularly the Aβ domain, which consists of the last 28 aa of the APP ectodomain and the first 12-14 aa of the tm-domain and is not present in APLPs, cannot play a pivotal physiological role. However, a recent study demonstrates a ferroxidase activity of APP and a role in neuronal iron-export. Intracellular iron accumulates in primary neurons of APP knock out mice. Moreover, APP knock out mice fed with an iron dietary exhibit increased Fe^{2+} levels, resulting in oxidative stress in cortical neurons (Duce et al., 2010).

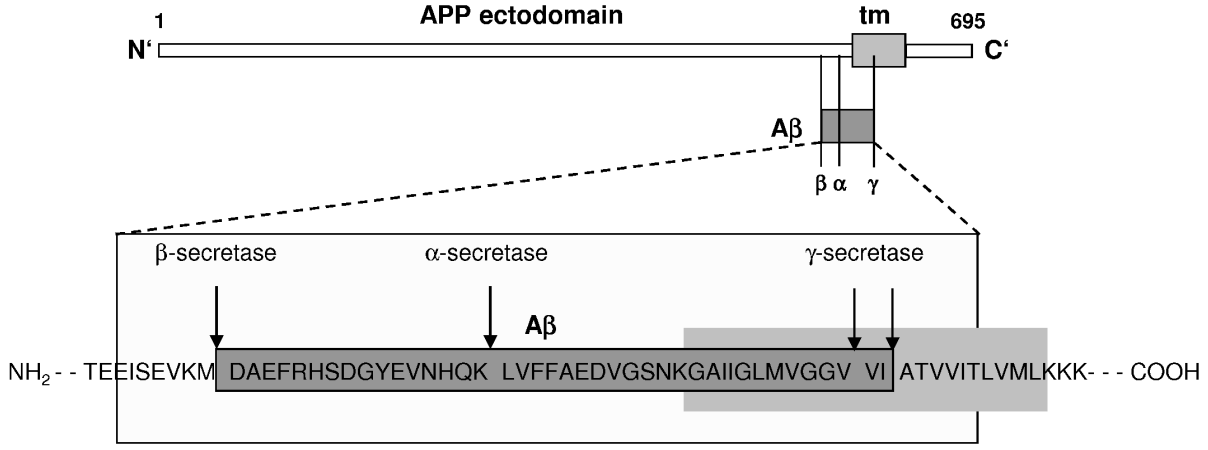

Figure 2: Scheme of the APP structure.

APP can be divided in a large extracellular ectodomain, a short single transmembrane (tm)-domain and a cytosolic tail. The Aβ domain (dark gray) is located at the end of the ectodomain and the beginning of the transmembrane domain. The box highlighted the Aβ and tm-domain as amino acid sequence. The cleavage site of the three secretases are indicated by arrows. Modified from "Cellular processing of β-amyloid precursor protein and the genesis of amyloid β-peptide" (Haass & Selkoe 1993).

1.1.4 APP processing

The release of Aβ from APP is mediated by two different proteases. These so-called secretases cleave APP sequentially in the lumen of cellular organelles e.g. Golgi, endosomes and lysosomes or at the cell surface. The first cleavage is catalyzed by β-secretase at position 1 of the Aβ domain (see fig. 2 and 3), thereby releasing the soluble APP fragment (sAPPβ) and a membrane bound C-terminal fragment (CTF) with a size of 99 aa (CTFβ or C99). Further processing of CTFβ by a multienzyme complex called γ-secretase leads to the production of Aβ and the release of the APP intracellular domain (AICD) into the cytosol (Haass et al., 1992b; Sastre et al., 2001; Haass & Steiner 2002). Since γ-secretase can cleave C99 at different sites, several Aβ variants with sizes of 37 aa–42 aa arise. However, $A\beta_{40}$ (~90 %) and $A\beta_{42}$ (~10 %) are the variants most frequently released from the membrane (Citron et al., 1996; Weggen et al., 2001; Wiltfang et al., 2002). Importantly, $A\beta_{42}$ is, based on its hydrophobicity, most prone to aggregate and form plaques (Barrow & Zagorski 1991; Jarrett et al., 1993). Alternatively, APP can be processed in the non amyloidogenic pathway which results in the generation of a small, non amyloidogenic peptide, named p3. In this pathway the first cleavage of APP within the Aβ domain at aa 16 (see fig. 2 and 11) is catalyzed by the α-secretase (Esch et al., 1990; Sisodia et al., 1990) releasing sAPPα into the extracellular space and a CTF which is 83 aa in size (CTFα or C83).

The subsequent γ-secretase cleavage of CTFα results in the release of the non amyloidogenic p3 peptide (Haass et al., 1993; Sastre et al., 2001) and AICD, like in the amyloidogenic pathway. The

AICD was shown to have gene regulatory function (Cao & Sudhof 2001; Kimberly et al., 2001; Alves da Costa et al., 2006), but other groups could not confirm these findings (Hass & Yankner 2005; Hebert et al., 2006). However, a recent paper demonstrates a function for the sAPPβ fragment as ligand for the death receptor 6 which is involved in axonal pruning and neuronal cell death (Nikolaev et al., 2009).

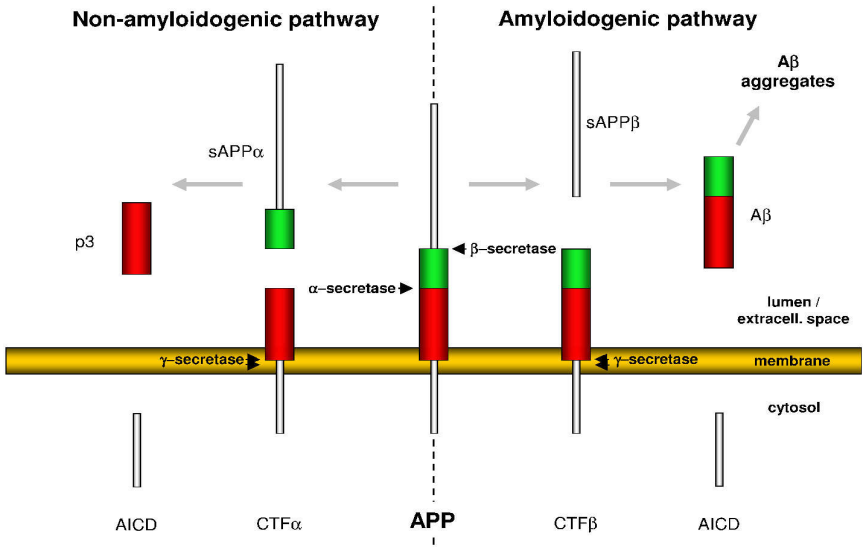

Figure 3: The APP processing.

In the amyloidogenic pathway APP is first cleaved by β-secretase generating sAPPβ and CTFβ. In the non-amyloidogenic pathway α-secretase cleaves first within the Aβ domain, thereby generating sAPPα and CTFα. The subsequent cleavage of the CTFs by γ-secretase results in the release of Aβ in the amyloidogenic and of p3 in the non-amyloidogenic pathway. Modified from "Cellular processing of β-amyloid precursor protein and the genesis of amyloid β-peptide" (Haass & Selkoe 1993).

1.1.5 Structural and functional insights in the APP processing enzymes

1.1.5.1 The a-secretase: ADAM-10, ADAM-17 and ADAM-9

All proteases which catalyze the cleavage of ectodomains are called sheddases. The main APP ectodmomain shedding in non-neuronal cells occurs by α-secretase cleavage between K16 and L17 of the Aβ region. There are three enzymes of the ADAM (a disintegrin and metalloprotease) protease family which were identified to have α-secretase properties: ADAM-10 (Lammich et al., 1999), ADAM-17 also known as tumor necrosis factor-α converting enzyme (Buxbaum et al., 1998) and ADAM-9 (Koike et al., 1999). Interestingly, the overexpression of ADAM-10 in mice increased α-secretase cleavage thereby lowering Aβ production (Postina et al., 2004). Moreover,

the ectodomain shedding of APP can be increased by activation of protein kinase C (Etcheberrigaray et al., 2004).

All ADAMs are type I transmembrane zinc metalloproteases and cleave APP on the secretory pathway from the trans Golgi network (TGN) to the plasma membrane or directly at the plasma membrane (Haass et al., 1992a; Sisodia 1992; Chyung & Selkoe 2003). During the past years the ADAM family appeared to be one of the most important groups of sheddases, with several substrates involved in various signaling pathways. In addition to APP, the type I transmembrane proteins TNFα, the Notch receptors, p75, TNFα-receptor and L-selectin are substrates of the ADAM family (Seals & Courtneidge 2003). Mice deficient for either ADAM-10 or ADAM-17 are lethal already in embryonic state, confirming the important physiological role of these sheddases (Peschon et al., 1998; Hartmann et al., 2002).

1.1.5.2 The β-secretase: BACE-1

The shedding of the APP ectodomain is essential for the release of Aβ, but for a long time the exact protein acting as β-secretase was unknown. In the late '90s a type I transmembrane aspartyl protease, the β-site APP cleaving enzyme-1 (BACE-1), also known as aspartic protease-2 or memapsin-2 (membrane-associated aspartic protease-2) could be identified as β-secretase (Hussain et al., 1999; Sinha et al., 1999; Vassar et al., 1999; Yan et al., 1999; Lin et al., 2000). Like all type I transmembrane proteins BACE-1 consists of an ectodomain, a transmembrane domain and a C-terminal cytosolic tail (Hussain et al., 1999; Sinha et al., 1999; Vassar et al., 1999; Yan et al., 1999; Lin et al., 2000). The ectodomain bears the typical DTGS and DSGT amino acid motifs, forming the catalytic center of aspartyl proteases (Hussain et al., 1999; Vassar et al., 1999; Yan et al., 1999). Mutation of one of these motifs abolishes the protease activity completely (Hussain et al., 1999).

As other aspartic proteases, BACE-1 contains a propeptide, located at the N-terminus of the enzyme, which is cleaved during maturation by furin or a furin-like protease (Bennett et al., 2000b; Capell et al., 2000; Creemers et al., 2001). Furthermore, the ectodomain contains four asparagine residues which undergo complex N-glycosylation during the transport from the ER to the Golgi (Capell et al., 2000; Huse et al., 2000). Fully matured BACE-1 is transported from the Golgi to the cell surface. The transport of BACE-1 is mediated by motifs located in the cytoplasmic domain, since the deletion of this part results in an accumulation of BACE-1 in the ER (Capell et al., 2000). From the cell surface, BACE-1 can be re-internalized into endosomal compartments from which it is either recycled back to the plasma membrane or transported to the

TGN (Walter et al., 2001a) or lysosomes (Koh et al., 2005). While the re-internalization is mediated by a di-leucine motif in the C-terminus (Huse et al., 2000; Pastorino et al., 2002), the transport to the TGN is controlled by the phosphorylation state of the adjacent serine residue S498 (Walter et al., 2001a). Both the di-leucine motif and serine 498 are part of a DISLL motif which follows the structure DxxLL, known to serve as the binding site for a particular group of transport proteins, the GGAs (Golgi associated, γ-adaptin ear containing, ARF binding proteins). These are monomeric adapter proteins which sort specific cargo-proteins like the mannose-6-phosphate receptor from the TGN to endosomal/lysosomal compartments (Bonifacino 2004; Robinson 2004). BACE-1 was shown to bind GGAs (He et al., 2002; Shiba et al., 2004). Moreover, it was shown that the DxxLL motif regulates the retrograde transport of internalized BACE-1 from endosomal compartments to the TGN in a phosphorylation dependent manner (Wahle et al., 2005). In addition to the critical DxxLL motif, the C-terminus of BACE-1 contains also three cysteine residues which can be palmitoylated (Benjannet et al., 2001). The palmitoylation leads to the insertion of a second membrane anchor which might take part in regulating the subcellular localization (Schweizer et al., 1996; Vetrivel et al., 2009). Although β-secretase activity was detected in various cell types and tissues, the highest BACE-1 activity was measured in neuronal tissue, particularly in neurons (Haass et al., 1992b; Shoji et al., 1992; Seubert et al., 1993). Biochemical studies revealed that BACE-1 shows highest activity at pH 5 (Vassar & Citron 2000; Walter et al., 2001b). Accordingly, BACE-1 was mainly found in endosomal and lysosomal compartments.

Less is known about the physiological role of BACE-1, since BACE-1 knock out mice show no overt phenotype. However, more careful analysis of BACE-1 deficient mice revealed a decreased myelination, suggesting a role of BACE-1 in the formation of myelin sheets. Responsible for this defect might be the impaired cleavage of the transmembrane protein neuregulin-1 by BACE-1 (Aoki et al., 2004; Hu et al., 2006; Willem et al., 2006; Hu et al., 2008). Physiologically neuregulin-1 plays a role in the maintenance of heart function and in myelination of axons. Other known BACE-1 substrates are beside APP also the APLPs (Li & Sudhof 2004), the sialyltransferase ST6Gal-I (Kitazume et al., 2003), the P-selectine glycoprotein ligand-1 (PSGL-1) (Lichtenthaler et al., 2003) and LRP (low density lipoprotein receptor related protein) (von Arnim et al., 2005).

In parallel to BACE-1 a homologue protein was identified as β-site APP cleaving enzyme-2. Both proteins have similar structural organization and share more than 50 % sequence identity on the amino acid level (Vassar et al., 1999; Yan et al., 1999; Acquati et al., 2000; Hussain et al., 2000; Lin et al., 2000). Consistent with the high molecular structure identity to BACE-1, BACE-2 undergoes comparable posttranslational modifications like complex N-glycosylation at asparagine

residues located in the ectodomain (Vassar & Citron 2000; Walter et al., 2001b). Immature BACE-2 also contains a propeptide which is cleaved during the maturation. However, while this maturation step is catalyzed by furin proteases in BACE-1, the propeptide of BACE-2 appears to be removed autocatalytically (Hussain et al., 2001; Yan et al., 2001). Although both enzymes are very similar, BACE-2 shows striking differences regarding stability and intracellular transport (Fluhrer et al., 2002). Compared to BACE-1 that is highly expressed in neurons, there is relative low expression of BACE-2 in the nervous system, but higher in peripheral tissues (Vassar et al., 1999; Bennett et al., 2000a). The highest expression in the nervous system is observed in glia cells (Dominguez et al., 2005). Since the *bace2* gene is localized on chromosome 21, a contribution of BACE-2 to the AD-like pathology in Down's syndrome and in AD was suggested (Yan et al., 1999; Solans et al., 2000; Vassar & Citron 2000; Walter et al., 2001b). Interestingly, BACE-2 mRNA and protein levels were increased in individuals with Down's syndrome (Motonaga et al., 2002; Barbiero et al., 2003).

As shown by cell biological studies, BACE-2 is able to cleave APP, but the cleavage efficiency at the β-secretase site is very low (Bayer et al., 1999; Farzan et al., 2000; Hussain et al., 2000; Lin et al., 2000; Yan et al., 2001). Rather, BACE-2 cleaves APP in an α-secretase-like manner within the Aβ domain between phe 19 and phe 20 as well as between phe 20 and ala 21 (Farzan et al., 2000; Yan et al., 2001; Fluhrer et al., 2002). Accordingly, protein expression studies in human brain of AD patients and aged-matched controls, can detect BACE-2, but the expression and activity is not significantly altered in AD brains (Stockley et al., 2006; Ahmed et al., 2010).

1.1.5.3 The γ-secretase

The γ-secretase is a multiprotein complex consisting of four essential components. The catalytic center of the complex is formed by PS1 or its homologue PS2 (Levy-Lahad et al., 1995; Sherrington et al., 1995), supported by three additional co-factors: nicastrin (Yu et al., 2000; Edbauer et al., 2002b; Kopan & Goate 2002; Lai 2002), APH-1 (anterior pharynx-defective-1) (Francis et al., 2002; Goutte et al., 2002; Lee et al., 2002; Luo et al., 2003) and PEN-2 (presenilin enhancer-2) (Francis et al., 2002; Steiner et al., 2002; Luo et al., 2003). These components appear in a stoichiometric ratio of 1:1:1:1 in the mature γ-secretase complex (Sato et al., 2007). Since the total molecular mass of the γ-secretase complex is higher than the summarized molecular masses of the single components, it was early considered that other unidentified proteins take part in the complex. In fact, it was shown that γ-secretase modulators (GSMs) like TMP21 (Chen et al., 2006; Pardossi-Piquard et al., 2009), CD147 (Zhou et al., 2005) and the recently found GSAP (γ-

secretase activating protein) (He et al., 2010) are associated with the γ-secretase complex and can modulate γ-secretase activity. However, purification of γ-secretase during which the GSMs are separated early from the rest of the γ-secretase complex, and subsequent activity assays with the purified γ-secretase, revealed that GSMs are not relevant for the basal activity of the γ-secretase complex. Thus, the four main components PS, nicastrin, APH-1 and PEN-2 are sufficient for an active γ-secretase complex (Winkler et al., 2009).

PS1 and PS2 are membrane proteins with nine transmembrane domains, bearing the two catalytic aspartate residues (Spasic et al., 2006). In the γ-secretase complex, presenilins are present as a heterodimer formed by a C-terminal and an N-terminal fragment, each of them containing one catalytic aspartate residue. The two fragments are most likely generated by autocatalytic endoproteolysis between tm-domain 6 and tm-domain 7 (Ratovitski et al., 1997; Capell et al., 1998; Wolfe et al., 1999a; Wolfe et al., 1999b; Kimberly et al., 2000).

Nicastrin, a glycosylated type I transmembrane protein was shown to be involved in the substrate recognition. Nicastrin binds the extracellular/lumenal N-terminus, generated upon ectodomain shedding of type I transmembrane proteins, thereby recruiting the substrate into the catalytic center. It was found that the recognition is not mediated by the amino acid sequence of the substrates. Only a short free N-terminal part above the cell membrane seems to be necessary (Yu et al., 2000; Shah et al., 2005).

PEN-2 and APH-1 are both polytopic transmembrane proteins. Only little is known about the function of these proteins. However, PEN-2 is supposed to support the endoproteolytic cleavage of presenilin, because PEN-2 deficiency stabilized the presenilin holoprotein (Hu & Fortini 2003; Luo et al., 2003; Takasugi et al., 2003; Prokop et al., 2004). Although the assembly of the whole γ-secretase complex is not yet fully understood, there is evidence that APH-1 supports this process and is involved in maturation and transport (Luo et al., 2003; Takasugi et al., 2003; Kaether et al., 2006a). There are studies showing that only fully assembled complexes can be transported via the secretory pathway to the plasma membrane and early endosomes where most of the γ-secretase is located (Walter et al., 1998; Annaert et al., 1999; Kaether et al., 2006a), while unassembled, single components were retained in the ER (Kaether et al., 2006a; Dries & Yu 2008).

To date a couple of different γ-secretase substrates are identified. Among these are APP, Notch (De Strooper et al., 1999; Saxena et al., 2001) and other proteins which have important physiological functions e.g. APLP-1 and -2 (Walsh et al., 2003), E- and N-cadherin (Marambaud et al., 2002), EphB (Georgakopoulos et al., 2006) and LRP (May et al., 2002). Another important protein which is processed by γ-secretase is the widely expressed cell-adhesion protein CD44 (Okamoto et al., 2001; Lammich et al., 2002; Murakami et al., 2003), implicated amongst others in

leukocyte homing and activation as well as cell migration.

Since the cleavage reaction occurs in all cases inside the plasma membrane and not in a water containing environment, the process is called regulated intramembrane proteolysis (RIP). To afford proteolysis within the membrane, it was suggested that the γ-secretase complex forms a water containing pore in which the cleavage reaction is catalyzed. Because of the high number of γ-secretase substrates and its less cleavage specificity, the γ-secretase was long time assumed to be a "proteasome of the membrane" (Kopan & Ilagan 2004). However, an unbiased proteomic screen revealed exact substrate characteristics, as the short ectodomain and permissive transmembrane and cytoplasmic domain (Hemming et al., 2008). Besides the release of gene regulatory intracellular domains, like the Notch ICD (De Strooper et al., 1999; Saxena et al., 2001), γ-secretase can directly affect the Wnt signaling pathway by direct interaction with GSK3β and β-catenin (Prager et al., 2007). PS1 mediated processing of Notch, which is involved in transcriptional regulation of developmental genes is a crucial function of γ-secretase. Because of this PS $^{-/-}$ mice and PS1/PS2 knockout mice resemble a Notch knock out phenotype to some extent, and are lethal directly after birth (Shen et al., 1997). However, PS2 $^{-/-}$ mice are viable, indicating that PS2 could not compensate PS1 deficiency.

There is evidence that γ-secretase function is also important for endocytosis. In presenilin deficient cells the endocytosis of the LDL-receptor is impaired, leading to upregulation of cholesterol biosynthesis (Tamboli et al., 2008).

Recently, a very interesting function of γ-secretase in neurogenesis was published. Neural progenitor cells (NPCs) from mice expressing a variant of presenilin linked to familiar AD (PS FAD) show a defect in proliferation (Choi et al., 2008). Moreover, NPCs cultured in medium of microglia from PS FAD mice exhibit a significant less proliferation rate than the NPCs in medium of control microglia. Based on these results a non-cell-autonomous mechanism was supposed by which γ-secretase modulates neurogenesis (Choi et al., 2008). In a subsequent study the authors could show that microglia from PS1 FAD mice produce altered chemokine levels and that these chemokines are closely linked to neurogenesis (Veeraraghavalu et al., 2010). Although γ-secretase expression was mainly shown in neurons. These results give the first hints for γ-secretase function in microglia. According to this, the presence of presenilin and nicastrin in microglia and reactive astrocytes following traumatic brain injury (Nadler et al., 2008) might be related to the modulation of neurogenesis.

1.2 Aβ clearance in the brain

While EOAD is predominantly caused by increased $A\beta_{42}/A\beta_{40}$ ratio or altered aggregation behavior of Aβ, the reasons for developing sporadic AD are largely unclear. Most likely, a misregulation of either Aβ production, Aβ clearance or both could contribute to sporadic pathogenesis. In fact, the activity of BACE-1 which catalyzes the rate limiting step in the generation of Aβ is increasing with age in humans (Tyler et al., 2002; Kern et al., 2006; Stockley et al., 2006) as well as in mice (Apelt et al., 2004). In contrast, the amount and activity of Aβ degrading enzymes is reduced with age (Wang et al., 2006). Moreover, there are findings that the ability of microglia to clear Aβ decreases also with age (Hickman et al., 2008).
There are different pathways by which Aβ can be cleared from the brain:

Efflux of soluble Aβ to the peripheral circulation through the blood brain barrier.

The blood brain barrier (BBB) is a highly specialized endothelial structure of the brain cells, separating together with astrocytes, pericytes and microglia components of the blood stream from neurons (Zlokovic 2008). To clear sAβ from the brain, it can be transported across the BBB into brain blood vessels by LRP1 mediated transcytosis (Shibata et al., 2000; Deane et al., 2008b; Deane et al., 2009). Therefore sAβ either binds directly (Deane et al., 2004) or in complex with ApoE (DeMattos et al., 2004; Bell et al., 2007; Deane et al., 2008a) or α2-macroglobulin (Narita et al., 1997; Qiu et al., 1999) to LRP-1, located on brain endothelial cells. A relatively minor part (10-15 % of total Aβ clearance) is directly transported by bulk flow of interstitial fluid into cerebrospinal fluid, followed by drainage into the blood stream (Shibata et al., 2000; Deane et al., 2009). Furthermore, there is an active transport of Aβ across the BBB, mediated by the P-glycoprotein efflux pump, highly expressed on the lumenal surface of brain capillary endothelial cells (Lam et al., 2001; Cirrito et al., 2005; Kuhnke et al., 2007).

Proteolytic degradation of Aβ.

sAβ has been shown to be sensitive to proteolytic degradation mediated by proteases which cleave Aβ additionally to their physiological substrates. The known proteases are neprilysin (NEP), insulin degrading enzyme (IDE), endothelin converting enzyme-1 (ECE1), angiotensin converting enzyme (ACE), plasmin and matrix metalloprotease-9 (MMP9) (Miners et al., 2008). With respect to Aβ degradation, NEP and IDE are the best characterized intracellular and extracellular enzymes in microglia and other cells (Iwata et al., 2000; Mukherjee & Hersh 2002; Jiang et

al., 2008).

NEP is a type II transmembrane protein of the zinc metalloprotease family, so its C-terminal domain is oriented to the extracellular space (Malito et al., 2008). NEP is able to degrade sAβ in the extracellular space while $A\beta_{40}$ can be degraded more efficiently than $A\beta_{42}$. There are several studies supporting the role of NEP as a rate-limiting Aβ degrading enzyme. NEP knockout in mice results in decreased degradation of injected radiolabeled Aβ as well as suppression of endogenous Aβ levels (Iwata et al., 2001). Furthermore, overexpression of NEP (8-fold) in APP transgenic mice revealed a 50 % decrease of soluble and insoluble $A\beta_{40}$ and $A\beta_{42}$ (Leissring et al., 2003).

IDE is also a zinc metalloprotease which is normally expressed in the cytosol of microglia, neurons and astrocytes but can be also found membrane localized or as a secreted protein. Microglia and astrocytes were found to secrete IDE (Malito et al., 2008) via an exosome mediated pathway, since IDE lack any signal sequence (Bulloj et al., 2010; Tamboli et al., 2010). In addition to insulin and numerous other substrates, sAβ has been reported to be a canonical substrate of IDE. The strongest evidence that IDE can indeed degrade sAβ has come from studies with $IDE^{-/-}$ and $IDE^{+/-}$ mice. While homozygous mice showed < 50 % increased Aβ levels compared to controls, heterozygous mice exhibit Aβ levels that were intermediate between the $IDE^{-/-}$ and the control mice (Farris et al., 2003). Further support came from the overexpression experiments of Leissring and colleagues as described already for NEP. In this study a 2-fold overexpression of IDE resulted in a 50 % decrease of Aβ (Leissring et al., 2003), suggesting that IDE is the more efficient Aβ degrading enzyme. Interestingly, the levels of IDE were found to be elevated in an AD mouse model, overexpressing APP_{swe} and PS1 Δexon 9 (Lazarov et al., 2005). However, it was also reported that levels of NEP, IDE and MMP9 were massively reduced in older mice concomitant with the upregulation of pro inflammatory cytokines (Hickman et al., 2008).

Uptake and degradation by microglia

Microglia were shown to internalize fibrillar Aβ (fAβ) and sAβ by phagocytosis and a process called macropinocytosis, respectively. The exact mechanisms are discussed in 1.4.1. However, by yet unknown mechanisms the phagocytosis efficiency of microglia is decreased in AD (discussed below).

1.3 Microglia

Microglia are resident macrophages of the central nervous system (CNS) and account for 5-10 % of the total cell population in the brain. They are derived from myeloid precursors, which was conclusively shown by absence of microglia in PU.1 null mice (McKercher et al., 1996), a transcription factor controlling gene expression during myeloid development. These precursors enter the CNS during development, proliferate and mature under the influence of the CNS microenvironment. In the adult brain microglia have a small cell soma, little perinuclear cytoplasm and a number of fine branched protrusions (Ransohoff & Perry 2009). By *in vivo* two-photon microscopy of mice expressing GFP in the gene coding for the fractalkine receptor it was shown that microglia in the "ramified", also known as "resting" state are very active. The processes and arborization of such cells are highly motile. *De novo* synthesis of the protrusions and withdrawal of the protrusions lead to permanent reorganization of the processes (Davalos et al., 2005; Nimmerjahn et al., 2005). Such dynamic structures enable the microglia to monitor their local environment without disturbing other cells in the CNS in particular neurons (Hanisch & Kettenmann 2007). This distinct phenotype is maintained by intensive contact of microglia to the cells in their immediate environment. A couple of receptor-ligand pairs, which are expressed on microglia and their neighboring cells, play a crucial role in this process. CD200 expressed on neurons binds to the CD200 receptor (CD200R) located on the microglia surface (Hoek et al., 2000; Wright et al., 2000). CD200R contains an immunomodulatory tyrosine inhibitory motif (ITIM) that averts activation of microglia via Src activation and recruitment of SHP-1 & 2 (Src homology region 2 domain-containing phosphatase). Other ligand–receptor pairs which can modulate the phenotype of microglia are CX3CL1–CX3CR1 (Cardona et al., 2006) and SIRPα–CD47 (Vernon-Wilson et al., 2000). Disruption of these cell–cell contacts through brain injury or disease results in a shift of the microglia activation state towards a phenotype characterized by shortened and extensively branched processes and hypertrophy of the cell body (Perry et al., 2010). The so-called "off-signaling" is only one important signaling principle which organizes the microglia responsiveness. The other principle, the "on-signaling" relies on receptors recognizing pathogen-associated molecular pattern molecules (PAMPs) or damage-associated molecular pattern molecules (DAMPs). PAMPs are proteins of microbiological origin, like lipopolysaccharide, peptidoglycan and nucleic acid variants associated with viruses. These molecules are recognized by different toll-like receptors (TLRs) or other pattern recognition receptors. DAMPs are mostly intracellular molecules which are released due to cell damage or cell death. Examples are heat shock proteins, HMGB1 (high-mobility group box 1) (Scaffidi et al., 2002), high concentrations of ATP (Davalos

et al., 2005) or UDP as well as DNA. Some of these DAMPs are also recognized by TLRs (for example DNA by TLR9) whereas the detection of ATP and UDP is accomplished by P2Y metabotropic receptors (Haynes et al., 2006; Koizumi et al., 2007). Another important DAMP receptor expressed on microglia is the receptor for advanced glycosylated end products (RAGE). Detection of PAMPs and DAMPs results in phagocytosis. The uptake of bacterial molecules is thereby accompanied by release of inflammatory-mediators (Hanisch et al., 2001; Hausler et al., 2002) whereas microglia which engulf apoptotic cells or myelin debris release anti-inflammatory factors (Magnus et al., 2001; Liu et al., 2006).

1.4 The role of microglia & inflammation in AD

Microglia play a multifaceted role in the pathogenesis of AD. To date, there is a controversial debate going on whether they are beneficial or detrimental. Their beneficial contribution is mostly linked with Aβ phagocytosis, as discussed in detail in 1.4.1 whereas the detrimental effects are connected with amplification of as well as response to inflammatory processes.

In brains of AD patients and in a well known mouse disease model the Tg2576 mouse, amyloid plaques are found associated with microglia, exhibiting an "activated" proinflammatory phenotype (Perlmutter et al., 1990; Frautschy et al., 1998). Moreover, *in vivo* two-photon microscopy revealed that surveying microglia rapidly extend their processes and finally migrate towards a new appeared plaque (Bolmont et al., 2008; Meyer-Luehmann et al., 2008). The number and size of microglia increase thereby in proportion to the size of plaques, suggesting a role of microglia in plaque maintenance (Bolmont et al., 2008; Meyer-Luehmann et al., 2008; Yan et al., 2009). In contrast, it was shown that the ablation of endogenous microglia in an AD mouse model has no effect on the plaque number and size over a period of 2-4 weeks. However, there was a 3-4 fold increase in soluble $A\beta_{40}$ and $A\beta_{42}$ measurable, meaning that microglia contribute to the removal of soluble Aβ species (Grathwohl et al., 2009).

1.4.1 Beneficial roles of microglia in Aβ clearance

Several cells and pathways were described to be necessary for the uptake of sAβ. The best described one is the uptake of sAβ by brain capillary endothelial cells in a LRP1 mediated pathway. Although, microglia expresses LRP (Marzolo et al., 2000) it is not the major pathway for the uptake of sAβ since treatment of microglia with the LRP antagonist receptor-associated protein (RAP) had no effect on the sAβ uptake (Mandrekar et al., 2009). However, it was also shown that

intracellular degradation of sAβ by microglia was induced in presence of ApoE, a ligand for LRP1 (Jiang et al., 2008), supporting the role of LRP1 in the microglia sAβ uptake. The receptor complex including scavenger receptors, CD36 and CD47 which is believed to be responsible for internalization of fAβ, plays no role in uptake of sAβ because the inhibition of individual receptor components didn't significantly impair the incorporation of sAβ in microglia (Mandrekar et al., 2009). In contrast, a macropinocytosis mediated uptake process was suggested, where sAβ is taken up to pinocytotic vesicles which are transported rapidly to endolysosomal compartments where the soluble peptides undergo degradation (Mandrekar et al., 2009).

Although some studies show no effect of microglia on plaque size, there are some findings indicating that microglia can ingest fAβ via receptor-mediated phagocytosis (Paresce et al., 1996; Koenigsknecht & Landreth 2004). However, it is not conclusively evidenced yet, whether microglia can degrade fAβ intracellularly. The findings vary from release of fAβ after internalization (Chung et al., 1999) to the retention of fAβ for some weeks before degradation (Paresce et al., 1997). The degradation of Aβ might depend on the activation status of microglia, since microglia activated with the macrophage colony-stimulating factor were able to degrade fAβ efficiently (Majumdar et al., 2007). Moreover, microglia displaying an activation status in which they produce proinflammatory cytokines, were unable to take up and degrade fAβ (Koenigsknecht-Talboo & Landreth 2005).

Several receptors have been shown to interact with fAβ. Contribution of Fc receptors (FcRs) was suggested, because opsonization of Aβ with anti-Aβ antibodies in the brain of mice resulted in a robust phagocytic response (Bard et al., 2000; Wilcock et al., 2003). Additionally, TLRs (Reed-Geaghan et al., 2009; Stewart et al., 2010), scavenger receptors of class A and B as well as integrins play an important role in the uptake of fAβ. All these receptors were thought to form a receptor complex which leads to induction of phagocytosis subsequent to receptor activation (Bamberger et al., 2003). Although a lot of studies indicate phagocytosis of Aβ *in vitro*, the unsolved question remains why they fail to clear amyloid deposits in the brain.

Besides their function as phagocytes, microglia also express Aβ degrading enzymes as explained in 1.2, which can degrade Aβ species directly in the extracellular environment.

Furthermore, microglia can contribute to neurogenesis when they are activated by T helper cell cytokines like IL-4 and low concentrations of interferon-γ (Butovsky et al., 2006).

1.4.2 Detrimental roles of microglia by chronic enhancement of inflammatory processes

Inflammation is an active defense mechanism against diverse insults, designed to remove the injurious stimuli and to inhibit or reverse their detrimental effects. Evidences that inflammatory processes play a role in AD came initially from epidemiological studies showing that people treated with non steroidal anti inflammatory drugs (NSAIDs) over a long period of time, have a reduced risk to develop AD (Andersen et al., 1995; Breitner et al., 1995). The induction of the inflammatory processes is ascribed to the accumulation of Aβ aggregates. These aggregates trigger cellular stress finally resulting in cell death. The binding of Aβ to RAGE on neurons results in oxidative stress and cytotoxicity (Yan et al., 1996). Moreover, the binding of Aβ to various microglial surface receptors, like RAGE, scavenger receptors as well as TLRs and their co-receptor CD14 can activate microglia (Liu et al., 2005). Such activated microglia secrete proinflammatory cytokines and produce reactive oxygen species (ROS) and nitric oxide (NO) (Mantovani et al., 2004; Cameron & Landreth 2010). These toxic substances can augment the oxidative stress and neuronal loss observed in AD brains (fig. 4).

The activation of the complement system by Aβ could further increase the inflammatory response of microglia and could directly attack neurons by forming membrane attack complexes (Rogers et al., 1992; Webster et al., 1997a; Webster et al., 1997b).

Massive cell death could then facilitate the inflammatory response of microglia through the reaction to DAMPs as explained in chapter 1.3 or by loss of microglia-neuron contacts needed for microglia suppression. Besides that it could be shown, that the release of proinflammatory cytokines can inhibit neurogenesis (Ekdahl et al., 2003; Monje et al., 2003).

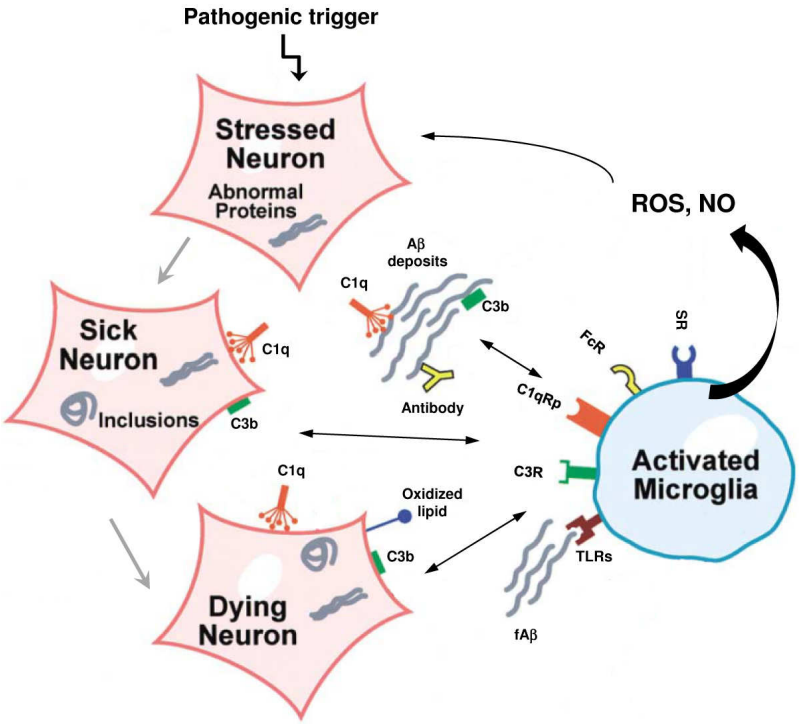

Figure 4: Scheme of some components of the inflammatory cascade.

A pathogenic trigger, like abnormal Aβ production and deposition elicit cellular stress and can result in dysfunction and degeneration of neurons. Complement factors bind either to Aβ and activate microglia or directly attack neurons. fAβ can directly bind to TLRs thereby activating microglia. Furthermore, activation could be initiated by binding of oxidized lipid via scavenger receptors. Activated microglia release ROS and NO which could stress neurons, starting the vicious circle again. C1qRp, C1q receptor for phagocytosis; CR3, complement receptor 3; FcR, Fc receptor; PSR, phosphatidyl serine receptor; SR, scavenger receptor. Modified from "Inflammation in Neurodegenerative Disease—A Double-Edged Sword" (Wyss-Coray & Mucke 2002).

1.5 Triggering receptors expressed on myeloid cells (TREMs)

The triggering receptors expressed on myeloid cells (TREMs) belong to the immunoglobulin superfamily cell surface receptors. They are glyco-proteins of 30-40 kDa, consisting of a single extracellular immunoglobulin-like domain, a single transmembrane region and a short cytoplasmic tail with no signal motifs (Bouchon et al., 2000). They are part of the huge group of type I transmembrane proteins. The transmembrane domain contains a charged lysine residue, important for the interaction with adapter proteins. In humans two forms of TREMs are expressed. In mice homologues of these receptors have been identified together with a third one (TREM3), which exists only as pseudogene in humans (Daws et al., 2001; Chung et al., 2002).

1.5.1 TREM1

TREM1 was the first receptor found of this family and was initially cloned by a cDNA screening from human natural killer cells (Bouchon et al., 2000). TREM1 is mainly expressed on blood neutrophils and monocytes/macrophages. Activation of the receptor by a yet unknown ligand and engagement with its adapter protein DNAX activating protein of 12 kDa (DAP12) triggers the generation of proinflammatory cytokines like interleukin-8 (IL-8), monocyte chemo attractant protein 1 (MCP1), MCP3 and macrophage inflammatory protein-1α (MIP1α) (Bouchon et al., 2000; Bleharski et al., 2003; Colonna & Facchetti 2003), but doesn't induce phagocytosis (Bleharski et al., 2003). Furthermore, TREM1 is highly expressed by neutrophils infiltrating tissues that are infected with bacteria or fungi as well as epithelial cells in these tissues (Bouchon et al., 2001a). According to this, the DAP12/TREM1 receptor system plays a crucial role in the amplification of inflammatory processes caused by infection.

1.5.2 TREM2

TREM2 was originally identified on monocyte-derived dendritic cells (DCs), where it promotes migration (Bouchon et al., 2001b). However, as TREM2 has not yet been detected on primary DCs, the involvement in DC biology remains unclear (Klesney-Tait et al., 2006). In contrast, it has clearly been showed that TREM2 is negatively regulating the response of macrophages to TLR activation. The concentrations of inflammatory cytokines like tumor necrosis factor (TNF) and IL-6 are exaggerated in macrophages of TREM2 deficient mice (Turnbull et al., 2006) as well as after knockdown of TREM2 by small interfering RNAs (siRNA) (Hamerman et al., 2006). Insight into two more functions of TREM2 was gained by studies of the rare genetic disorder, polycystic lipomembraneous osteodysplasia with sclerosing leukoencephalopathy (PLOSL or Nasu-Hakola disease). Patients exhibit multiple bone cysts and develop a progressive presenile dementia in the fourth decade of life. In the white matter of brains of autopsied patients sclerotic lesions including activated microglia were identified (Kitajima et al., 1989; Verloes et al., 1997; Tanaka 2000). Genetic analysis revealed that loss of function mutations in the TREM2 gene and in the gene for the adapter protein DAP12 are causative for this disease (Paloneva et al., 2000; Paloneva et al., 2002). It was shown that TREM2 and DAP12 are involved in the genesis of osteoclasts which are multinucleated cells of myeloid origin involved in bone resorption and homeostasis. Peripheral mononuclear blood cells from TREM2 or DAP12 deficient PLOSL patients failed to differentiate into osteoclasts (Paloneva et al., 2003). However, these findings from humans could not be reproduced in TREM2 deficient mice, so the function of TREM2 in

osteoclastogenesis remains unclear. The finding that TREM2 mutations can also cause early-onset dementia without bone cysts, suggests that TREM2 is active in the CNS (Chouery et al., 2008). Indeed TREM2 was found by *in situ* hybridization to be expressed in microglia, but the levels of expression and the percentages of expressing cells vary in different brain regions. The highest percentages were found in cortical regions (Schmid et al., 2002). The receptor is expressed at the cell surface but predominantly distributed into two pools: one in the Golgi complex and one population in exocytic vesicles, which are continuously shuttling to and from the cell surface (Sessa et al., 2004). Activation of TREM2 in microglia induces the expression of chemokine receptors and cell migration. Additionally, a decrease in phagocytosis of apoptotic neurons was observed after knockdown with siRNA (Takahashi et al., 2005; Takahashi et al., 2007). Interestingly, this knockdown resulted in an upregulation of inflammatory cytokines, suggesting an anti-inflammatory function (Takahashi et al., 2007). Since the ligand(s) for TREM2 are still unknown it was unclear how TREM2 recognizes apoptotic cells, till Hsieh *et al.* described a ligand expressed on apoptotic neurons (Hsieh et al., 2009). Another endogenous ligand was described as heat shock protein 60 (Hsp60) a mitochondrial chaperon which can be released from both healthy and dying cells (Stefano et al., 2009). Moreover, other potential binding partners have been reported, like polyanionic microbial products such as LPS or peptidoglycan (Daws et al., 2003). This was supported by the finding that TREM2 can bind several species of bacteria and fungi (Daws et al., 2003) and that TREM2 can serve as an phagocytic receptor for these microbes (N'Diaye et al., 2009). Nevertheless, specific molecules mediating the activation have not been identified. One possible explanation could be that TREM2 participates in a multimeric receptor complex, containing TREM2, a ligand, DAP12, plexin-A1 – a receptor known to control axon guidance – and the plexin-A1 ligand semaphorin 6D (Takegahara et al., 2006; Ford & McVicar 2009). However, in all scenarios DAP12 is indispensable for the function of TREM2.

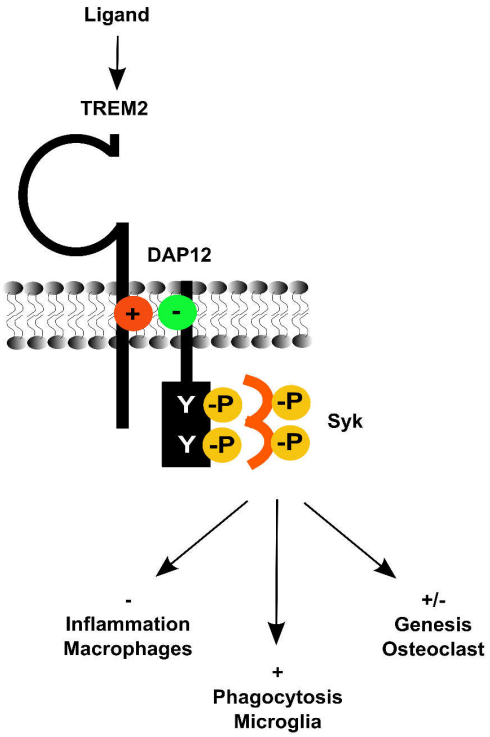

Figure 5: General understanding of the TREM2/DAP12 signaling pathway.

Ligand binding to TREM2 leads to engagement with the ITAM motif containing adapter protein DAP12 via the charged amino acid residues in the transmembrane domains of the two proteins. Phosphorylation of the two tyrosine residues in the ITAM domain, recruits the spleen tyrosine kinase (Syk), leading to activation of this kinase. The final downstream effects like negative regulation of inflammatory processes in macrophages, the activation of phagocytosis in microglia and the regulation of osteoclastogenesis are the result of a phosphorylation cascade of several proteins initiated by Syk. Modified from "The TREM receptor family and signal integration" (Klesney-Tait et al., 2006).

1.6 DAP12 – structure and signaling

DAP12 is a small signaling protein with a molecular mass of ~12 kDa, expressed in myeloid and NK cells. It is composed of a small extracellular part (~14 aa) that contains a cysteine residue to facilitate the formation of homodimers through disulfide bonds, followed by a transmembrane region and a cytosolic domain (Lanier et al., 1998), so DAP12 belongs like TREM2 to the type I transmembrane proteins. The transmembrane region contains a charged amino acid residue (aspartic acid) that allows electrostatic interaction with associated receptors like TREM2 (see fig. 5). The cytosolic domain embeds the conserved signaling element, the so-called immunoreceptor tyrosine-based activation motif (ITAM). The ITAM itself consists of a highly conserved sequence D/E XX **Y** XX L/I(X6-8) **Y** XX L/I (Reth 1989) which is essential for the signaling of

DAP12 containing receptor complexes. Besides DAP12 there are more adapter proteins known which signal via an ITAM domain. However, the general signaling pathway is similar for all of these proteins. The binding of a ligand leads to the clustering of the receptor e.g. TREM2 with DAP12. As a result, Src-family kinases become activated by dephosphorylation of their regulatory C-terminal tyrosine and subsequently phosphorylate DAP12 at the two tyrosines in the ITAM domain thereby recruiting the spleen tyrosine kinase (Syk) in myeloid cells or the Zeta-chain associated kinase of 70 kDa (Zap-70) in NK cells. Interaction of the kinase Src homology 2 (SH2) domains with the phosphorylated tyrosine residues induces the activation of the kinases. They in turn phosphorylate several downstream substrates forming signaling complexes that communicate to a number of pathways in the cell, like mitogen-activated protein kinase (MAPK) or phospholipase Cγ (PLCγ) leading to different cellular responses (fig. 5), for review see (Hamerman et al., 2009; Mocsai et al., 2010). The exact member of the Src-family kinases involved in the DAP12/TREM2 signaling in microglia is unknown. Mutations of either ITAM or the SH2 domains in the kinases completely block the signaling function, showing that both are absolutely necessary for the function of the associated immunoreceptors (Hamerman et al., 2009). It is known that DAP12 can mediate either activatory or inhibitory processes. The regulation of multinucleated giant cell formation (Helming et al., 2008), osteoclast fusion and the initiation of phagocytosis are three examples for an activatory signaling (see 1.5.2). The inhibitory signaling is generally observed when cells are stimulated simultaneously by a DAP12-associated receptor and a distinct receptor system, like TLRs. DAP12 deficient macrophages produce increased levels of inflammatory cytokines after stimulation of TLRs (Hamerman et al., 2005). As previously described for TREM2, DAP12 negatively regulates the transcription of genes coding for TNF, IL-1β and inducible nitric oxide-synthase (iNOS) (Takahashi et al., 2005). DAP12 signals not only in concert with immunoreceptors, also a signaling with integrins has been described. The interaction of DAP12 with the microglial CD11b integrin for example regulates neuronal apoptosis during development. Since the TREM2/DAP12 system regulates several functions in microglia, it is interesting to study this regulation in context to AD.

1.7 Rationale

Microglia have been shown to phagocytose Aβ in a FcR-mediated process upon passive immunization with anti-Aβ antibodies (Bard et al., 2000; Bacskai et al., 2002; Wilcock et al., 2003) as well as active immunization with $A\beta_{42}$ (Schenk et al., 1999). However, phagocytosis of Aβ without vaccination appears to be less efficient. The reason for this defect remains unclear. Since phagocytosis is a specific form of endocytosis and γ-secretase has been shown to regulate endocytosis (Tamboli et al., 2008), a contribution of γ-secretase in phagocytotic processes might be possible. There are some studies suggesting expression of γ-secretase components in microglia. However, a function of γ-secretase in these cells is still unknown.

Thus, the main goal of this project was to investigate the expression and function of γ-secretase in microglia. By pharmacological and genetic approaches it should also be tested whether γ-secretase is functionally involved in phagocytosis.

One potential candidate might be the microglial receptor TREM2. As type I transmembrane protein TREM2 might represent a γ-secretase substrate. Since TREM2 has been shown to be involved in phagocytotic processes of apoptotic neurons in the brain, processing of this receptor might alter phagocytosis of Aβ by microglia.

2 MATERIAL & METHODS

Except as noted otherwise, all chemicals used for the described experiments were purchased with a purity grade of "per analysi" from Sigma-Aldrich (Steinheim, Germany), Roche (Basel, Switzerland), Roth (Karlsruhe, Germany) or Applichem (Darmstadt, Germany). The specific cloning primers were obtained from Sigma-Aldrich, and the restriction enzymes from Fermentas (St. Leon-Rot, Germany). The radiochemicals were from Hartmann Analytic (Braunschweig, Germany). Cell culture media and additives were purchased from Invitrogen, cell culture plastics from Corning.

Table 1: Equipment

Cell culture equipment	
-80 °C Freezer	Thermo
Cell culture hood	Thermo
37 °C CO_2 incubator	Binder
Water bath	Medigen
Centrifuge (5804)	Eppendorf
Blotting- and cloning equipment	
Protein-electrophoresis chamber	Höfer
Blotting chamber	Höfer
Chemiluminescence Imager (ChemiDoc XRS) with software Quantity One	Bio-Rad
Cooling system (E100)	Lauda
DNA-electrophoresis chamber	Amersham
Trans-UV illuminator (GVM 20)	Syngene
General laboratory devices	
Microcentrifuge(5415D)	Eppendorf
refrigerated Microcentrifuge (5415R)	Eppendorf
refrigerated Centrifuge (5804R)	Eppendorf
Cycler (Mastercycler Personal)	Eppendorf
Gradientcycler (Mastercycler Gradient)	Eppendorf
37 °C incubator	Binder
Autoclave	H+P
Heeting Block (SBH 130 D)	Stuard Scientific
Magnetic stirrer	Velp Scientifica
pH Meter (MP 225)	Mettler Toledo

Photometer (Genesis)	Thermo
Sonifier (Sonopuls, UW 2070)	Bandelin
Thermomixer (Thermomixer compact)	Eppendorf
Overhead rotor	Scientific Industries
Vortex (MS 2 Minishaker)	IKA
Analytical Balance (Labstyle 204)	Mettler Toledo
Balance (PL 202-S)	Mettler Toledo
Microtiterplate Reader (Multiskan RC)	Thermo

Special devices	
Fluorescence microscope (AxioVert 200) with software AxioVision	Zeiss
Phosphoimager	Fuji

2.1 Cell biological techniques

2.1.1 Cell culture

Cell culture medium (DMEM +/+)
Dulbecco´s Modified Eagle´s Medium (DMEM) Glutamax™ containing 4.5 g/l D-glucose supplemented with 10 % heat inactivated fetal calf serum (FCS) and 1 % PenStrep solution (50 U/ml Penicillin, 50 µg/ml Streptomycin)
Phosphate Buffered Saline (PBS)
140 mM NaCl, 10 mM Na_2HPO_4, 1.75 mM KH_2PO_4, dH_2O, pH 7.4
Trypsin-EDTA Solution
0.05 % (w/v) trypsin (Invitrogen), 0.53 mM EDTA, dH_2O
Cryo medium
90 % FCS supplemented with 10 % dimethylsufoxide (DMSO)

Frozen cells were rapidly thawed in a water bath. Cells were washed once with cell culture medium (300 x g, 3 min) and plated on a new dish in fresh cell culture medium. Cells were maintained in a CO_2 incubator at 37 °C, 95 % humidity and 5 % CO_2. When cells reached confluence of 70-90 %, they were split. Cells were therefore washed once with PBS before they were detached from the surface by 1 ml of Trypsin-EDTA solution per 10 cm dish and plated onto a new culture dish in a ratio of 1:20-1:2. If an exact cell number was needed, cells were counted in a Neubauer counting-chamber. For cryo conservation cells of a 90 % confluent 6 cm dish were detached as described above, pelleted (300 x g, 3 min), resuspended in 1-2 ml cryo medium and finally stored in a -80 °C freezer or for long term storage in liquid nitrogen.

Table 2: Cell lines

Cell line	species/cell type	Media and Constituents
HEK 293	human embryonic kidney cell	DMEM Glutamax™ containing 4.5 g/l D-Glucose supplemented with 10 % heat inactivated fetal calf serum (FCS), 50 U/ml Penicillin, 50 µg/ml Streptomycin
HEK 293 PS1 WT	human embryonic kidney cell stably expressing hPS1 WT	like HEK 293 + 100 µg/ml Zeocin
HEK 293 PS1 DN	human embryonic kidney cell stably expressing hPS1 DN	like HEK 293 + 100 µg/ml Zeocin
HEK 293 PS1 L166P	human embryonic kidney cell stably expressing hPS1 L166P	like HEK 293 + 100 µg/ml Zeocin
HEK 293 PS1 M146L	human embryonic kidney cell stably expressing hPS1 M146L	like HEK 293 + 100 µg/ml Zeocin
HEK 293 PS1 ΔEx9	human embryonic kidney cell stably expressing hPS1 ΔEx9	like HEK 293 + 100 µg/ml Zeocin
HeLa	human cervical cancer cells	DMEM Glutamax™ containing 4.5 g/l D-Glucose supplemented with 10 % heat inactivated fetal calf serum (FCS), 50 U/ml Penicillin, 50 µg/ml Streptomycin
COS-7	monkey kidney cells	DMEM Glutamax™ containing 4.5 g/l D-Glucose supplemented with 10 % heat inactivated fetal calf serum (FCS), 50 U/ml Penicillin, 50 µg/ml Streptomycin
ESdM	mouse microglia-like cell line derived from embryonic stem cells	DMEM/F12 (1:1) supplemented with 1 % N2 Supplement, 50 U/ml Penicillin, 50 µg/ml Streptomycin, 0.153 % Glucose, 0.48 mM glutamine
BV-2	mouse microglia cell line	DMEM/F12 (1:1) supplemented with 1 % N2 Supplement, 50 U/ml Penicillin, 50 µg/ml Streptomycin, 0.153 % Glucose, 0.48 mM glutamine

2.1.2 Cell culture of ES cell derived microglia

Cell culture medium
DMEM/F12 (1:1) supplemented with 1 % N2 Supplement, 50 U/ml Penicillin, 50 µg/ml Streptomycin, 0.153 % Glucose, 0.48 mM glutamine
Cryo medium
90 % FCS supplemented with 10 % dimethylsufoxide (DMSO)

The cells (provided by Prof. Neumann, Institute of Reconstructive Neurobiology, Bonn) were thawed as described in 2.1.1 and plated on a 10 cm dish in fresh cell culture medium. Since these cells only proliferate to low densities, they were split at a confluence of 60-70 %. For splitting, cells were scraped off with a cell scraper and plated to a new dish in a 1:3-1:5 ratio. For cryo conservation cells of a 70 % confluent 10 cm dish were detached by scraping, pelleted (300 x g, 5 min), resuspended in 2-3 ml cryo medium and finally stored in liquid nitrogen.

2.1.3 Transient transfection

Opti-MEM ® I (Invitrogen)
DMEM +/-
Dulbecco´s Modified Eagle´s Medium (DMEM) Glutamax™ containing 4.5 g/l D-glucose supplemented with 10 % FCS

Cells were grown to 80 % confluence and transfected with Lipofectamin 2000 (Invitrogen) according to manufacturer´s instruction (for each 6 cm dish 5 µg DNA and 7.5 µl Lipofectamin 2000). During the transfection time of 5-6 h, cells were incubated in DMEM +/-. Medium was changed and cells were incubated for another 24 h at 37 °C, 5 % CO_2. To achieve good transfection results the concentration of the used DNA solution should be > 0.5 µg/ml.

2.1.4 Immunocytochemistry (ICC)

Phosphate Buffered Saline (PBS), sterile
140 mM NaCl, 10 mM Na_2HPO_4, 1.75 mM KH_2PO_4, dH_2O, pH 7.4
DMEM -/-
Dulbecco´s Modified Eagle´s Medium (DMEM) Glutamax™ containing 4.5 g/l D-glucose
Poly-L-lysine solution
100 µg/ml sterile poly-L-lysine in PBS
Distilled Water, sterile (dH_2O) (Invitrogen)
Paraformaldehyde solution (PFA; 4 %)
4 % (w/v) Paraformaldehyde in PBS
Triton X-100 solution (0.25 %)
0.25 % (v/v) Triton X-100 (Sigma-Aldrich) in PBS
Blocking solution
10 % (w/v) BSA in PBS (for neurons: 10 % BSA in PBS + 0.25 % Triton X-100) or DMEM
Primary antibody solution
Primary antibody in appropriate concentration (see Table 7) in PBS or DMEM supplemented with 5 % BSA (for neurons: additionally with 0.125 % Triton X-100)
Secondary antibody solution
Secondary antibody in appropriate concentration (see Table 8) in PBS or DMEM with 5 % BSA (for neurons: additionally with 0.125 % Triton X-100)

For immunocytochemistry cover slips (CS) were used which were coated with poly-L-lysine for 1 h at 37 °C, washed three times with sterile distilled water (dH_2O) and once with PBS. 150000 cells were seeded in one 6 well (containing 3 CS). After 24 h cells were transfected as described in 2.1.3. Cells were then washed three times with PBS and fixed in 4 % Paraformaldehyde (Birnboim & Doly 1979) for 10 min. To remove residual PFA cells were washed three times with PBS. Cells were then permeabilized by incubation in Triton X-100 for 10 min at room temperature (RT) and incubated in incubated in blocking solution for 1 h at RT. The protein of interest was then stained by incubation in 100 µl primary antibody solution for 1 h at RT, followed by intensive washing 3 x with PBS. The washing was repeated 3 times with 5 min incubation in between. After incubation with secondary antibody solution (100 µl) for 1 h at RT, the unbound secondary antibody was removed by intensive washing as described above. Finally CS were washed once with dH_2O and embedded on a slide with ImmuMount (Thermo). The slides were kept dark at 4 °C. Slides were analyzed with a fluorescence microscope.

To selectively detect cell surface proteins, cells were stained prior to fixation. For this purpose, cells were kept on ice for the whole staining procedure. As blocking solution 10 % BSA in DMEM -/- was used. The primary and the secondary antibody was diluted in DMEM -/- with 5 % BSA. All washing steps were conducted in DMEM -/-. After the last washing, the cells were fixed in 4 % PFA. For visualization of the total protein expression, standard immunostaining as described in 2.1.4 was used.

2.2 Molecularbiological techniques

2.2.1 Polymerase chain reaction (PCR)

PCR reaction mix	
10X Pfu Buffer with $MgSO_4$	5 µl
dNTP Mix, 10 mM each	1 µl (0.2 mM of each)
Forward primer	1.0 µM
Reverse primer	1.0 µM
Template DNA	10-100 ng
Pfu DNA Polymerase	2.5 U (1 µl)
add to 50 µl total volume with nuclease-free water	

The DNA constructs used in this project (see Table 3) were generated by PCR using the primers listed in Table 4. The PCR reaction mix was prepared on ice. For amplification the PCR program was run for 30 cycles after one initial DNA denaturating step (2 min, 95 °C). Every program included the following steps:

1. Denaturation: 95 °C, 0.5 min
2. Annealing: 50-80 °C (depends on primer), 0.5 min
3. Elongation: 72 °C, 0.5-2 min (depends on construct length)

The exact PCR programs are listed in Table 5.

The point mutations in DAP12 were generated by a three-step cloning strategy. At first two PCRs were conducted using the cloning primers in combination with the opposite mutation primers (step 1 & 2). The products of step 1 and 2 were then used as template which was amplified using the cloning primers.

To continue the cloning the amplified PCR products were analyzed according to their size in a 1-2 % agarose gel (see 2.2.2). The bands were cut out of the gel and the DNA was isolated as described in 2.2.3.

Table 3: List of the DNA constructs used for the project

Name	Vector	restriction enzymes	PCR program
Flag-TREM2-mycHis	pSecTag Hygro B	Hind III/Xho I	B2
Flag-DAP12-HA	pSecTag Hygro B	Hind III/Xho I	B2
myc-TREM2	pSecTag Hygro B	Sfi I/Hind III	MutHG
DAP12-HA	pSecTag Hygro B	Hind III/Xho I	GC
Flag-DAP12 D52A-HA	pSecTag Hygro B	Hind III/Xho I	B2 (all three steps)
Flag-DAP12 Y92F Y103F-HA	pSecTag Hygro B	Hind III/Xho I	Mut; B2; Mut
DAP12 Y92F Y103F-HA	pSecTag Hygro B	Hind III/Xho I	Mut; B2; Mut
myc-TREM2-GFP	pSecTag Hygro B	Sfi I/Hind III	MutHG
TREM2-GFP	pSecTag Hygro B	Sfi I/Hind III	MutHG
Flag-TREM2ΔECD-mycHis	pSecTag Hygro B	Hind III/Xho I	B2
TICD-mycHis	pSecTag Hygro B	Hind III/Xho I	B2

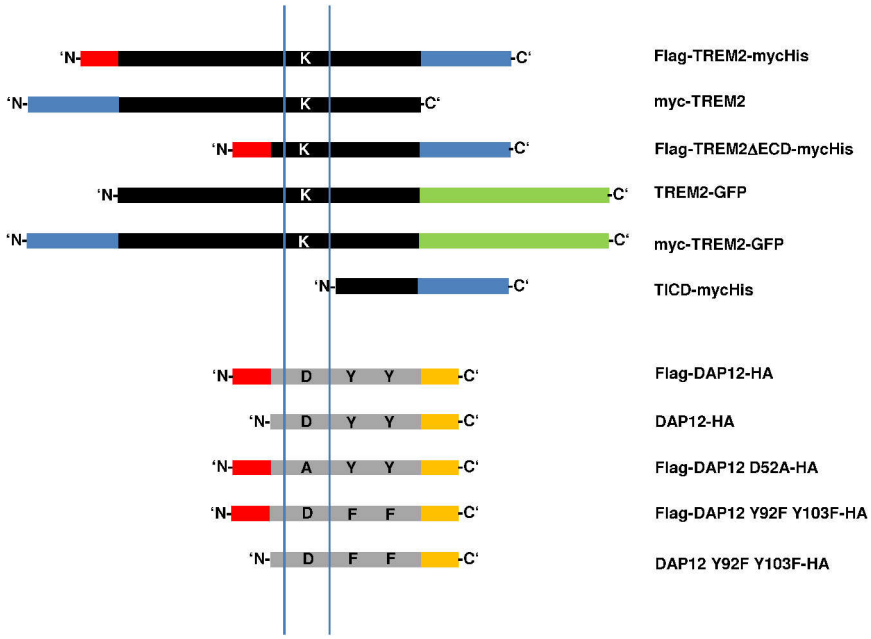

Figure 6: Schematic drawings of the different constructs used in this study.

Illustrated are the different TREM2, DAP12 and BACE constructs. The two thin blue lines indicate the membrane. N- and C-terminus as well as important amino acids are highlighted.

Table 4: Overview of cloning primers

Name	Primer	
Flag-TREM2-mycHis	FW:	gcgaagcttgattacaaagacgatgacgataagaacaccacggtgctg
	RV:	gcgctcgagtcgtacctccgggtccagtg
Flag-DAP12-HA	FW:	gcgaagcttgattacaaagacgatgacgataagttaagtcccgtacaggcc
	RV:	gcgctcgagctaaagagcgtaatctggaacatcgtatgggtatctgtaatattgcctctgtg
myc-TREM2	FW:	ggcccagccggccatggcatcaatgcagaagctgatctcagaggaggacctgaacaccacggtgctg
	RV:	gcgaagcttttcacgtacctccgggtccagtg
DAP12-HA	FW:	gcgaagcttatgggggctctggag
	RV:	gcgctcgagctaaagagcgtaatctggaacatcgtatgggtatctgtaatattgcctctgtg
Flag-DAP12 D52A-HA	FW:	gcgaagcttgattacaaagacgatgacgataagttaagtcccgtacaggcc
	Mut. Pr. FW:	ctgggtgctttggtgttgactctgctgattgcc
	Mut. Pr. RV:	caccaaagcacccagaacaatcccagccag
	RV:	gcgctcgagctaaagagcgtaatctggaacatcgtatgggtatctgtaatattgcctctgtg
Flag-DAP12 Y92F Y103F-HA	FW:	gcgaagcttgattacaaagacgatgacgataagttaagtcccgtacaggcc
	Mut. Pr. FW:	tcgccttttcaggagcttcagggtcagagaccagaagtattcagtgac
	Mut. Pr. RV:	gaggtcactgaatacttctggtctctgaccctgaagctcctgaaaaggcga
	RV:	gcgctcgagctaaagagcgtaatctggaacatcgtatgggtatctgtaatattgcctctgtg
myc-TREM2-GFP	FW:	ggcccagccggccatggcatcaatgcagaagctgatctcagaggaggacctgaacaccacggtgctg
	RV:	gcgaagcttcgtacctccgggtccagtg
Flag-TREM2 CTF-mycHis	FW:	gcgaagcttgattacaaagacgatgacgataagagcacctccaggaatcaagagacc
	RV:	gcgctcgagtcgtacctccgggtccagtg
B1 TMCT GFP	FW:	cccggatccgatgagtcaaccctcatgaccata
	RV:	cccctcgagtcacttcagcagggagatgtca
B2 TMCT mCherry	FW:	cccggatccagcaactgtgtccccgct
	RV:	cccctcgagtcatttccagcgatgtctgaccagaga
B2 TMCT V513L mCherry	FW:	cccggatccagcaactgtgtccccgct
	RV:	cccctcgagtcatttccagcgatgtctgagcagaga
B2 TMCT V513L E509D mCherry	FW:	cccggatccagcaactgtgtccccgct
	RV:	cccctcgagtcatttccagcgatgtctgagcagagaggagtcatcatt
TICD-mycHis	FW:	gcgaagcttgtggccaggggcaggcag
	RV:	gcgctcgagtcgtacctccgggtccagtg

Table 5: Detailed PCR programs

B2		GC		Mut		MutHG	
						95 °C – 1 s pause	
95 °C – 3 min		95 °C – 3 min		95 °C – 3 min		95 °C – 3 min	
95 °C – 1 min 50 °C – 1 min 72 °C – 2 min	10 x	95 °C – 0.5 min 50 °C – 0.5 min 72 °C – 1.5 min	25 x	95 °C – 1 min 50 °C – 1 min 72 °C – 3 min	30 x	95 °C – 1 min 50 °C – 1 min 72 °C – 3 min	10 x
95 °C – 1 min 60 °C – 1 min 72 °C – 2 min	20 x	72 °C – 4 min		72 °C – 5 min		95 °C – 1 min 70 °C – 1 min 72 °C – 3 min	20 x
72 °C – 7 min		72 °C – 7 min				72 °C – 5 min	

2.2.2 Separation and visualization of DNA fragments

TBE Buffer
9 mM Tris-Borat, 2 mM EDTA, dH_2O, pH 8.0
6 x orange loading dye
60 % Glycerin, 0.15 % Orange G, 60 mM EDTA, 10 mM Tris, dH_2O, pH 7.6
GelRed (Biotium Inc.)
10000 x in water

Agarose gels allow the separation of DNA by their fragment length in an electric field. To separate 100-10000 bp gels of 1-2 % were used. For visualization of the DNA the agarose gels were supplemented with 2 µl GelRed/100 ml gel. The DNA samples were mixed with 6 x orange loading dye before they were loaded in the gel. The gel was then run in TBE buffer at 110 V.

2.2.3 Isolation of DNA fragments from agarose gels

Wizard® SV Gel and PCR Clean up system (Promega)
dH_2O

The desired bands were cut out of the gel on an UV illuminator. The DNA was isolated using the *Wizard® SV Gel and PCR Clean up system* (Promega) according to the manufacturers' instructions. After elution in nuclease free dH_2O, the DNA was used directly for further cloning steps.

2.2.4 Restriction digestion

Restriction enzymes (see Table 3, Fermentas)
dH_2O

Restriction digestion of DNA was conducted in the buffer recommended for each enzyme. For double digestion the ideal buffer for both enzymes was chosen by the *Double Digest* tool available on the Fermentas web site. For preparative purposes 2-5 µg DNA were digested with 5-10 U of the appropriate enzyme in 20 µl at 37 °C for 4-16 h.

2.2.5 Dephosphorylation of linearized DNA

Shrimp alkaline phosphatase (SAP, 1 U/µl, Fermentas)
dH_2O

To prevent self re-ligation of the linearized plasmid DNA, the free 5'-phosphate group was removed by adding 2 U shrimp alkaline phosphatase for the last hour directly to the restriction digestion.

2.2.6 Ligation

T4 DNA-ligase (5 U/µl, Fermentas)
dH_2O

The insertion of passenger DNA into the dephosphorylated linearized vector via the DNA-ligase of the bacteriophage T4 was carried out in a molar ratio of 1:3 (vector:insert). At least 100 ng insert were incubated together with the reaction buffer and 5 U T4 ligase for 16 h at RT. 1/3 of the ligation mixture was then used for the transformation in competent *E. coli* cells (see 2.2.8).

2.2.7 Generation of chemo competent E. coli Top10

TFB I
100 mM RbCl, 50 mM $MnCl_2$, 30 mM potassium acetate, 10 mM $CaCl_2$, 15 % Glycerol, pH 5.8
TFB II
10 mM MOPS, 10 mM RbCl, 75 mM $CaCl_2$, 15 % Glycerol, pH 6.8
Low salt Lauria-Bertani (LB) medium
1 % (w/v) tryptone, 0.5 % (w/v) yeast extract, 0.5 % (w/v) NaCl, dH_2O, pH 7.0 (autoclaved)

At first, 200 ml LB medium in a 1 l flask were inoculated with 2 ml of an overnight culture. The culture was incubated for 2 h under rotation (250 rpm) at 37 °C. Cells were pelleted by centrifugation (1500 x g, 10 min, 4 °C). After resuspending the pellet in 30 ml ice cold TFB I by pipetting, a centrifugation step followed to pellet the cells again. This pellet was then resuspended in 4 ml ice cold TFB II. Finally, the solution was divided into 50 µl aliquots and freezed at -80 °C for long term storage.

2.2.8 Transformation of E. coli Top10

SOC medium
0.5 % (w/v) yeast extract, 2 % (w/v) tryptone, 10 mM NaCl, 2.5 mM KCl, 20 mM $MgSO_4$, 20 mM glucose
LB agar plates
1 % (w/v) tryptone, 0.5% (w/v) yeast extract, 0.5% (w/v) NaCl, 15 g/l agar, dH_2O, pH 7.0 (autoclaved); before pouring the plates the antibiotics were added to the warm (~ 40-50 °C) solution.
Selection antibiotics
Kanamycin: 30 µg/ml (Stock: 30 mg/ml, dH_2O); Ampicillin: 100 µg/ml (Stock: 100 mg/ml, dH_2O)

For transformation of the chemo competent bacteria with plasmid DNA, the thawed cells were mixed with 1/3 of the ligation mixture, or in case of re-transformation with 0.5 µg plasmid DNA and incubated for 30 min on ice. After a heat shock of exact 30 s at 42 °C the cells were placed back on ice. 250 µl of pre-warmed SOC medium were added to each vial and the cells were incubated for 1 h at 37 °C at 500 rpm in a shaking incubator. To spread the transformed cells onto a LB agar plate, the cells were pelleted at 300 x g for 3 min, the supernatant was removed except 50 µl. The pellet was resuspended in these 50 µl and the solution was plated on an agar plate supplemented with the appropriate antibiotic.

2.2.9 Cryo conservation of transformed E. coli

Conservation medium
70 % (v/v) Glycerol, dH_2O (autoclaved)
Low salt Lauria-Bertani (LB) medium
1 % (w/v) tryptone, 0.5 % (w/v) yeast extract, 0.5 % (w/v) NaCl, dH_2O, pH 7.0 (autoclaved)

0.8 ml of a fresh bacteria culture was transferred into a screw cap tube, 0.5 ml conservation medium was added, gently mixed and freezed at -80 °C. For re-utilization of the transformed bacteria a bit of the frozen medium was scratched with a sterile pipette tip and transferred into a test tube filled with 3 ml LB medium. For an overnight culture the test tube was then incubated overnight (~16 h) in a shaking incubator at 37 °C and 250 rpm.

2.2.10 Extraction of plasmid DNA from E. coli

Resuspension buffer
50 mM Tris, 10 mM EDTA, 100 µg/ml RNase A, pH 8.0
Lysis buffer
200 mM NaOH, 1 % (w/v) SDS
Neutralization buffer
3 M Potassium acetate, pH 5.5
PureYield Plasmid Midiprep System (Promega)
GeneJET™ Plasmid Miniprep Kit (Fermentas)

For the extraction of DNA out of *E. coli* cells an alkaline procedure was used as described by Birnboim & Doly (Birnboim & Doly 1979). Briefly, 1 ml of the overnight culture was centrifuged (1 min, 12000 x g) and the pellet resuspended in 100 µl resuspension buffer. 100 µl lysis buffer were added. After mixing by inverting and an incubation of 3 min, 175 µl neutralization buffer were added to precipitate proteins and associated genomic DNA. Solution was cleared by centrifugation (10 min, 12000 x g) and the DNA precipitated as described in 2.2.11. The obtained DNA solution was used for restriction digestion (see 2.2.4).

For preparative extraction the *PureYield Plasmid Midiprep System* (Promega) or for small amounts the *GeneJET™ Plasmid Miniprep Kit* (Fermentas) was used. Both kits were used as described in the manufacturers' manual. The DNA was general eluted in nuclease-free dH_2O. In case that the concentration of the gained DNA solution was too low for effective transfection (2.1.3), the DNA was concentrated by ethanol precipitation (2.2.12).

2.2.11 Precipitation of DNA by isopropanol

Isopropanol
70 % Ethanol
RNase-H_2O
Sodium acetate
3 M Sodium acetate, dH_2O, pH 5.2
RNase water
RNase 10 µg/ml, dH_2O

To isolate the pure DNA from the crude solution obtained from the alkaline extraction (2.2.10) the cleared supernatant was supplemented with 420 µl isopropanol and 35 µl sodium acetate. After a spin of 10 min at 12000 x g, the supernatant was discarded and the pellet washed with 600 µl 70 % ethanol (EtOH). After a further spin (10 min, 12000 x g) the pellet was air dried. Finally, the dried DNA pellet was resuspended in 50 µl RNase-H_2O.

2.2.12 Precipitation of DNA by ethanol

absolute Ethanol
Sodium acetate
3 M Sodium acetate, dH_2O, pH 5.2
70 % Ethanol
Nuclease-free dH_2O

To concentrate diluted DNA solutions, the DNA solution was mixed by vortexing with 1/10 volume with sodium acetate and 3 volumes of absolute ethanol and aliquoted to 2 ml tubes. After incubation for 15 min at -20 °C and a 30 min spin (12000 x g, 4 °C), the pellets were washed with 70 % EtOH and again centrifuged (5 min, 12000 x g, 4 °C). In the end the pellets were resuspended in the required amount of nuclease-free water to gain an applicable concentration for transient transfection (2.1.3).

2.2.13 DNA sequencing

BigDye Terminator v1.1 Cycle Sequencing Kit (Applied Biosystems)

The cDNA-constructs were sequenced using the *BigDye Terminator v1.1 Cycle Sequencing Kit* (Applied Biosystems) as described in the manufacturers' guidelines.

2.2.14 Photometric determination of DNA concentration

The DNA was diluted 1:20 in dH_2O and measured at 260 nm in a quartz cuvette (A_{260}). The blank value was determined using dH_2O as well. The concentration was then calculated using the following equation:

$$c[\mu g/ml] = A_{260} \cdot dilution\ factor\ (DF) \cdot multiplikation\ factor\ (F)$$

(F=50, V=20)

2.3 Proteinbiochemical techniques

2.3.1 Extraction of membrane proteins out of eukaryotic cells

Phosphate Buffered Saline (PBS)
140 mM NaCl, 10 mM Na_2HPO_4, 1.75 mM KH_2PO_4, dH_2O, pH 7.4
Hypoton buffer:
10 mM Tris, 1 mM EDTA, 1 mM EGTA, dH_2O, pH 7.6
STEN-lysis buffer:
50 mM Tris, 150 mM NaCl, 2 mM EDTA, 1 % (v/v) NP40 (Sigma-Aldrich), 1 % (v/v) Triton X-100 (Sigma-Aldrich), dH_2O, pH 7.4
25 x Protease inhibitor (PI) cocktail
(Complete, Roche), dH_2O

Cells were washed once with PBS, scraped and pelleted in 1 ml PBS. The cells were incubated in 0.8 ml hypoton buffer for 15 min on ice and lysed by drawing 20 x through a 0.6 mm needle. To clear the homogenate from nuclei and mitochondria it was spun for 10 min at 300 x g and 4 °C. The separation of the cytosol fraction and the membrane vesicles was accomplished by a second centrifugation step (60 min, 12000 x g, 4 °C). Before the protein concentration was measured by the BCA assay, as described in 2.3.3, the membrane pellet was lysed in 50 µl STEN lysis buffer, incubated for another 15 min on ice and sedimented by a 15 min spin at 12000 x g and 4 °C. Protein extracts were either stored at -20 °C or directly used for SDS electrophoresis (see 2.3.6).

2.3.2 Protein extraction out of eukaryotic cells

PBS
140 mM NaCl, 10 mM Na_2HPO_4, 1.75 mM KH_2PO_4, dH_2O, pH 7.4
RIPA lysis buffer
50 mM Tris, 150 mM NaCl, 0.5 % (w/v) Sodium deoxycholic acid, 0.1 % (w/v) SDS, 1 % (v/v) NP-40, pH 7.4
STEN lysis buffer
50 mM Tris, 150 mM NaCl, 2 mM EDTA, 1 % (v/v) NP40 (Sigma-Aldrich), 1 % (v/v) Triton X-100 (Sigma-Aldrich), dH_2O, pH 7.4

Cells were washed once with PBS and lysed in 0.8 ml RIPA or STEN lysis buffer for 15 min on ice. The homogenates were cleared from the insoluble material by centrifugation for 15 min at 12000 x g and 4 °C. For further use protein extracts were stored at -20 °C or loaded on gels for SDS electrophoresis (see 2.3.6).

2.3.3 Protein estimation

BCA protein assay kit (Thermo Scientific)
Bradford reagent (Bio-Rad)

Two different methods for protein estimation were used depending on the detergents exerted for protein extraction.

I) BCA method, first described by Smith and co-workers (Smith et al., 1985)

This method is divided into two reactions. In a first reaction, the so-called Biuret reaction are Cu^{2+} ions reduced by negatively charged hydroxyl groups to Cu^{+}. These copper ions complex then two bicinchoninic acid molecules, resulting in a violet complex which can be photometrically measured.

For the estimation the *BCA protein assay kit* (Thermo Scientific) was used. The protein extracts were diluted 1:10-1:20 with water and mixed with the kit reagents according to the manual. After incubation for 30 min the absorption at 562 nm was measured. The protein concentration was finally calculated by means of a standard curve.

II) Bradford method, first described by (Bradford 1976)

In this method basic and aromatic protein side chains react with Coomassie G-250, which is part of the Bradford reagent (Bio-Rad), shifting its absorption maximum to 595 nm.

For estimation protein extracts in different dilutions were mixed 1:5 with Bradford reagent, incubated for 5 min at RT and subsequently the absorption measured at 595 nm. The protein concentration was finally calculated by means of a standard curve.

2.3.4 Immunoprecipitation (IP)

STEN buffer
50 mM Tris, 150 mM NaCl, 2 mM EDTA, 0.2 % (v/v) NP40 (Sigma-Aldrich), pH 7.6
STEN-NaCl
50 mM Tris, 500 mM NaCl, 2 mM EDTA, 0.2 % (v/v) NP40 (Sigma-Aldrich), dH_2O, pH 7.6
PBS
140 mM NaCl, 10 mM Na_2HPO_4, 1.75 mM KH_2PO_4, dH_2O, pH 7.4
Loading dye (5 x)
50 % (v/v) Glycerin, 7.5 % (w/v) SDS, 0.1 M DTT, 0.025 mg/ml Bromphenol blue in stacking gel buffer
Protein A sepharose (Zymed)
Protein G sepharose (Invitrogen)

Specific proteins can be isolated by specific antibodies coupled to protein A (against rabbit IgG) or protein G sepharose (against mouse IgG) from cell lysates (see 2.3.2). To prevent unspecific binding of proteins the lysates were pre-cleared with 30 µl uncoupled protein A sepharose beads for 1 h at 4 °C on a rotatory shaker. The sepharose was sedimented (2 min, 9300 x g, 4 °C) and the supernatant incubated with fresh sepharose beads and generally 1-3 µg of the specific antibody for 2-16 h at 4 °C under constant rotation. Afterwards the beads were sedimented (2 min,

9300 x g, 4 °C) and the supernatant discarded. The beads were then washed once with STEN-NaCl and three times with STEN buffer. Therefore the beads were incubated for 5 min on a rotatory shaker at 4 °C before they were pelleted (2 min, 9300 x g, 4 °C). Finally the beads were sucked dry by the use of a syringe and 0.4 mm needle, taken up in 20 µl of 2 x loading dye and boiled 5 min at 95 °C. The samples were then used for SDS electrophoresis (see 2.3.6).

2.3.5 Co-immunoprecipitation of DAP12 and TREM2

Brij97 lysis buffer
0.875 % Brij 97, 0.125 % Igepal, 10 mM Tris, 150 mM NaCl
Protein G sepharose (Invitrogen)

Co-immunoprecipitation (co-IP) is a technique to detect protein-protein interactions. For co-IP of DAP12 and TREM2, the Brij97 lysis buffer described by Voehringer and colleagues (Voehringer et al., 2004) was used. Cells were lysed, according to 2.3.2 in 800 µl Brij97 lysis buffer. 20 µl of the cell lysate was taken and the rest pre-cleared as described in 2.3.4. During the pre-clearing the protein concentration was estimated by BCA according to 2.3.3. For IP, which was accomplished for 16 h, as described in 2.3.4, 1 mg protein per sample was used in equal volumes. After the IP the procedure was continued as described in 2.3.4 with the exception that the washing steps were performed with Brij97 lysis buffer.

2.3.6 Sodium dodecyl sulfate polyacrylamide gel electrophoresis (SDS-PAGE)

Stacking gel buffer (4 x) (Upper-Tris)
500 mM Tris, 0.4 % (w/v) SDS, dH_2O, pH 6.8
Separation gel buffer (4 x)
1.5 M Tris, 0.4 % (w/v) SDS, dH_2O, pH 8.8
SDS loading dye (5 x)
50 % (v/v) Glycerin, 7.5 % (w/v) SDS, 0.1 M DTT, 0.025 mg/ml Bromphenol blue in stacking gel buffer
Ammonium persulfate (APS, Sigma)
10 % (w/v) Ammonium persulfate, dH2O
N,N,N´,N´-Tetramethylethylenediamine (TEMED, Roth)
Running buffer
25 mM Tris, 200 mM Glycine, 0.1 % (w/v) SDS, dH_2O
Acrylamide/Bisacrylamide solution
30 % (v/v) Acrylamide/Bisacrylamide in the ratio of 37.5:1
PageRuler™ protein ladder (Fermentas)
PageRuler™ prestained protein ladder (Fermentas)
SeeBlue® prestained standard (Invitrogen)
SeeBlue® Plus prestained standard (Invitrogen)

The separation of proteins on the basis of their molecular weight was carried out in 1.5 mm thick gels which were casted under the conditions listed in Table 6.

Table 6: Composition of the SDS-PAGE gels

	Separation gel			Stacking gel
	12 %	**10 %**	**7 %**	**4 %**
dH_2O	7 ml	8.3 ml	10.3 ml	6.2 ml
Acrylamide/Bisacrylamide	8 ml	6.7 ml	4.7 ml	1.3 ml
Lower-Tris	5 ml	5 ml	5 ml	-
Upper-Tris	-	-	-	2.5 ml
APS	50 µl	50 µl	50 µl	25 µl
TEMED	50 µl	50 µl	50 µl	25 µl
∑	20 ml	20 ml	20 ml	10 ml

For the discontinuous electrophoresis a stacking gel is poured atop of a separation gel. First the separation gel, whose percentage was chosen according to needed molecular weight range, was prepared and polymerized in a gel caster with a thin 70 % EtOH film on top. After full polymerization EtOH was carefully removed and the stacking gel casted on top of the separation gel. For pocket formation a comb sealed the stacking gel. 5 x SDS sample buffer was added to the samples prior to 5 min of boiling at 95 °C. Approximately 20-30 µg protein was loaded per lane with the help of a Hamilton syringe. The electrophoresis was performed at 30 mA per gel and a maximum voltage of 180 V. As molecular weight standard, PageRuler™ (Fermentas) or PageRuler™ prestained were loaded along with the samples.

Alternatively, precasted 4-12 % Bis-Tris polyacrylamide gels were used (Variogel®, Anamed or NuPAGE® gels, Invitrogen). Here, samples were prepared and buffers were used according to the manufacturer's instructions. For NuPAGE® gels SeeBlue® or SeeBlue® Plus were loaded as protein standard.

2.3.7 Western immunoblotting (WB)

Blotting buffer
5 mM Tris, 200 mM Glycine, 10 % (v/v) methanol, dH_2O
Ponceau solution
3 % (w/v) Ponceau S, 3 % (w/v) trichloroacetic acid, dH_2O
TBS/T
10 mM Tris, 150 mM NaCl, 0.1 % (v/v) Tween20, dH_2O, pH 7.5
PBS/T
PBS, 0.05 % (v/v) Tween20, pH 7.4
TBS/T blocking solution
TBS/T, 4 % (w/v) BSA (Roth)
PBS/T blocking solution
PBS/T, 4 % (w/v) skimmed milk powder (Roth)
Antibody solutions
TBS-T/PBS-T, specific antibody (for dilution see Table 7)
ECL (1:1 mix of W1 and W2)
W1: 0.1 M Tris pH 8.5, 0.4 mM cumaric acid, 0.25 mM luminol, dH_2O
W2: 0.1 M Tris pH 8.5, 0.018 % H_2O_2, dH_2O
ECL™ advanced Western Blotting Detection Reagent (GE Healthcare)

The proteins which were separated by their size in the SDS gel were transferred to nitrocellulose membranes by WB to allow immuno detection. Before blotting, membranes were equilibrated in blotting buffer. The proteins were transferred to the membrane in a blotting chamber at a constant current of 400 mA with a maximum voltage of 120 V for 2 h at 4 °C.

After a completed transfer the efficiency was controlled by Ponceau staining. The membrane was incubated in Ponceau solution for 2 min and washed several times with dH_2O till the bands become visible. To prevent unspecific antibody binding the membrane was incubated for 1.5 h in 4 % skimmed milk in PBS/T. The blocked membranes were incubated in primary antibody solution (for dilution see Table 7) overnight at 4 °C or for 2 h at RT. In order to remove excess of primary antibody the blot was washed four times with PBS/T for 5 min. Afterwards the blot was incubated in secondary antibody solution (for dilution see Table 8) for 1 h at RT followed by again washing four times with PBS/T. The secondary antibody is conjugated to HRP, which allows a detection by ECL reagent. The enzyme catalyzes a reaction that leads to chemiluminescence. The emitted light was recorded by an ECL Imager (Bio-Rad). Weaker signals were analyzed with the help of ECL™ advanced western Blotting Detection Reagent (GE Healthcare). The quantification of specific signals was conducted by the software *Quantity One*®.

Table 7: Primary antibodies that were used for western immunoblotting (WB), immunocytochemistry (ICC), surface stainings (SurfS), immunoprecipitation (IP) and co-immunoprecipitation (CoIP)

Antibody	Target protein	WB	ICC	SurfS	IP	CoIP	Species	Company
α-DAP12	DAP12	1:250	1:50				goat	Santa Cruz Biotech.
α-GFP	GFP	1:10000			2 µg		mouse	Roche
α-HA	HA-tag	1:500	1:400	1:200		4 µg	mouse	Sigma
α-msGGA1	GGA1	1:500					rabbit	Abcam
α-TREM2	TREM2	1:250	1:50				rat	R&D System
β-actin	Actin	1:2000					mouse	Sigma
140	APP	1:500					rabbit	Lab AG Walter
2972	GST	1:500					rabbit	Lab AG Walter
5313	APP	1:1000					rabbit	(Walter et al., 2000)
7520	BACE 1	1:1000	1:300				rabbit	(Capell et al., 2000)
7523	BACE 1	1:1000					rabbit	(Capell et al., 2000)
AP-1	AP-1		1:300				mouse	Sigma
c-myc0	c-myc	1:1000	1:1000	1:500	3 µg	4 µg	mouse	(Wahle et al., 2005)
Calnexin H-70	Calnexin	1:1000					mouse	Santa Cruz Biotech.
EEA1	EEA1	1:2500	1:300				mouse	BD Biosciences
Flag M2	Flag-tag	1:500	1:400	1:200	3 µg	3 µg	mouse	Sigma
Flotillin	Flotillin	1:250					mouse	BD Biosciences
Giantin	Giantin		1:2500				mouse	
TGN46	TGN46	1:250					rabbit	Sigma

Table 8: Secondary antibodies that were used for western immunoblotting (WB), immunocytochemistry (ICC) and surface stainings (SurfS)

Antibody	Target protein	WB	ICC	SurfS	-conjugated	Company
α-gt-HRP	goat IgG	1:1000			HRP	Sigma
α-ms-HRP	mouse IgG	1:50000			HRP	Sigma
α-rat-HRP	rat IgG	1:50000			HRP	Sigma
α-rb-HRP	rabbit IgG	1:50000			HRP	Sigma
ms-Alexa 350	mouse IgG		1:250	1:100	Alexa 350	Invitrogen
ms-Alexa 488	mouse IgG		1:750	1:400	Alexa 488	Invitrogen
ms-Alexa 594	mouse IgG		1:750	1:400	Alexa 594	Invitrogen
rb-α-ms	mouse IgG		1:500			Sigma
rb-Alexa 350	rabbit IgG		1:250	1:100	Alexa 350	Invitrogen
rb-Alexa 488	rabbit IgG		1:750	1:400	Alexa 488	Invitrogen
rb-Alexa 594	rabbit IgG		1:750	1:400	Alexa 594	Invitrogen

2.3.8 Coomassie staining of proteins in polyacrylamide gels

Coomassie staining solution
50 % (v/v) Isopropanol, 10 % (v/v) acetic acid, 0.5 % (w/v) Coomassie brilliant-blue R, dH_2O
Destaining solution
20 % (v/v) Isopropanol, 10 % (v/v) acetic acid, dH_2O

Alternatively to WB the polyacrylamide gels were directly stained with Coomassie. Therefore the gels were incubated in Coomassie staining solution for 30 min at RT. To remove excess of bound Coomassie the gels were incubated for another 2-4 h in destaining solution.

2.3.9 Precipitation of soluble proteins from cell culture supernatants by trichloroacetic acid (TCA)

DOC solution
2 % (w/v) Sodium deoxycholic acid
Trichloroacetic acid (TCA)
100 % (v/v) TCA, dH_2O
Acetone
Tris/SDS Buffer
50 mM Tris, 1 % SDS, dH_2O
SDS loading dye (5 x)
50 % (v/v) Glycerin, 7.5 % (w/v) SDS, 0.1 M DTT, 0.025 mg/ml bromphenol blue in stacking gel buffer

1.5 ml supernatant was collected from cultured cells, cleared from cell debris by centrifugation (10 min, 300 x g) and 1.3 ml transferred into a new tube. DOC solution was added to a final concentration of 0.02 %, mixed vigorously and incubated for 15 min at RT. TCA was added to an end concentration of 10 %. After an incubation of 1 h at RT a spin of 10 min at 12000 x g and 4 °C followed. The supernatant was discarded and the pellet washed twice with ice cold acetone.

Therefore, 200 µl of acetone was added to the pellet, incubated for 15 min on ice and spun 10 min at 12000 x g and 4 °C. The washed pellet was air-dried, resuspended in 35 µl Tris/SDS buffer and incubated for 10 min at 50 °C. Finally, 10 µl 5 x loading dye were added.

2.3.10 Expression and isolation of glutathione S-transferase (GST) fusion proteins

IPTG solution (1000 x)
100 mM IPTG, dH_2O
Lysozyme solution (stock)
100 mg/ml, dH_2O
Elution buffer
50 mM Tris, 10 mM glutathione (reduced), dH_2O, pH 8.0
Equilibration buffer
50 mM Tris, dH_2O, pH 8.0
GSH-sepharose (Amersham)
Triton solution
25 % Triton X-100, dH_2O

400 ml LB medium were inoculated with 10 ml of an overnight culture and incubated at 250 rpm and 37 °C to an OD_{600} of 0.6-0.8. The expression of the fusion protein was induced by adding IPTG to a final concentration of 0.1 mM. To reach a good amount of fusion protein the culture was incubated for another 5 h under the conditions mentioned above. The cells were pelleted (30 min, 3500 x g, 4 °C) and frozen at -20 °C. Later the pellet was resuspended in 20 ml PBS containing 5 mg/ml lysozyme and incubated for 30 min on ice. The cell suspension was then 10 times sonicated for 30 s with an idle period of 20 s each plus one final sonification step for 1.5 min. 400 µl Triton solution was added and the mixture incubated 45 min under constant agitation. The solution was then cleared from the insoluble fragments by centrifugation (30 min, 3500 x g, 4 °C). In the next step the supernatant was diluted 1:5 with PBS, mixed with 2 ml GSH-sepharose and incubated at 4 °C on an overhead shaker for 2 h. The GSH-beads were pelleted (5 min, 2000 x g, 4 °C) and washed in the same way five times with PBS. After the last washing step, beads were taken up in 10 ml PBS and carefully packed to a poly-prep chromatography column (Amersham). In the column the beads were washed two times with equilibration buffer. Finally the fusion proteins were eluted from the beads by adding 10 ml elution buffer, thereby the eluate was collected in 0.5 ml fractions. Using the Bradford method (see 2.3.3) the protein concentration of each fraction was measured and the purity controlled by Coomassie staining (2.3.8) of an polyacrylamide gel.

2.3.11 Biotinylation of cell surface proteins

Poly-L-lysine solution
100 µg/ml sterile poly-L-lysine in PBS
PBS
140 mM NaCl, 10 mM Na_2HPO_4, 1.75 mM KH_2PO_4, dH_2O, pH 7.4
Biotin solution
0.5 mg/ml sulfo-NHS-biotin (Pierce) in PBS
Glycine solution
20 mM glycine in PBS
SDS loading dye (5 x)
50 % (v/v) Glycerin, 7.5 % (w/v) SDS, 0.1 M DTT, 0.025 mg/ml bromphenol blue in stacking gel buffer
STEN lysis buffer
50 mM Tris, 150 mM NaCl, 2 mM EDTA, 1 % (v/v) NP40 (Sigma-Aldrich), 1 % (v/v) Triton X-100 (Sigma-Aldrich), dH_2O, pH 7.4

Cells were cultured in poly-L-lysine coated 6 cm dishes to a confluence of 80-90 %. The cells were washed twice with ice cold PBS and incubated in 2 ml biotin solution for 30 min on ice under constant gentle shaking. The biotin solution was removed and the cells were washed three times with glycine solution. The glycine solution of the last wash was left on cells for 15 min on ice. The cells were then washed once with ice cold PBS prior to lysis by addition of 900 µl STEN lysis buffer and incubation for 15 min on ice. After the removal of insoluble cell fractions by centrifugation (10 min, 12000 x g, 4 °C), 50 µl of washed streptavidin-sepharose was added to the lysates and the mixture was incubated overnight at 4 °C on a overhead shaker. Finally, the streptavidin-sepharose was washed four times for 10 min each with STEN buffer, pelleted by centrifugation (3 min, 600 x g, 4 °C) and boiled in 20 µl of 2 x SDS loading dye. All samples were analyzed by SDS-PAGE and WB as described in sections 2.3.6 and 2.3.7.

2.3.12 Radio-labeling with ^{32}P-orthophosphate

Poly-L-lysine solution
100 µg/ml sterile poly-L-lysine in PBS
PBS
140 mM NaCl, 10 mM Na_2HPO_4, 1.75 mM KH_2PO_4, dH_2O, pH 7.4
Phosphate free DMEM (Invitrogen)
Labeling medium
Phosphate free DMEM, 0.5 mCi/dish [^{32}P]-ortho phosphate
RIPA lysis buffer
50 mM Tris, 150 mM NaCl, 0.5 % (w/v) Sodium deoxycholic acid, 0.1 % (w/v) SDS, 1 % (v/v) NP-40, pH 7.4

Cells were grown to a confluence of 80-90 % on poly-L-lysine coated 6 cm dishes and incubated for 1 h in phosphate-free medium. After incubation for 1 h in labeling medium in a CO_2 incubator, cells were washed once with PBS and lysed in 1 ml RIPA lysis buffer. The protein of interest was finally isolated by IP as described in 2.3.4. The [^{32}P]-phosphate incorporation was visualized by autoradiography.

2.3.13 TREM2 shedding assay

PBS
140 mM NaCl, 10 mM Na_2HPO_4, 1.75 mM KH_2PO_4, dH_2O, pH 7.4
DMEM -/-
PDBu (stock solution)
10 mM PDBu in DMSO
Batimastat (stock solution)
10 mM Batimastat in DMSO
DMSO
Poly-L-lysine solution
100 µg/ml sterile poly-L-lysine in PBS

80-90 % confluent cells were washed once carefully with warm PBS and incubated then for 4 h in 2 ml DMEM -/- supplemented with 1 µM PDBu, 10 µM Batimastat or DMSO as control respectively. After the incubation supernatants were collected, cleared and used for TCA precipitation (see 2.3.9). Cells were scraped and used for membrane preparation as shown in 2.3.1. Alternatively the assay was combined with cell surface protein staining as described in 2.1.4. Therefore the cells were grown on poly-L-lysine coated CS to the required confluence. CS were then placed on parafilm and the cells were incubated with 150 µl DMEM -/- with the chemicals mentioned above for 4 h. Finally the parafilm with the CS was transferred on ice prior to following the cell surface staining protocol 2.1.4.

2.3.14 TREM2 activation assay

Poly-L-lysine solution
100 µg/ml sterile poly-L-lysine in PBS
PBS
140 mM NaCl, 10 mM Na_2HPO_4, 1.75 mM KH_2PO_4, dH_2O, pH 7.4
Phosphate free DMEM (Invitrogen)
Labeling medium
Phosphate free DMEM, 0.5 mCi/dish [^{32}P]-ortho phosphate
RIPA lysis buffer
50 mM Tris, 150 mM NaCl, 0.5 % (w/v) Sodium deoxycholic acid, 0.1 % (w/v) SDS, 1 % (v/v) NP-40, pH 7.4
Orthovanadate (stock solution)
20 mM sodium orthovanadate, dH_2O
DMEM -/-

In principle the TREM2 activation assay follows the protocol for Radio-labeling with ^{32}P-ortho-phosphate (2.3.12). Since the natural ligand of TREM2 is still unknown, the activation of the TREM2/DAP12 system was achieved by cross-linking of two TREM2 molecules via the N-terminal located myc-tag by an anti-myc antibody. Thus, after 1 h incubation in labeling medium, cells were treated with 10 µg/ml anti-myc antibody. To stabilize the phosphorylation of DAP12 some dishes (as indicated in fig. 7) were also treated with orthovanadate to a final concentration of 200 µM. The cells were then incubated for another hour and it was continued as described in 2.3.12.

Alternatively the TREM2 activation assay was performed as a non radioactive variant. Therefore,

after reaching 80-90 % confluence, the cells were washed once carefully with PBS prior to incubation for 1 h with 2 ml of DMEM -/- supplemented with 10 µg/ml anti-myc antibody. Afterwards, the supernatants were collected, cleared by centrifugation (300 x g; 10 min) and used for TCA precipitation as described in 2.3.9. The cells were used for membrane preparation (2.3.1).

2.3.15 Aβ-Phagocytosis assay

FAM-$A\beta_{42}$
15 µM FAM-$A\beta_{42}$ (AnaSpec) in PBS, aged 3 days at 37 °C
0.2 % Trypan Blue
125 µg/ml Trypan Blue in PBS, pH 4.4
H33342 solution
50 µg/ml Hoechst 33342 in PBS
DMEM +/+

10000 BV-2 cells/well for 4 h incubation or 5000 cells/well for 18 h incubation were plated into a 96-well plate. Cells were incubated for 1 h at 37 °C prior to adding the Aβ solution to a final concentration of 0.5 µM. After incubation for 4-18 h the medium was aspirated using a multichannel pipette. 100 µl Trypan Blue solution was added to each well and the plate was incubated for 1 min at RT. The Trypan Blue solution was removed again and the emission at ~535 nm (excitation ~485 nm) was measured in a plate reader. 100 µl H33342 solution was added to each well and the plate incubated for 30 min. After complete removal of the H33342 solution the emission at ~465 nm (excitation ~360 nm) was measured in a plate reader.

2.4 Densitometric quantification of signals and statistical analysis

Protein signals were quantified by densitometric analysis using Quantity One® software. Statistical analysis of the experiments were carried out by a two-sided student's t-test or to compare more than two individual groups by an One-way Anova test. If not indicated differently in the figure caption in the result part, the diagrams show the mean values and the corresponding standard error (SEM) of three independent experiments. To classify and indicate significant values the following P-values were used: $P < 5$ %, *; $P < 1$ %, **; $P < 0{,}1$ %, ***.

3 RESULTS

3.1 Proteolytic processing of TREM2 by γ-secretase

3.1.1 Expression of PS1 in microglia

While PS1 expression in neurons (Naruse et al., 1998) and astrocytes (Weggen et al., 1998; Diehlmann et al., 1999) is well established, less is known about the role of PS1 in microglia. Only the upregulation of PS1 and nicastrin in microglia after traumatic brain injury was shown, suggesting the presence of a functional γ-secretase complex in these cells (Nadler et al., 2008). In the active γ-secretase, PS is present as a heterodimer consisting of an C-terminal and a N-terminal part (see 1.1.5.3). To test the expression of PS1 and PS2 in microglia, the microglial cell line BV-2 as well as primary murine microglia were tested. Western immunoblotting demonstrates the expression of PS1 CTF in BV-2 cells, mouse embryonic fibroblasts as well as primary microglia (fig. 7 A). The detection of a CTF and N-terminal fragment (NTF) of PS1 and PS2 indicates the presence of a functional γ-secretase in these cells (fig. 7 B). Accordingly, the treatment of BV-2 cells with the γ-secretase inhibitor DAPT led to accumulation of APP CTF (fig. 7 C). As indicated by immunofluorescence microscopy, APP CTF accumulates at the cell surface upon treatment of BV-2 cells with the γ-secretase inhibitor DAPT (fig. 7 D). All together these experiments indicate presence of functional γ-secretase complex in microglia.

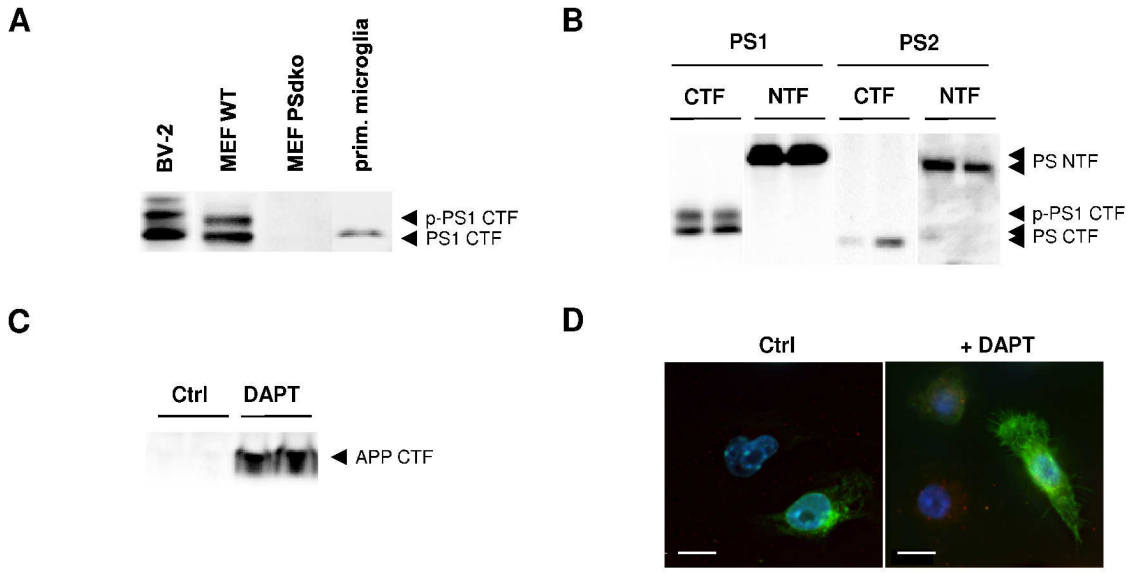

Figure 7: Detection of functional γ-secretase in microglia.

(A) Detection of PS1 CTF in purified membranes of BV-2 cells, MEF, MEF deficient for both PS1 and PS2 (MEF PSdko) and primary microglia by western immunoblotting. Cell membranes were prepared as described in methods section (2.3.1) **(B)** Detection of NTF and CTF of both PS variants in purified membranes of BV-2 cells by western immunoblotting. **(C, D)** BV-2 cells were incubated in absence or presence of 1 μM DAPT for 24 h. APP CTF was detected by the APP antibody 140 in purified membranes by western immunoblotting (C). C99-eGFP was detected in fixed transiently transfected BV-2 cells in immuno stainings (D). Scale bars represents 10 μM

3.1.2 γ-secretase dependent processing of TREM2

Having established the presence of active γ-secretase in a microglia cell line and primary microglia, the next step was to test the proteolytic cleavage of TREM2. As explained in the introduction γ-secretase processes type I transmembrane proteins after shedding of their ectodomain. If TREM2 acts as γ-secretase substrate, the pharmacological inhibition of PS1 should lead to accumulation of a small TREM2 fragment. To prove this, HEK293 cells were transfected with cDNA (see table 3, fig. 6) encoding TREM2 (Flag-TREM2-mycHis) and DAP12 (Flag-DAP12-HA). TREM2 failed to appear in single transfected HEK293 cells, consistent with findings of Bouchon and co-workers, showing that TREM2 expression was partially increased by co-transfection of DAP12 cDNA (Bouchon et al., 2000). Thus, in all experiments TREM2 was co-expressed with DAP12. The transfected HEK293 cells were incubated in absence or presence of the γ-secretase inhibitor DAPT (Dovey et al., 2001) and subjected to membrane preparation.

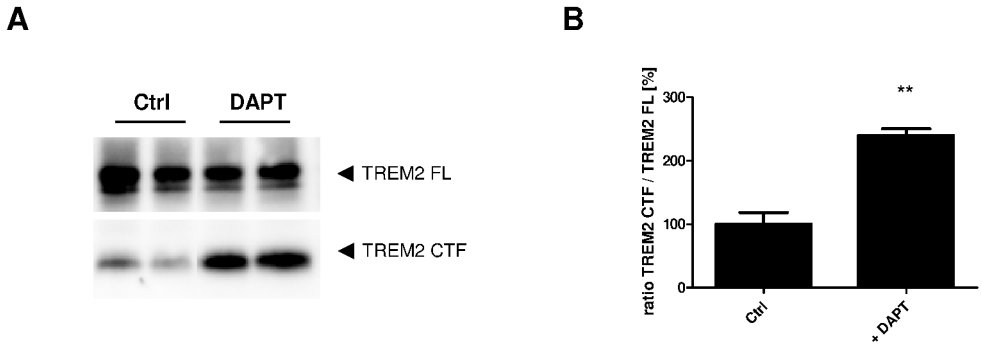

Figure 8: Pharmacological inhibition of γ-secretase leads to the accumulation of a TREM2 C-terminal fragment.

(A) HEK293 cells were transiently co-transfected with Flag-DAP12-HA and Flag-TREM2-mycHis (see table 3, fig. 6). Cells were incubated for 24 h in the presence or absence of 10 μM DAPT. After membrane preparation (2.3.1) and separation by SDS-PAGE (2.3.6), proteins were detected by western immunoblotting (2.3.7) with an anti-myc antibody. **(B)** Quantification of (A) by ECL imaging, displayed as ratio of TREM2 CTF to TREM2 FL

In control cells a strong band migrates at 40 kDa and a weak band at 17 kDa. Based on the size of the bands, the upper one represents most likely the full-length variant of TREM2 (TREM2 FL) and the lower one might be a CTF of TREM2. Accordingly, this band increases significantly upon incubation with DAPT, while the upper band remains constant. This confirms the lower band as TREM2 CTF and indicates that TREM2 represents an immediate γ-secretase substrate (see fig. 8). Since DAP12 expression is not altered upon γ-secretase inhibition (data not shown), the potential processing of DAP12 was not analyzed further in this study.

To corroborate the accumulation of TREM2 CTF through inhibition of γ-secretase in a genetic model, HEK293 cells stably overexpressing the wild-type or a dominant negative variant of human PS1 were co-transfected with DAP12 and TREM2 (fig. 9 A, C). After membrane preparation TREM2 was detected by an anti-myc antibody. In PS1 DN HEK293 cells a small C-terminal fragment appears, similar to the fragment accumulating after DAPT treatment.

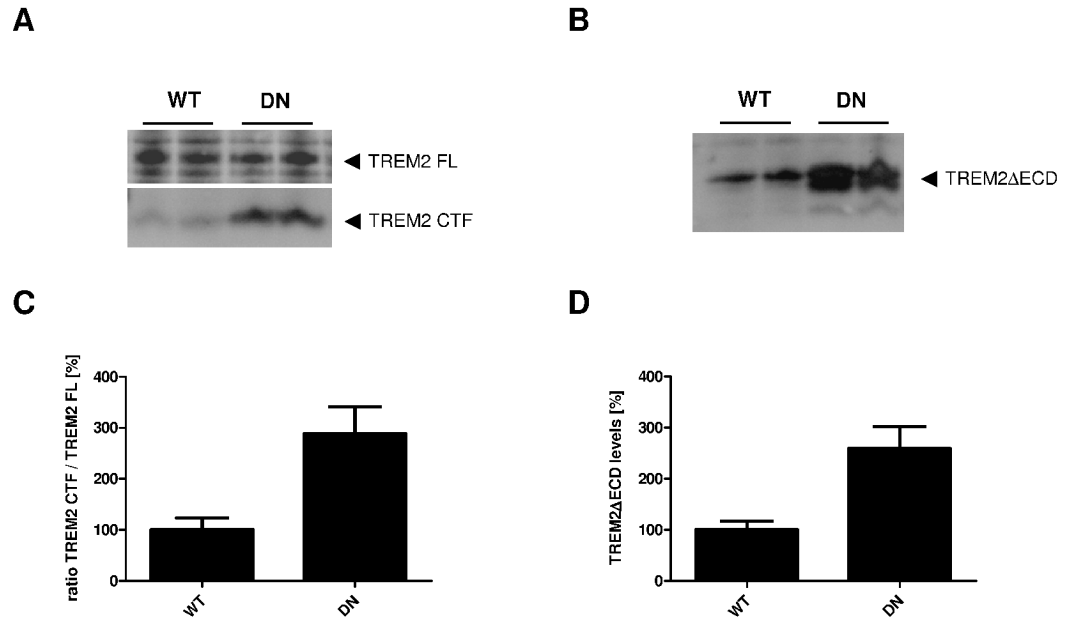

Figure 9: TREM2 is proteolytically processed by γ-secretase.

(A, B) HEK293 cells stably expressing PS1 WT or DN variants were transfected with Flag-TREM2-mycHis and Flag-TREM2ΔECD-mycHis respectively in combination with Flag-DAP12-HA. After membrane preparation (2.3.1) and SDS-PAGE (2.3.6), TREM2 was detected by western immunoblotting (2.3.7) with an anti-myc antibody. **(B, C)** Quantification of (A, B) two independent experiments by ECL imaging, displayed as ratio of TREM2 CTF to TREM2 FL and TREM2ΔECD levels respectively.

To further proof the γ-secretase dependent TREM2 CTF processing, an artificial TREM2 CTF construct (TREM2ΔECD; see fig. 6) was cloned. As usually considered, such a construct encoding a TREM2 variant that consists only of the C-terminal domain, the tm-domain and 14 aa of the ectodomain should be processed directly, because γ-secretase processes C-terminal stubs of proteins with a short (~10-15 aa) ectodomain (Hemming et al., 2008). Thus, HEK293 cells were transfected with TREM2ΔECD and DAP12 (fig. 9 B, D). Importantly, TREM2ΔECD strongly accumulates in PS1 DN cells comparable to the CTF derived from the full-length TREM2.

Fig. 8 and 9 show that γ-secretase inhibition either by a pharmacological or genetic approach leads to the accumulation of TREM2 CTFs. Next, it was investigated whether PS1 FAD mutants (De Strooper 2007; Wolfe 2007) also affect the proteolytic processing of TREM2. To test this, HEK293 cells stably overexpressing two of the most severe FAD mutants were co-transfected with TREM2 and DAP12 (fig. 10). The strongest TREM2 CTF accumulation (80 % more compared to WT) is detected in the PS1 DN cells. More importantly, there is also a significant accumulation (30 % more compared to WT) of TREM2 CTFs in cells expressing the PS1 L166P FAD mutation. Cells expressing PS1 ΔEx9 also show a trend towards TREM2 CTF accumulation (fig. 10).

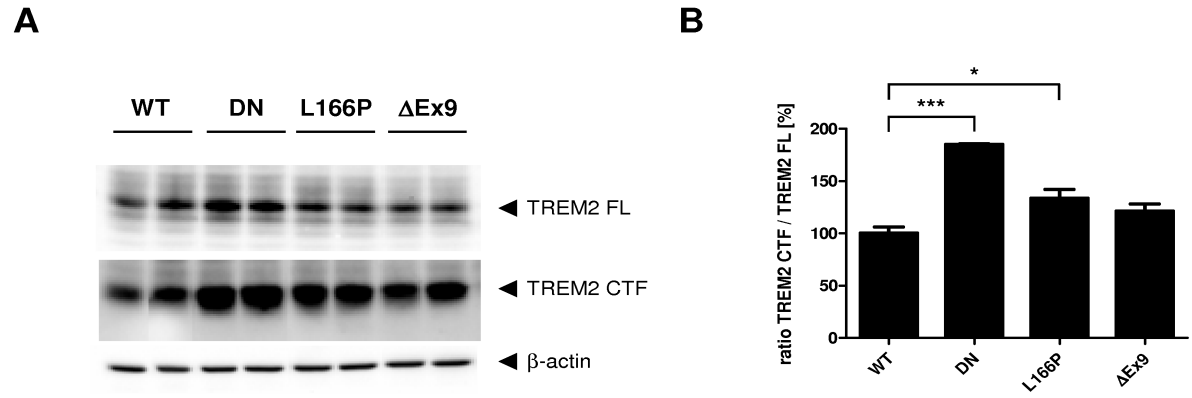

Figure 10: FAD mutations of PS1 lead to accumulation of TREM2 CTFs.

(A) HEK293 cells stably overexpressing the indicated PS1 mutants or PS1 WT were transiently co-transfected with Flag-TREM2-mycHis and Flag-DAP12-HA. After membrane preparation (2.3.1) and separation by SDS-PAGE (2.3.6), the TREM2 full-length (FL) and TREM2 CTF was detected by western immunoblotting (2.3.7) with an anti-myc antibody. β-Actin was detected as loading control. **(B)** Quantification of (A) was done by ECL imaging, ratio of TREM2 CTF to TREM2 FL is displayed.

Taken together, it was shown that the inhibition of γ-secretase either by a pharmacological approach or in cells expressing mutant variants of PS1 results in accumulation of TREM2 CTFs. Furthermore, the artificial construct TREM2ΔECD which is similar to a direct γ-secretase construct accumulates after genetic PS1 inhibition. Thus, these data demonstrate that TREM2 is a γ-secretase substrate.

The next step was to find out more about the localization of this cleavage process and whether TREM2 is also subjected to ectodomain shedding.

3.2 Characterization of γ-secretase dependent processing and localization of TREM2

3.2.1 Cleavage of TREM2 occurs at the cell surface

The γ-secretase substrates APP CTF and Notch are cleaved either on the plasma membrane or in endosomal/lysosomal compartments (Matsuda et al., 2009; Sorensen & Conner 2010). Since TREM2 could interact with cell surface molecules on apoptotic cells (Hsieh et al., 2009) or bacteria (Daws et al., 2003), the localization of TREM2 in cells with or without inhibited γ-secretase was analyzed by immunocytochemistry.

HeLa cells were transfected with TREM2 and incubated for 24 h in the presence and absence of

DAPT respectively (fig. 11). Since staining with an anti-flag antibody was not possible, the cells were stained with an anti-myc antibody.

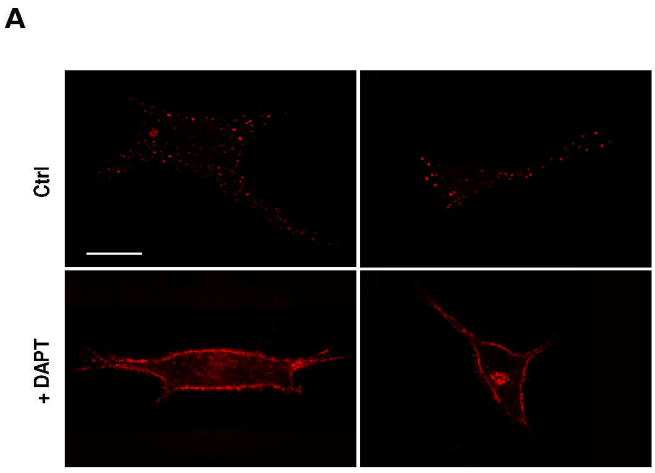

Figure 11: Inhibition of γ-secretase changes the localization of TREM2.

HeLa cells were transiently transfected with a Flag-DAP12-HA and Flag-TREM2-mycHis and incubated with or without 10 μM DAPT for 24 h. Cells were fixed with PFA and permeabilized with Triton X-100 followed by staining with anti-myc antibodies and a secondary Alexa 594-coupled antibody to detect TREM2. For a detailed protocol see 2.1.4. Scale bar represents 20 μM. Two representative images of each group are shown.

While TREM2 FL detected via the C-terminal myc-tag is mainly localized in vesicular compartments in untreated cells, the DAPT treatment leads to strong localization at the membrane (fig. 11). The increased signal at the plasma membrane could either be attributed to TREM2 FL which is transported to the cell surface in response to the DAPT treatment or to accumulation of TREM2 CTF.

To specifically test whether TREM2 CTF accumulates at the cell surface of transfected COS7 cells, TREM2ΔECD was stained at the surface of living cells as described in 2.1.4. In untreated COS7 cells TREM2ΔECD shows a dotted pattern, which is typical for cell surface stainings (fig. 12). In contrast to this, upon DAPT treatment the TREM2ΔECD positive structures on the cell surface increase strongly in size (fig. 12).

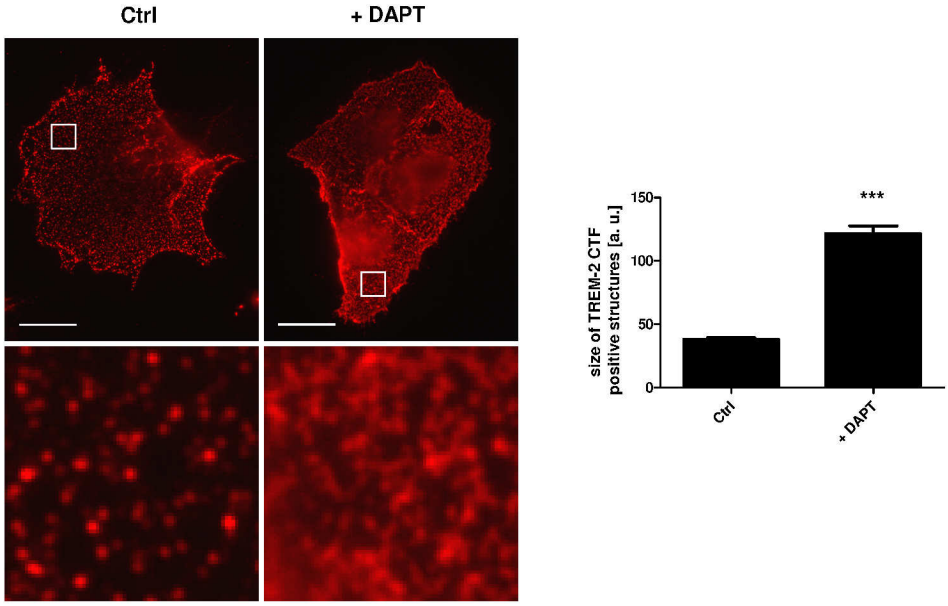

Figure 12: Inhibition of γ-secretase alters the distribution of TREM2 at the cell surface.

COS7 cells transiently transfected with Flag-TREM2ΔECD-mycHis and DAP12-HA were incubated for 24 h with or without 10 µM DAPT and stained on ice against the Flag-tag of TREM2ΔECD by an anti-Flag antibody and an Alexa 594-coupled secondary antibody. For quantification 10 different areas (75 px x 75 px, white square) of five different cells of each group were randomly chosen and the areas of the Flag-positive structures were measured. Scale bar represents 20 µM. One representative image of each group is shown.

Next, the accumulation of TREM2 CTF was quantified by cell surface-biotinylation (fig. 13). As shown before (fig. 8), TREM2 CTFs accumulate in DAPT treated cells, while TREM2 FL is not changed (fig. 13 A, C). Notably, the increasing amount of biotin-labeled TREM2 CTFs demonstrate accumulation at the cell surface (fig. 13 B, D), thereby confirming the observed surface staining of the artificial TREM2 CTF upon γ-secretase inhibition (fig. 12). Since biotin-labeled TREM2 FL doesn't increase (fig. 13 B) the enhanced reactivity at the cell surface detected by immunocytochemistry (fig. 11) cannot be caused by TREM2 FL accumulation.

TREM2 signaling is dependent on the engagement of the receptor with the adapter DAP12 via a charged aspartate in the tm-region of DAP12 (see 1.5.2 and 1.6). To test whether this interaction can regulate the cleavage of TREM2 an interaction mutant of DAP12 was cloned by substituting the aspartate at position 52 against alanine (DAP12 D52A, see fig. 6) (Hamerman et al., 2006).

The TREM2 CTF accumulation at the cell surface relating to DAP12 interaction was checked by a second biotinylation experiment with HEK293 cells expressing TREM2 and DAP12 D52A (fig. 14)

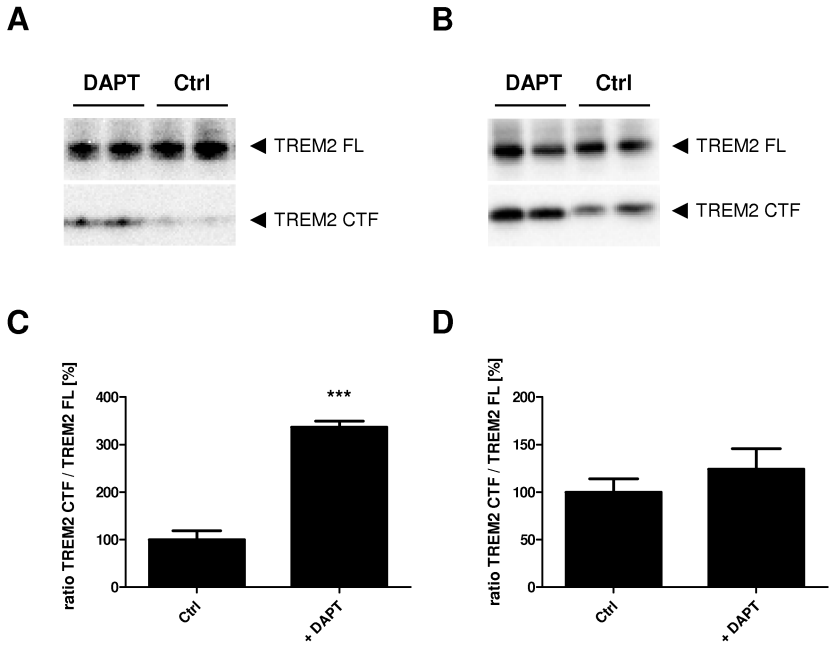

Figure 13: TREM2 CTFs accumulate at the cell surface after γ-secretase inhibition.

HEK293 cells were transfected with Flag-TREM2-mycHis in combination with Flag-DAP12-HA and incubated for 24 h in absence or presence of 10 μM DAPT. Surface proteins were biotinylated wit sulfo-NHS-biotin for 30 min followed by lysis and streptavidin-IP (2.3.11). Aliquots of cell lysates **(A)** and streptavidin-IPs **(B)** were separated by SDS-PAGE. TREM2 was detected by western immunoblotting with an anti-myc antibody. **(C, D)** Quantification of (A, B) by ECL imaging, ratio of TREM2 CTF and TREM2 FL is displayed.

Both in lysates (fig. 14 A, C) and at the plasma membrane (fig. 14 B, D) TREM2 FL is not changed upon DAPT treatment. However, CTFs in DAPT treated cells accumulate significantly in lysates as well as at the plasma membrane, indicating that TREM2 CTF cleavage occurs independently of interaction with DAP12.

The interaction with DAP12 was demonstrated to regulate the surface expression of TREM2 FL (Bouchon et al., 2000). The only known interaction site so far is the charged amino residue in the transmembrane region of both proteins. Although the interaction mutant DAP12 D52A was expressed together with TREM2 in the previous experiment, TREM2 FL is detectable at the plasma membrane. This finding suggests that transport of TREM2 to the cell surface can occur independently of DAP12. Alternatively, there might be other unknown motifs involved in the interaction between TREM2 and DAP12 or other signaling related proteins regulate the cell-surface expression of TREM2.

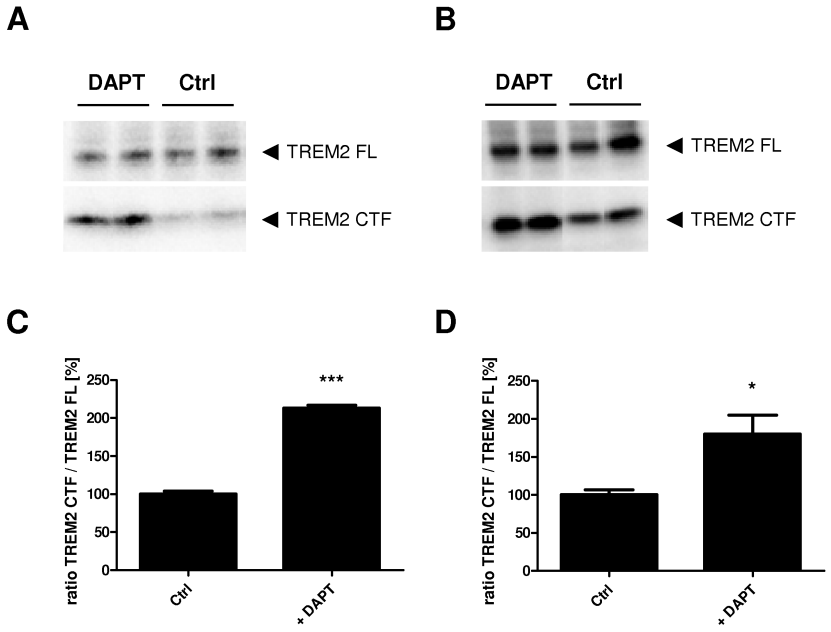

Figure 14: Interaction with DAP12 is not prerequisite for γ-secretase mediated TREM2 cleavage.

HEK293 expressing Flag-TREM2-mycHis in combination with Flag-DAP12 D52A-HA were incubated for 24 h in absence and presence of 10 µM DAPT. After biotinylation with sulfo-NHS-biotin, lysis and streptavidin-IP (2.3.11) aliquots of cell lysates **(A)** and streptavidin-IPs **(B)** were separated by SDS-PAGE. TREM2 was detected by western immunoblotting with an anti-myc antibody. **(C, D)** Quantification of (A, B) was done by ECL imaging.

3.2.2 γ-secretase mediated processing in response to the activation of TREM2.

There are several ways to inactivate receptors upon ligand binding and activation. The ligand-receptor complexes could be taken up by endocytosis and be further degraded. Alternatively, the complexes could be cleaved directly at the membrane. It is known that ligand binding could induce the shedding of the ECD of Notch, allowing subsequent γ-secretase cleavage which leads to an increase in Notch ICD, a small fragment transported to the nucleus where it has gene regulatory function (Schroeder et al., 1998; Mumm et al., 2000). The induced receptor cleavage is also known for G-protein coupled receptors like the V2 vasopressin receptor (Kojro & Fahrenholz 1995), thereby downregulating the receptors.

However, nothing is known about the downregulation of the TREM2/DAP12 signaling. To test whether TREM2 activation alters γ-secretase processing HEK293 PS1 WT and DN cells, expressing myc-TREM2-GFP/DAP12-HA were subjected to a non-radioactive TREM2 activation assay as described in 2.3.14 (fig. 15). Since no ligand of TREM2 is known, myc-tagged TREM2 was activated by ligation with an anti-myc antibody.

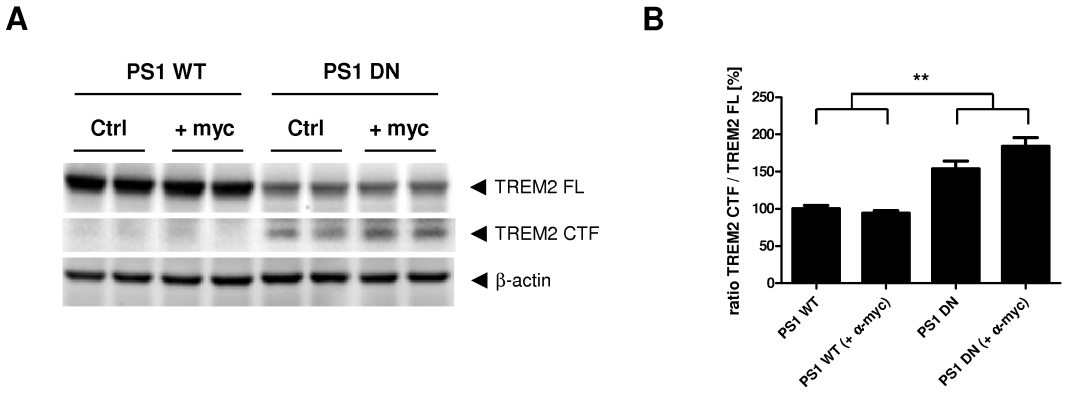

Figure 15: γ-secretase cleavage in response to activation of TREM2.

(A) HEK293 cells stably expressing PS1 WT and DN were transiently transfected with myc-TREM2-GFP. 24 h after transfection medium was changed against DMEM -/- or DMEM -/- supplemented with 10 µg/ml anti-myc antibody and cells were incubated for 1 h (for detailed protocol see 2.3.14). Membrane proteins were isolated as described in 2.3.1. After SDS-PAGE TREM2 FL & CTF were detected by western immunoblotting with an anti-GFP antibody. **(B)** Quantification of TREM2 FL and CTF by ECL imaging, normalized to β-actin which served as loading control. Ratio of TREM2 CTF/FL is shown.

Upon activation, levels of TREM2 FL changes neither in PS1 WT nor in PS1 DN cells. However, as previously shown, TREM2 CTF accumulates in HEK293 PS1 DN cells (fig. 15). Notably, after TREM2 activation by antibody cross-linking a slight increase in TREM2 CTFs is observed in HEK293 PS1 DN as compared to PS1 WT cells, but this difference doesn't reach significance.

Taken together, all these data indicate that proteolytic processing of TREM2 CTFs occurs at the plasma membrane dependent on the activation state of TREM2.

3.2.3 TREM2 ICD is not translocated to the nucleus

γ-secretase cleavage of substrate CTFs results in release of ICDs to the cytosol (see 1.1.4). The ICD of Notch is known to translocate to the nucleus upon generation, regulating expression of various target genes. The ICDs of several other γ-secretase substrates are very unstable due to efficient proteolytic degradation. Since detection of TREM2 ICD (TICD) after overexpression of TREM2 FL by western immunoblotting and immunostainings was not possible (not shown), an artificial TICD construct was generated starting one amino acid behind the putative tm-domain (see table 3, fig. 6). To test the localization of this fragment, HeLa cells were transiently transfected and subjected to immunofluorescence stainings (fig. 16). The transfected TICDs reveal no nuclear staining, but a vesicular stain, distributed over the whole cell.

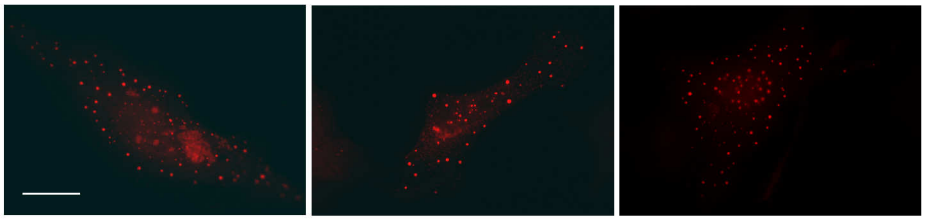

Figure 16: TREM2 ICD is not translocated to the nucleus

HeLa cells were transiently transfected with TREM2 ICD-mycHis. After fixation and permeabilization, TREM2 ICD was stained with an anti-myc antibody and an Alexa 594-coupled secondary antibody. Three representative cells are shown. Scale bar represents 20 µM.

3.2.4 TREM2 ectodomain shedding by an protease of the ADAM or MMP family.

γ-Secretase processing requires prior cleavage of large ectodomains (Hemming et al., 2008) (see 1.1.5.3).

The accumulation of TREM2 CTFs upon γ-secretase inhibition (see chapters 3.1.2 and 3.2.1) strongly indicates that TREM2 can undergo ectodomain shedding (see fig. 8, 9 A, 13, 14). Thus, it was first checked whether an ectodomain of TREM2 is detectable in the supernatant of TREM2 expressing cells. HEK293 PS1 WT and PS1 DN cells were transfected with myc-TREM2-GFP construct and used for a shedding assay (see 2.3.13). Since it is known that ligand binding could induce ectodomain cleavage (Bozkulak & Weinmaster 2009; Rahimi et al., 2009), the production of a ECD was analyzed with or without TREM2 activation (see 2.3.14).

Importantly, two TREM2 ECD bands are detected in the supernatants (fig. 17) of both PS1 WT and PS1 DN cells, indicating that the generation of this derivative is γ-secretase independent. The two bands might represent differently glycosylated forms of TREM2, because two potential sites for N-glycosylation (aa 20 and aa 79) are present in the ectodomain of TREM2 (UniProtKB, Q99NH8).

While levels of TREM2 FL and ECD decrease significantly in HEK293 PS1 WT cells after ligation of myc-tagged TREM2 with an anti-myc antibody, TREM2 ECD is unaffected in HEK293 PS1 DN after ligation of TREM2 (fig. 17 B). Although, TREM2 FL levels decrease significantly in HEK293 PS1 DN as compared to HEK293 PS1 WT cells, the levels of TREM2 FL are unchanged with or without activation (fig. 17 C).

Notably, the detection of the ECD band, demonstrates existence of a shedding process and rules out that CTFs are generated by ECD degradation processes.

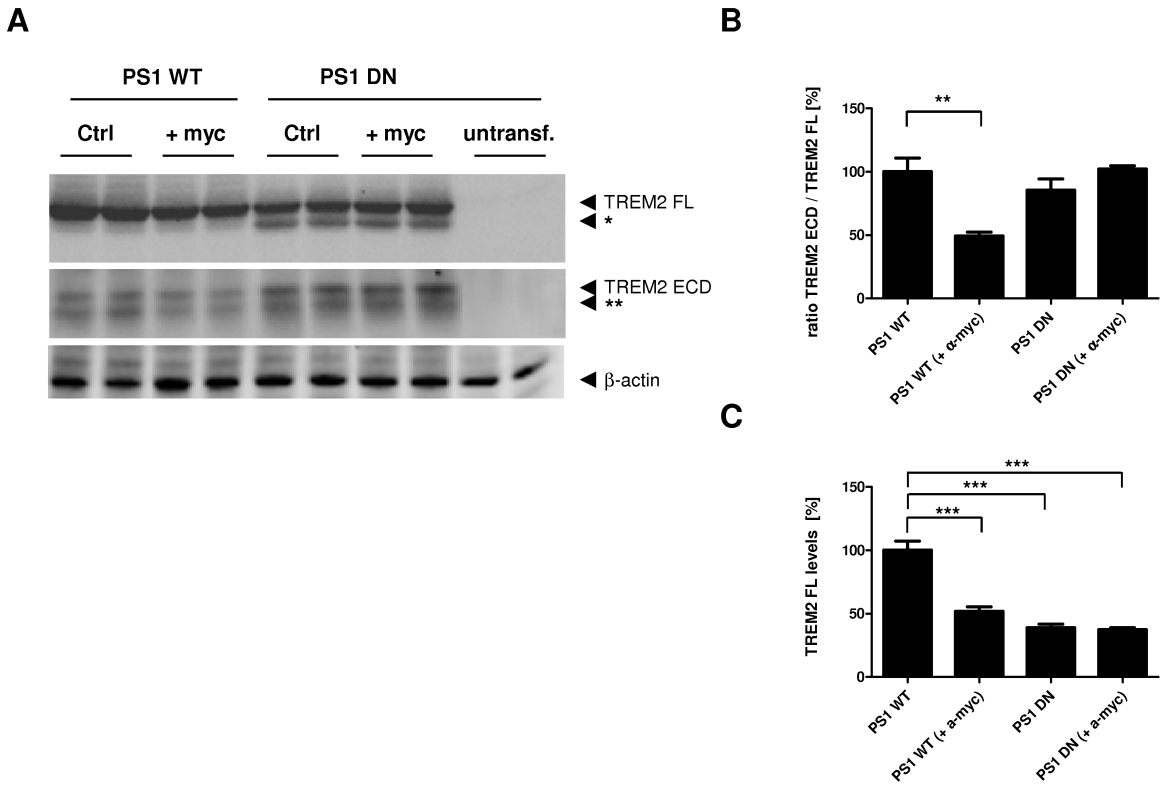

Figure 17: TREM2 ECD can be detected in supernatant of TREM2 overexpressing cells.

(A) HEK293 PS1 WT and DN cells were transiently transfected with myc-TREM2-GFP and DAP12-HA. 24 h after transfection medium was changed against DMEM -/- or DMEM -/- supplemented with 10 µg/ml anti-myc antibody and cells were incubated for 1 h. Membrane proteins were isolated (2.3.1) and TREM2 ECD was precipitated with TCA of cleared cell culture supernatant according to 2.3.9. All proteins were separated by SDS-PAGE (2.3.6). TREM2 FL and ECD were detected by western immunoblotting with an anti-myc antibody. β-actin served as loading control. The bands indicated with * and ** might represent differently glycosylated forms of TREM2. **(B, C)** Quantification of the detected bands by ECL imaging. Ratio of TREM2 ECD/FL and TREM2 FL levels are shown.

Proteases of the MMP (matrix metallo protease) family or the ADAM (A disintegrin and metalloprotease) are known to act as sheddases (Edwards et al., 2008). Other proteases which can act as sheddases are BACE-1 and BACE-2. So far, members of the ADAM protease and MMP family as well as BACE-2 are known to be expressed in microglia (Satoh & Kuroda 2000; Dominguez et al., 2005; Woo et al., 2008; Pul et al., 2009). In contrast BACE-1 is expressed mainly in neurons whereas there is minor expression in glia cells (Sinha et al., 1999; Vassar et al., 1999), so the expression of BACE-1 was first revealed in microglia derived from mouse embryonic stem cells (ESdM) (Napoli et al., 2009; Beutner et al., 2010), obtained from the group of Prof. Neumann (Institute of Reconstructive Neurobiology, Bonn). Two bands of 60-70 kDa are detected by IP (fig. 18 A), which are also present in HEK293 cells. These two variants might represent immature and mature form of BACE-1 (Vassar et al., 1999), showing that BACE-1 is present in microglia and can probably serve as sheddase for TREM2 in these cells. In order to study a putative

TREM2 shedding mechanism, HEK293 cells were transfected with DAP12 and TREM2 together with or without one of the putative sheddases BACE-1 (fig. 18), ADAM-10 and BACE-2 (fig. 19). Since the ECD could not be detected in this experiment, the effect of the three putative sheddases is only expressed as changes in the FL and CTF band of TREM2.

Overexpression of BACE-1 leads to a strong decrease of TREM2 FL but no increase of TREM2 CTF, nonetheless resulting in an increased ratio of TREM2 CTF/FL (fig. 18 B, C).

Interestingly, while the overexpression of BACE-1 alone results in a strong increase of sAPP, co-expression with TREM2 diminishes this effect (fig. 18 B). One explanation for this effect might be a substrate competition for BACE-1.

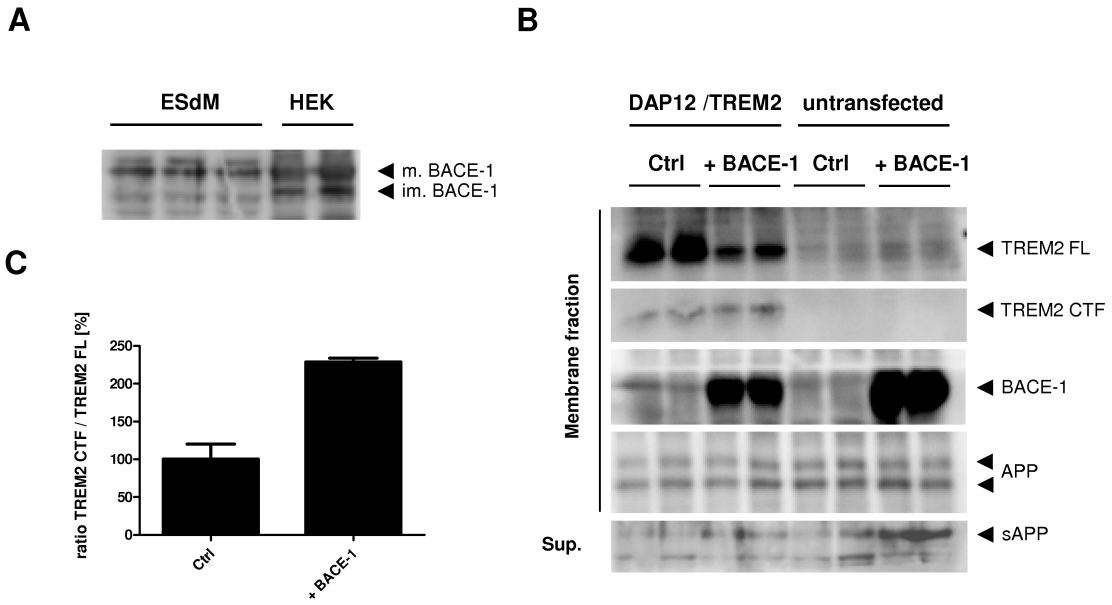

Figure 18: BACE-1 overexpression increases the ratio of TREM2 CTF/TREM2 FL.

(A) Detection of endogenous BACE-1 in ESdMs and HEK293 cells. BACE-1 was detected after IP (2.3.4) and SDS separation (2.3.6) in western immunoblotting (2.3.7) by the polyclonal antibody 7520. **(B)** HEK293 cells were transfected with Flag-TREM2-mycHis and Flag-DAP12-HA in combination with BACE-1 or with BACE-1 alone. Membrane proteins (Membrane fraction) were isolated as described in 2.3.1. Cell culture supernatants were cleared and extracellular proteins (Sup.) precipitated with TCA (2.3.9). After separation by SDS-PAGE (2.3.6), indicated proteins were detected by western immunoblotting (2.3.7). TREM2 FL and CTF were detected with an anti-myc antibody, BACE with the polyclonal antibody 7520, APP and sAPP with the polyclonal antibodies 140 and 5313 respectively. **(C)** TREM2 FL and CTF bands of two independent experiments were quantified by ECL imaging and shown as ratio of TREM2 CTF/FL.

Comparable effects are observed after overexpression of the putative sheddases ADAM-10 and BACE-2. Since CTF levels are unchanged, the alteration of the TREM2 CTF/TREM2 FL ratio results mainly from the decreased TREM2 FL levels (fig. 18, 19). An explanation might be the

alteration of protein expression due to triple transfection. This would also explain the decreased levels of all sheddases, when they were expressed in combination of DAP12 and TREM2.

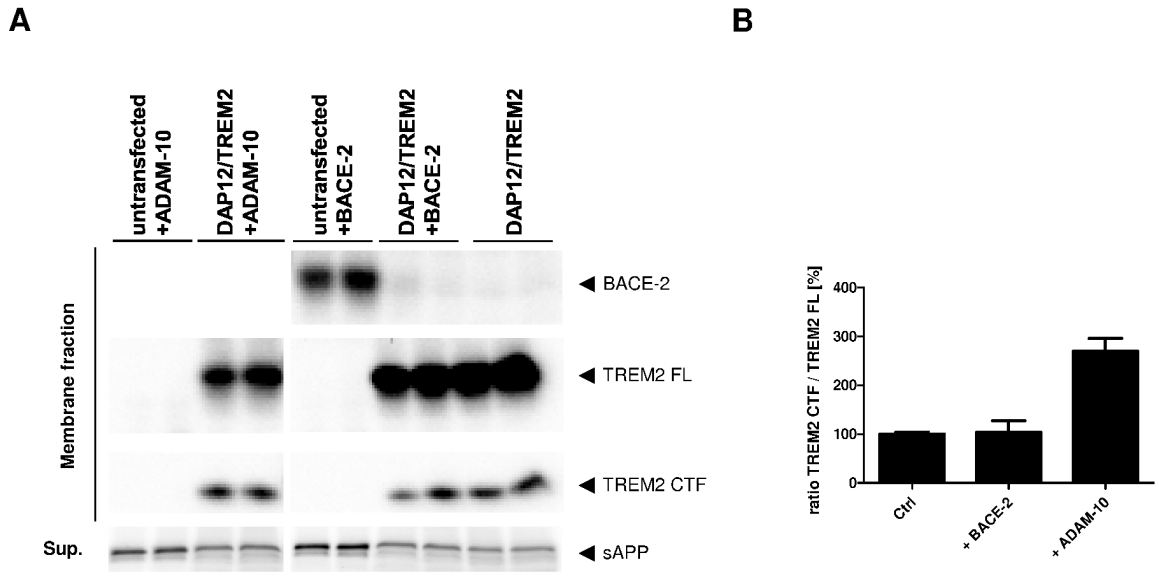

Figure 19: ADAM-10 overexpression increases ratio of TREM2 CTF/TREM2 FL.

(A) HEK293 cells were transfected with Flag-TREM2-mycHis and Flag-DAP12-HA in combination with ADAM-10 or BACE-2. To control the effect of triple transfection additionally untransfected HEK293 cells were transfected with one of the proteases alone. Membrane proteins (Membrane fraction) were isolated as described in 2.3.1 whereas extracellular proteins (Sup.) were precipitated with TCA from cleared cell culture supernatants (2.3.9). After separation by SDS-PAGE (2.3.6), indicated proteins were detected by western immunoblotting (2.3.7). TREM2 FL and CTF were detected with an anti-myc antibody, BACE-2 with the polyclonal antibody 7524 and sAPP with the polyclonal antibody 5313. **(B)** TREM2 FL and CTF bands were quantified by ECL imaging, ratio of TREM2 CTF to FL is shown.

To further characterize the identity of the TREM2 sheddase, experiments were carried out using pharmacological inhibitors or activators of ADAM and MMPs protease families.

Batimastat is a well known metalloprotease inhibitor with broad specificity for MMPs and ADAMs in the used concentration. The phorbol ester PDBu is an activator of protein kinase C (PKC) which was shown to stimulate shedding of cell surface proteins (Horuk & Gross 1990). Pervanadate, a potent tyrosine phosphatase inhibitor was also shown to activate sheddases of the ADAM and the MMP families (Codony-Servat et al., 1999; Gutwein et al., 2003).

TREM2/DAP12 transfected HEK293 cells were incubated with these substances to investigate the involvement of ADAMs in the shedding of TREM2.

The treatment with the metalloprotease inhibitor Batimastat results in an increase of the TREM2 FL band just as a decrease of the TREM2 CTF band (fig. 20 A, B), while TREM2 ECD levels are slightly elevated (fig. 20 A, C). This leads to the assumption that proteases of the

ADAM or MMP families participate in shedding of the TREM2 ectodomain. Besides inhibition of the putative TREM2 sheddase, Batimastat might also inhibit subsequent degradation of the ECD, thereby stabilizing this fragment in supernatants. This might contribute to the altered levels of TREM2 ECD.

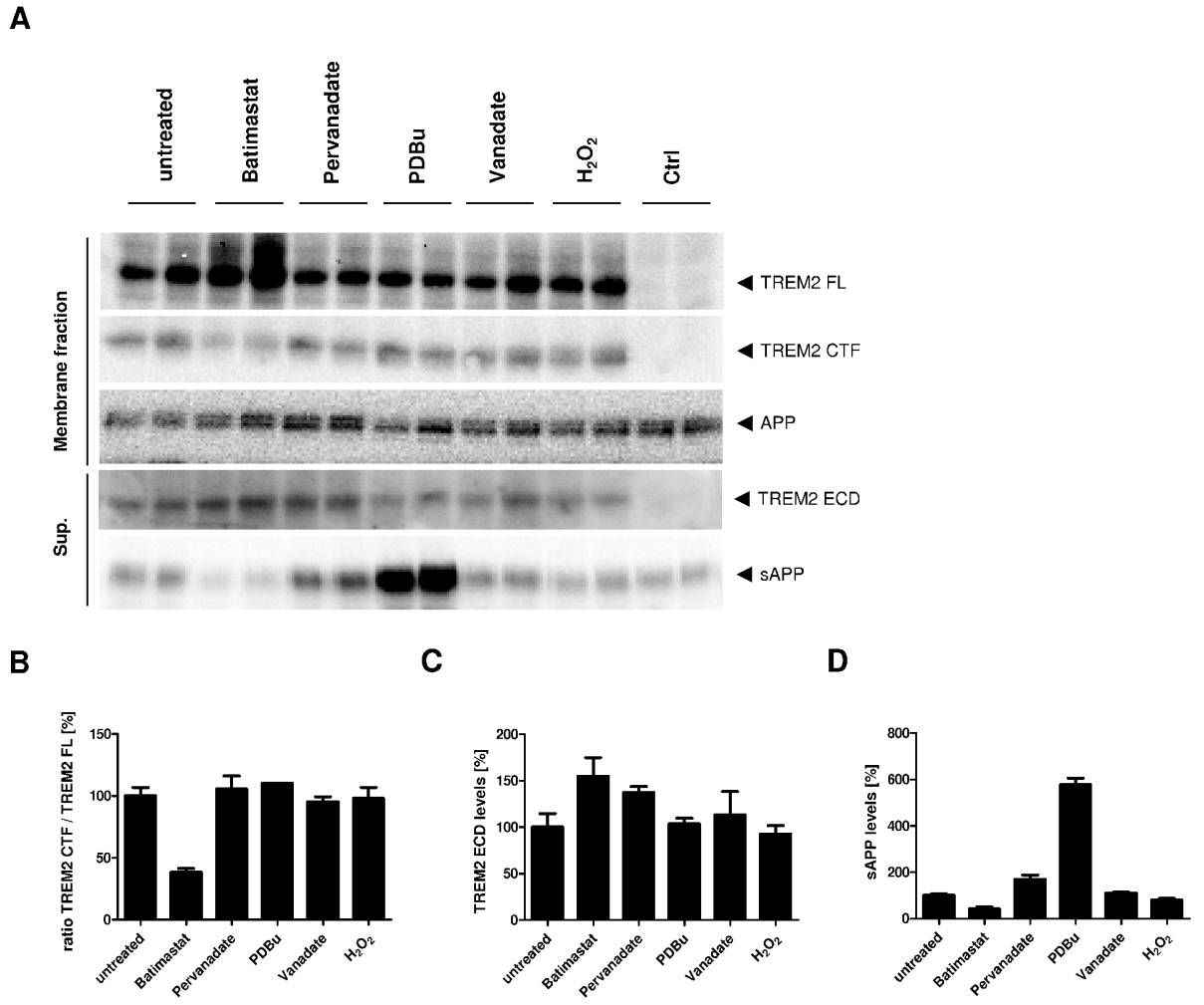

Figure 20: Pharmacological modulation of TREM2 shedding.

(A) Membrane proteins were isolated from HEK293 cells (2.3.1) transfected with Flag-DAP12-HA and Flag-TREM2-mycHis treated with Batimastat (10 μM), PDBu (1 μM), pervanadate (100 μM), vanadate (100 μM) or H_2O_2 (100 μM) for 4 h respectively. Soluble proteins were precipitated out of cleared cell culture supernatants (2.3.9). Both membrane proteins (Membrane fraction) and precipitated proteins (Sup.) were separated on SDS-gels (2.3.6). After western immunoblotting, TREM2 FL and CTF were detected by an anti-myc antibody, APP by the polyclonal antibody 140 and sAPP by 5313. **(B, C, D)** Quantification of two independent experiments by ECL imaging. Ratios of TREM2 CTF to FL, TREM2 ECD to FL and sAPP levels are shown.

Pervanadate which is an 1:1 mixture of vanadate and H_2O_2 was shown to activate MMP-1 (Codony-Servat et al., 1999) and ADAM-10 (Gutwein et al., 2003). The incubation with pervanadate and the control substances vanadate and H_2O_2, has no effect on TREM2 shedding

(fig. 20 A, B), suggesting that MMP-1 and ADAM-10 might not represent major TREM2 sheddases. However, TREM2 ECD levels are slightly increased with pervanadate (fig. 20 A, C). Paradoxically, the well established shedding activators PDBu and pervanadate don't alter the shedding of TREM2, demonstrated by the unaltered TREM2 CTF/FL ratio and ECD levels. However, as expected sAPP levels increase upon treatment with PDBu and pervanadate, confirming the activity of both modulators.

In fig. 20 the effect of different shedding modulators is addressed, but the levels of TREM2 ECD don't match to the TREM2 CTF/FL ratio. To further establish an effect of these modulators on the TREM2 FL-expression at the cell surface, myc-TREM2-GFP was analyzed by a microscopic approach. In the used construct, the myc-tag allows the specific detection of TREM2 FL at the plasma membrane, whereas the GFP-tag allows estimation of the total expression.

COS7 cells transfected with DAP12-HA and myc-TREM2-GFP were incubated with the indicated substances and myc-tagged extracellular part of TREM2 was stained at the surface of living cells as described in 2.1.4.

In untreated and DMSO treated cells, only minor amounts of TREM2 are detected at the cell surface, suggesting that TREM2 undergoes efficient constitutive shedding in COS7 cells (fig. 21 G, H, I). The amount of surface localized TREM2 FL is significantly decreased when cells were incubated for one hour with PDBu (fig. 21 D, E, F). In contrast, the treatment with the broad sheddase inhibitor Batimastat results in a markedly increase of myc-positive dots on the cell surface (fig. 21 A, B, C). The quantification of 10 cells with five randomly chosen squares of 75 x 75 px each, yield an averaged number of 25 dots for Batimastat. Both untreated and DMSO treated cells show less than 10 dots per square.

Interestingly, the GFP staining which represents the C-terminal part of TREM2 is similar under all tested conditions. This suggests that large fractions of TREM2 are localized in intracellular compartments which would be consistent to the localization pattern of TREM2 observed in microglia (Sessa et al., 2004; Prada et al., 2006). However, it is also possible that TREM2 exists predominantly in a variant lacking the lumenal domain on the cell surface (fig. 21 B, E, H, K).

Taken together, these experiments clearly show that TREM2 undergoes shedding. However, the nature of the involved protease could not be clarified completely. The sensitivity to PDBu and Batimastat substantiate the suspicion that ADAMs, most likely ADAM-17 are involved in the shedding process, but involvement of other proteases like BACE-1 or MMPs could not be ruled out.

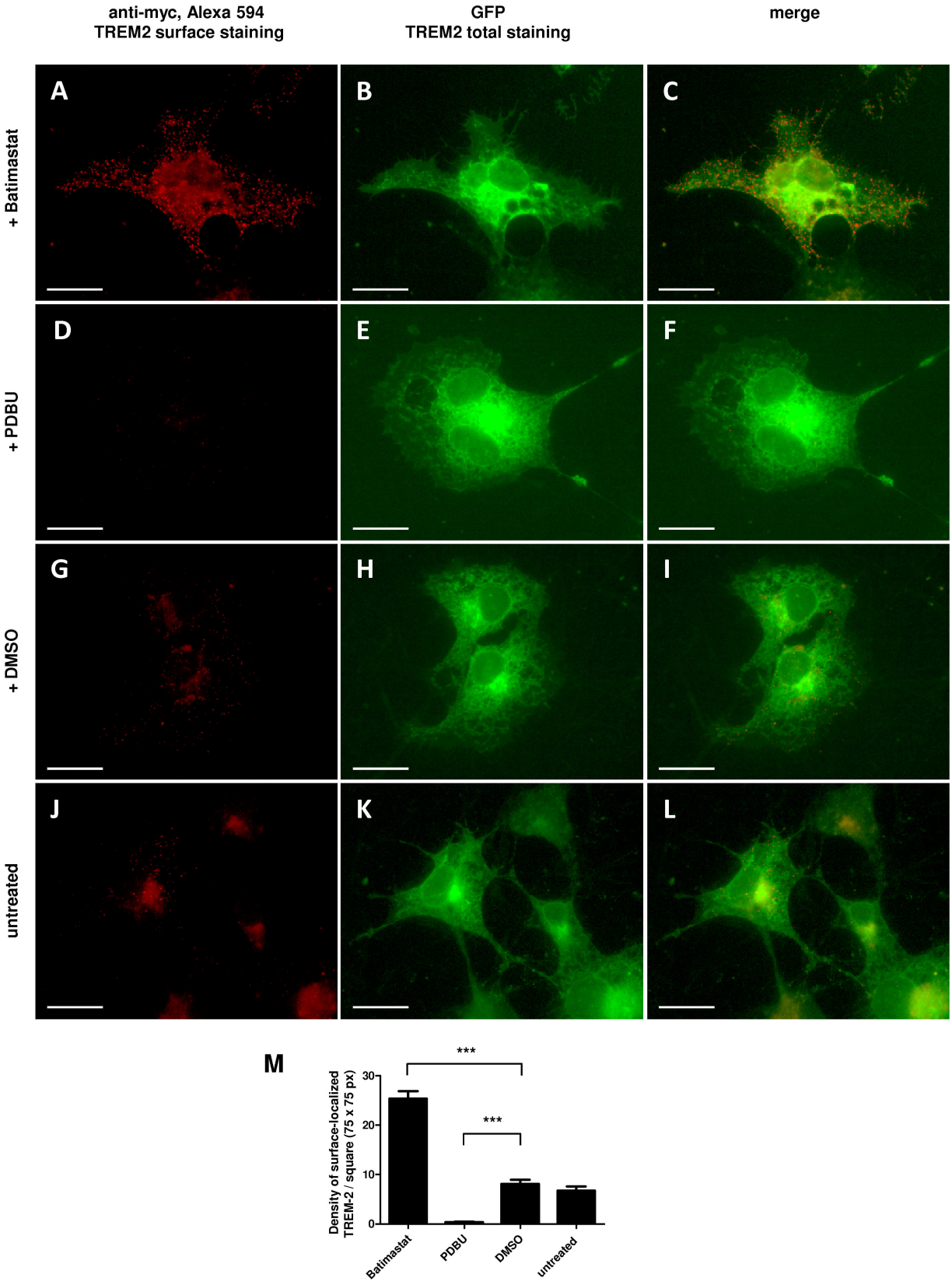

Figure 21: Treatment with Batimastat increases the TREM2 surface expression.

(A-L) COS7 cells were transfected with myc-TREM2-GFP and DAP12-HA. Cells were then treated with the indicated substances, (A-C) Batimastat (10 µM), (D-F) PDBu (1 µM) and (G-I) DMSO as control. After 1 h incubation the surface localization of TREM2 was visualized by an surface staining using an anti-myc antibody in combination with the Alexa 594-coupled secondary antibody. **(M)** Numbers of the cell surface located myc-positive dots were counted in 5 randomly chosen sectors of 75 x 75 px of 10 cells each. Scale bars represent 20 µm.

3.3 Role of TREM2 processing in the interaction with DAP12

3.3.1 Inhibition of γ-secretase facilitates co-localization of TREM2 and DAP12 at the cell surface.

After showing that TREM2 is cleaved by a sheddase generating a C-terminal fragment which is subsequently cleaved by the γ-secretase (see chapters 3.1 and 3.2), it was next investigated whether processing alters the interaction of TREM2 with its co-repressor DAP12.

To test this, COS7 cells transfected with Flag-TREM2ΔECD-mycHis and DAP12-HA, were treated with or without DAPT and subjected to surface immunostaining (see 2.1.4). To visualize a putative co-localization of DAP12 with the accumulated TREM2ΔECD, cells were fixed and permeabilized after surface staining and stained for total DAP12 expression via the C-terminal HA-tag of the DAP12 construct.

The total DAP12 stain shows a diffuse but in some areas dotted pattern (fig. 22 B, E). The co-localization between TREM2ΔECD and DAP12 is very limited (fig. 22 C, F). Upon γ-secretase inhibition with DAPT, the surface staining of TREM2 increases and changes from a punctuated to a more elongated, spiry shape, distributed over the whole cell. Interestingly, DAP12 shows very similar changes in the localization (fig. 22 H, K), reaching complete co-localization (fig. 22 I, L), indicating that TREM2 CTF interacts with DAP12 at the cell surface and affect its localization upon γ-secretase inhibition.

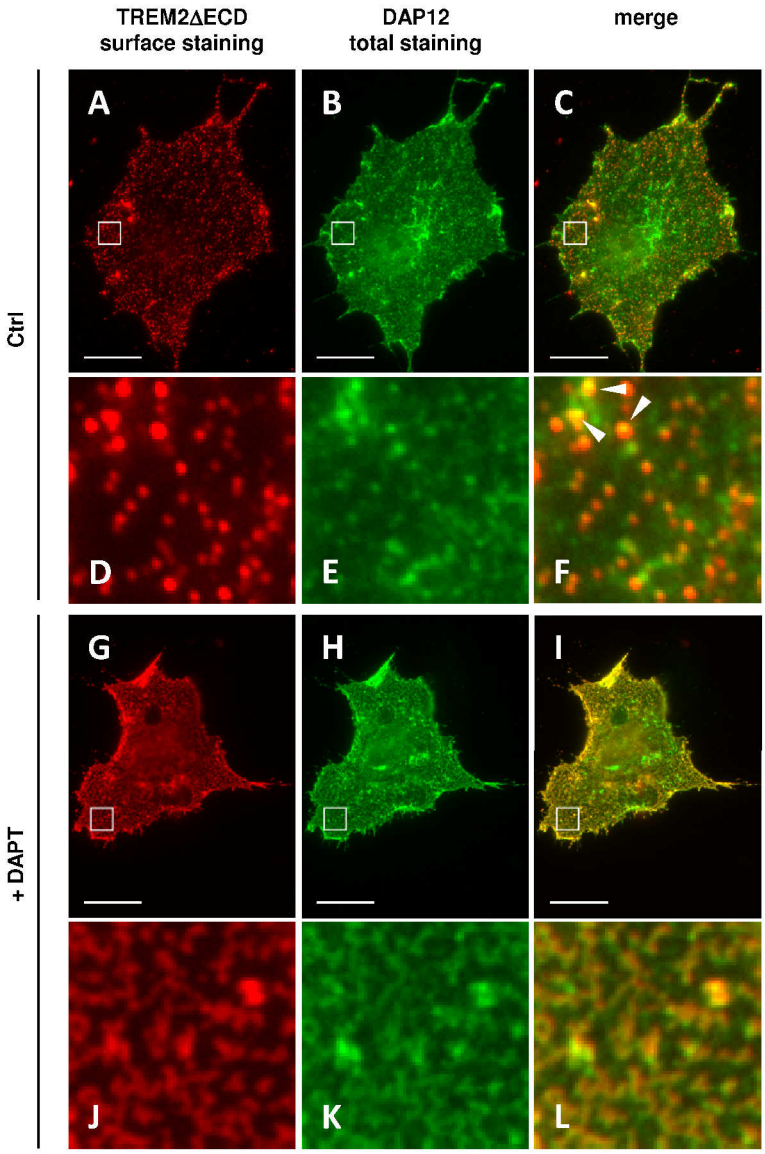

Figure 22: Co-localization of TREM2ΔECD and DAP12 upon cell treatment with DAPT.

COS7 transiently transfected with Flag-TREM2ΔECD-mycHis and DAP12-HA were incubated 24 h with or without 10 µM DAPT and stained on ice against the Flag-tag of TREM2ΔECD by an anti-Flag antibody and the secondary antibody Alexa 594. After the specific cell surface staining the cells were fixed in 4 % PFA, permeabilized with Triton X-100 and stained against DAP12 with an anti-HA antibody and the secondary antibody Alexa 488.

3.3.2 Processing of TREM2 alters the interaction with DAP12

To further analyze whether the interaction of TREM2 and DAP12 is dependent on γ-secretase activity, co-immunoprecipitation experiments were performed in transfected HEK293 cells treated with or without DAPT as well as in HEK293 PS1 WT and DN (fig. 23 C).

As shown in fig. 23 A and C, complexes of TREM2 and DAP12 can be isolated out of cell lys-

ates. Interestingly, the interaction of TREM2 FL with DAP12 markedly decreases in cells expressing the dominant negative form of presenilin (fig. 23 A, B), indicating that loss of γ-secretase function impairs interaction of TREM2 FL with DAP12. Decreased complex formation is also detected upon pharmacological γ-secretase inhibition with DAPT (fig. 23 C, D). However, these findings are completely contrary to trapping of DAP12 at the cell surface after DAPT treatment as shown in fig. 22.

To control the identity of the precipitated proteins, in one lane of each blot the protein was precipitated with the antibody later used for detection (lane labeled with IP control). Precipitation out of single transfected HEK293 cells results in a clean lane, evidencing the specificity of the performed co-IPs.

One explanation for the contrary findings might base on the experimental conditions. The main pool of TREM2 is located in the Golgi and in exocytic vesicles and only a minor part is located at the membrane. While the surface staining experiment in fig. 22 visualizes TREM2/DAP12 interaction at the cell surface, the Co-IP strategy addresses TREM2/DAP12 interaction in the whole cell. Thus, if binding of DAP12 by TREM2 CTF occurs only at the cell surface, precipitation of the intracellular TREM2 would mask the cell surface effect. Moreover, the decrease of TREM2/DAP12 interaction upon γ-secretase inhibition might be explained by massive translocation of DAP12 from intracellular pools to the cell membrane.

3.3.3 Inhibition of γ-secretase suppresses phosphorylation of DAP12 upon TREM2 activation

Ligand-dependent activation of TREM2 causes the interaction with the co-receptor DAP12 which subsequently induces phosphorylation of DAP12 (Takaki et al., 2006; Lanier 2009), triggering activation of microglia or inducing phagocytosis (Neumann & Takahashi 2007; Takahashi et al., 2007). Therefore, a potential involvement of γ-secretase in the regulation of phosphorylation of DAP12 was analyzed.

Cells co-expressing TREM2 and DAP12 were labeled with ^{32}P-orthophosphate in absence or presence of DAPT to inhibit γ-secretase. The two weak bands in the first lane of fig. 24. represent the phosphate incorporation of DAP12 one hour after activation of TREM2. As compared to control cells, presence of orthovanadate strongly increases phosphorylation of DAP12, indicating that DAP12 is efficiently dephosphorylated by phospho-tyrosine phosphatases. This in fact also indicates that the phosphorylation of DAP12 takes place at tyrosine residues. Two tyrosine

residues in DAP12 are located within the ITAM domain, which have been shown to be important for DAP12 signaling (Lanier et al., 1998; McVicar et al., 1998).

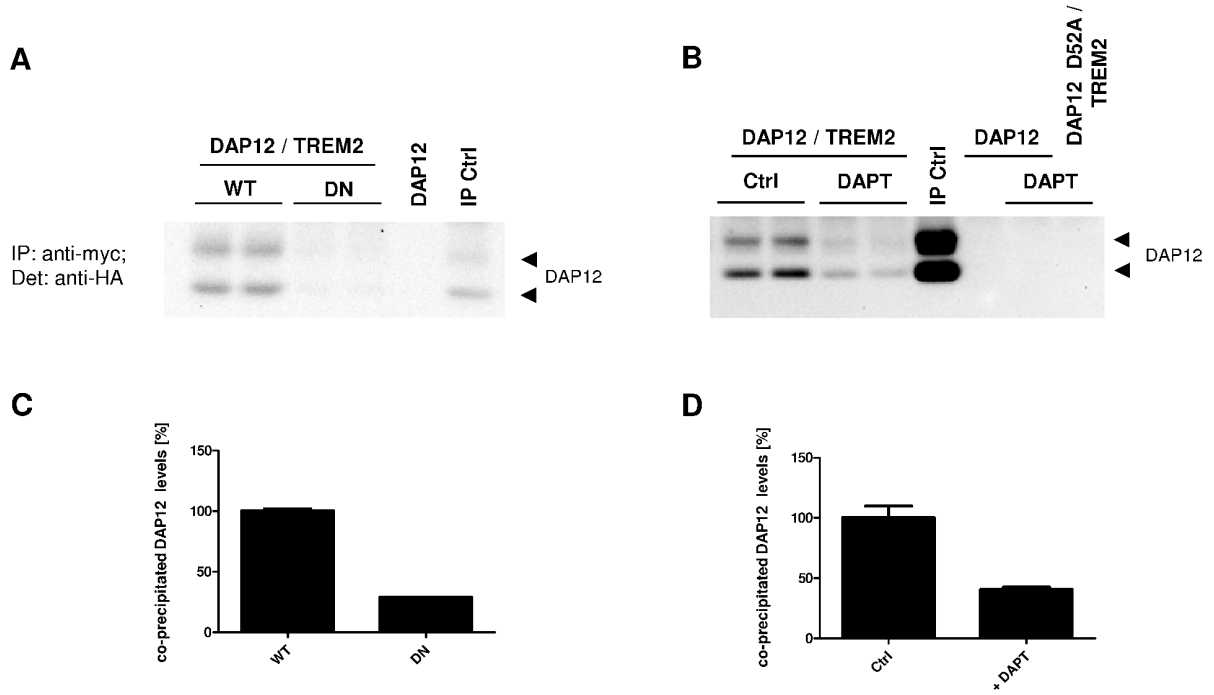

Figure 23: Inhibition of γ-secretase alters the association of TREM2 and DAP12.

(A) HEK293 PS1 WT and DN cells were transiently co-transfected with Flag-TREM2-mycHis and Flag-DAP12-HA. Cell lysates were precipitated with an anti-myc monoclonal antibody (2.3.5). Co-precipitated DAP12 was detected by western immunoblotting by an anti-HA antibody. Specificity of the co-IPs is indicated by the lack of signals when DAP12 alone was transfected (lane labeled with DAP12). Last lane (labeled with IP control) represents a control in which the protein was detected with the antibody used for precipitation. **(B)** HEK293 cells were co-transfected with TREM2-mycHis and DAP12-HA and incubated for 24 h with or without 10 µM DAPT. TREM2 was immunoprecipitated (2.3.5) with an anti-myc antibody and separated by SDS-PAGE (2.3.6). DAP12 was visualized with an anti-HA antibody. Lane 5 (labeled with IP Ctrl) represents a control in which DAP12 was immunoprecipitated and detected with an anti-HA antibody. To test the specificity of the co-IP two lanes represent control cells in which only DAP12 was transfected (labeled with DAP12). The last lane (labeled with D52A/TREM2) represents a control were the interaction site mutant of DAP12, in which the charged aspartate is mutated against alanine was transfected. **(C, D)** The DAP12 bands of two independent experiments (A, B) were quantified by ECL imaging.

Notably, DAPT treatment selectively decreases the phosphorylation of the lower migrating variant of DAP12 (fig. 24). The nature of these two bands is unclear but they might represent differentially phosphorylated forms of DAP12. Thus, inhibition of γ-secretase might selectively affect the phosphorylation of a single Tyr residue of DAP12. As a control, a DAP12 mutant in which both tyrosines (Y92, Y103) of the ITAM domain were mutated against phenylalanine (Hamer-

man et al., 2005) was transfected. This variant is not phosphorylated. Western immunoblotting (fig. 24, lower panel, WB) indicates that equal amounts of DAP12 are precipitated.

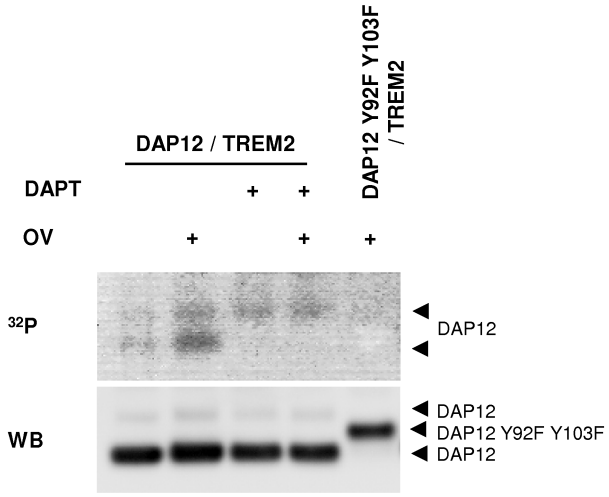

Figure 24: Inhibition of γ-secretase impairs the phosphorylation of DAP12.

HEK293 cells were transiently transfected with myc-TREM2 in combination with DAP12-HA and incubated for 24 h in presence or absence of 10 μM DAPT. As control, a mutant where both phosphorylation sites in the ITAM domain of DAP12 were mutated against phenylalanine (DAP12 Y92F Y103F-HA) was co-transfected with TREM2 (last lane). Cells were starved for 30 min in phosphate-free media and then incubated with ^{32}P-orthophosphate for 1 h. The TREM2/DAP12 system was then activated by incubation with 10 μg/ml anti-myc antibody. After further incubation of 1 h in presence or absence of 200 μM orthovanadate (OV), cells were lysed and an IP was performed with anti-HA antibodies to precipitate HA-tagged DAP12. Proteins were separated on a tris-tricine gel and transferred to a nitrocellulose membrane. Radiolabeled proteins were visualized by autoradiography (upper panel, ^{32}P). After exposure, DAP12-HA was detected on the same membrane by western immunoblotting with anti-HA antibody (lower panel, WB)

3.4 Inhibition of γ-secretase inhibition in microglia.

The data of fig. 23 and 24 indicate that the inhibition of TREM2 cleavage influences the interaction of TREM2 with DAP12. Interestingly, the subsequent phosphorylation of the DAP12 ITAM domain is inhibited and might interfere with downstream signaling. These processes might finally alter microglia specific processes like phagocytosis, cell-adhesion or migration.

3.4.1 Inhibition of γ-secretase in PS1 FAD mutants decrease phagocytosis of Aβ

γ-secretase is known to play an important role in endocytosis of lipoprotein receptors in mouse embryonic fibroblasts (Tamboli et al., 2008). Since phagocytosis is a special form of endocytosis it could be assumed that γ-secretase is also involved in phagocytosis processes. However, besides

the presented TREM2 processing nothing is known about the function of γ-secretase in microglia.

To test the involvement of γ-secretase in the phagocytosis of fAβ by microglia cells, BV-2 cells stably expressing PS1 WT, PS1 DN or PS1 L166P were generated. These stable BV-2 clones were incubated with fluorescently labeled fAβ. After 18 h the phagocytosis was measured by micro-titer plate based photospectrometry (fig. 25; see 2.3.15).

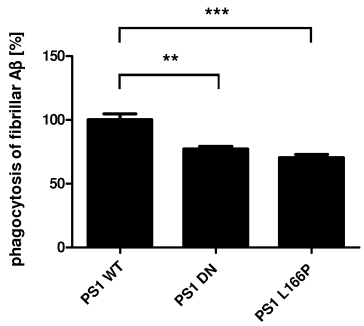

Figure 25: γ-secretase is involved in the phagocytosis of fibrillar Aβ.

BV-2 cells stably expressing PS1 WT, DN or the mutant variant L166P where incubated with fluorescent labeled fibrillar Aβ for 18 h. After quenching excessive Aβ outside the cells, the fluorescence was measured in a fluorescence spectrometer. For detailed protocol see 2.3.15.

The expression of the DN variant of presenilin and the mutated variant L166P reduces the phagocytosis of fAβ significantly, showing that γ-secretase might be involved in phagocytosis of Aβ in microglia cells.

4 DISCUSSION

Phagocytosis of cell debris, apoptotic cells, lipids, aggregated proteins or other waste material is one of the main function of microglia. Depending on the ingested material they exert either pro- or an anti-inflammatory responses.

In the AD brain, microglia with a proinflammatory phenotype are found in proximity to Aβ plaques, suggesting Aβ phagocytosis (Perlmutter et al., 1990; Frautschy et al., 1998; Bolmont et al., 2008; Meyer-Luehmann et al., 2008). There are several *in vitro* studies showing the ability of microglia to phagocytose Aβ (Koenigsknecht & Landreth 2004; Mandrekar et al., 2009; Hjorth et al., 2010; Nagano et al., 2010; Smith et al., 2010). *In vivo* uptake of injected sAβ and fAβ by microglia has also been demonstrated (Weldon et al., 1998; Takata et al., 2003). However, the ablation of microglia don't result in significant decrease of plaque growth or plaque development (Grathwohl et al., 2009), suggesting only a minor role of microglia in plaque formation, maintenance and clearance *in vivo*. Nevertheless, activation of microglia and phagocytosis of Aβ play an important role in AD as demonstrated by studies with APP transgenic mice lacking the chemokine receptor CCR2. These mice show less microglia activation and Aβ phagocytosis, resulting in increased AD progression and mortality (El Khoury et al., 2007).

Since Aβ accumulates in the brain of AD patients, there is obviously an insufficient clearance of Aβ by microglia under physiological conditions, because one function of microglia is the removal of waste material from the CNS (see 1.3). However, whether microglial phagocytosis in AD brain is defective is unclear..

Since γ-secretase has been linked to endocytosis processes previously (Tamboli et al., 2008), it might also be implicated in the regulation of phagocytosis in microglia.

Indeed, a very recent paper demonstrated a role of the γ-secretase component PS in the phagocytosis of Aβ. The treatment of the microglial cell line N9 with γ-secretase inhibitors decreased the phagocytosis of $fA\beta_{42}$. The phagocytosis was further diminished after shRNA mediated knock down of PS1 as well as in primary microglia of PS2 knock out mice (Farfara et al., 2010). However, the molecular mechanisms underlying γ-secretase dependent regulation of phagocytosis is unknown.

In this work it it shown that the triggering receptor TREM2 which is expressed on several myeloid cells including microglia is cleaved by γ-secretase. Prior to the γ-secretase cleavage the ectodomain of TREM2 is shed by a metalloprotease. The inhibition of TREM2 processing alters the interaction with its co-receptor DAP12. Moreover, blocking of the γ-secretase cleavage impairs

phosphorylation of the ITAM motif of DAP12, which is necessary for downstream signaling of TREM2 and DAP12.

Thus, cleavage of TREM2 and impaired DAP12 signaling could be a link between PS deficiency and phagocytosis defects, as observed in PS deficient microglia cells (Farfara et al., 2010)(see also chapter 3.4.1).

In accordance with this hypothesis TREM2/DAP12-dependent signaling was previously shown to regulate levels of proinflammatory cytokines after activation of TLRs (Hamerman et al., 2006). and linked to phagocytosis processes (Takahashi et al., 2005; Takahashi et al., 2007; Hsieh et al., 2009; N'Diaye et al., 2009).

4.1 Proteolytic processing of TREM2

Regulated intramembrane proteolysis (RIP) is a sequential mechanism liberating proteins from the lipid-bilayer. In the first step, cleavage by a sheddase, results in release of the ectodomain and the generation of a membrane-bound fragment of the protein. This part which consists of a small lumenal stub, a tm-domain and a cytoplasmic domain is then cleaved by a protease within the tm-domain, releasing both the lumenal part and the C-terminal domain from the membrane.

4.1.1 Shedding of the TREM2 ectodomain

Detection of soluble TREM2 ectodomain in cell culture supernatants (see chapter 3.2.4) established the shedding of TREM2. Well established sheddases are the members of the ADAM and the MMP families. Additionally, aspartate proteases like BACE-1 and -2 are also known to act as sheddases. While the members of the APP family (APP and APLPs) are the only known substrate for BACE-2, BACE-1 has several substrates. One of the first identified substrates of BACE-1 was the sialyltransferase ST6Gal I (Kitazume et al., 2003). However, the most studied substrates are APP (Hussain et al., 1999; Sinha et al., 1999; Vassar et al., 1999; Yan et al., 1999; Lin et al., 2000) and neuregulin which is involved in myelination processes (Hu et al., 2006; Willem et al., 2006; Hu et al., 2008). By the use of different protease modulators this work indicates that a protease of the ADAM or MMP family can shed TREM2 ectodomain (fig. 20, 21). However, these data don't rule out that other proteases, which might not be affected by the used modulators, contribute to TREM2 shedding. It might also be possible that TREM2 ectodomain shedding occurs by different proteases dependent on the intracellular localization and transport of both the protease and TREM2. This is known for APP, which ectodomain can either be shed

by ADAMs (Buxbaum et al., 1998; Koike et al., 1999; Lammich et al., 1999), BACE-1 or -2 (Hussain et al., 1999; Sinha et al., 1999; Vassar et al., 1999; Yan et al., 1999; Lin et al., 2000) or MMPs (Higashi & Miyazaki 2003; Ahmad et al., 2006; Yin et al., 2006; Talamagas et al., 2007). To further identity the TREM2 sheddase, surface stainings as shown in fig. 21 after treatment with more specific inhibitors are required. Alternatively, the generation of the TREM2 ECD could be measured after siRNA mediated knockdown of specific proteases or in knock out cells.

APP has been shown to be constitutively shed by ADAMs (Slack et al., 2001). Recently ADAM-10 has been established as the constitutively active α-secretase of APP in primary neurons (Kuhn et al., 2010). The low staining of myc-TREM2-GFP on the cell-surface of untreated COS7 cells (see fig. 21 G-L) suggests that TREM2 might be shed constitutively as well. However, the shedding could further be induced by treatment with the phorbol ester PDBu (see fig. 21 D-F). The effect of PDBu is most likely based on the property of phorbol ester to activate PKC (Blumberg 1988) and the resulting stimulation of ADAMs as shown for APP (Jolly-Tornetta & Wolf 2000; Skovronsky et al., 2000). The way in which PKC stimulates ADAMs is still not fully understood. Three main pathways are suggested. PKC can either phosphorylate the ADAMs directly, as has been shown by Jacobsen and colleagues (Jacobsen et al., 2010) or PKC can affect the translocation of ADAMs (Yang et al., 2007; Kohutek et al., 2009). Furthermore, PKC increases vesicle budding from the Golgi (Xu et al., 1995), thereby increasing the transport of both substrate and proteases to cell compartments where cleavage can occur. This would explain how the effect of the PKC activator TPPB which increases ADAM activity can be blocked by the transport inhibitor Brefeldin A (Yang et al., 2007).

In addition to phorbol ester, ADAM mediated shedding of APP was shown to be inducible by insulin growth factor-1 in a PKC dependent manner (Jacobsen et al., 2010).

The reduced ECD levels in HEK293 PS1 WT cells after ligation of TREM2 by an anti-myc antibody (see fig. 17) indicate that ligand binding to TREM2 might protect the full length receptor from ectodomain shedding. A possible explanation might be that ligand binding induces dimerization of TREM2, resulting in a sterical blockade of an interaction with the respective sheddase. Such an effect was shown for binding of growth hormones to the growth hormone receptor (Zhang et al., 2001). Alternatively, ligand engagement could directly alter the three dimensional structure of TREM2 thereby masking the sheddase cleavage site. This is known for Notch but in contrast to the findings regarding TREM2, binding of the Notch ligand is necessary to induce shedding of Notch ECD (Mumm & Kopan 2000; Mumm et al., 2000). Before ligand binding, Notch is locked in a protease-resistant state. Exposure to the ligand results in a conformational shift, unfolding the sheddase cleavage site (Bozkulak & Weinmaster

2009). The induction of shedding by ligand binding has also been shown for the vascular endothelial growth factor (VEGF) receptor-1 which is rendered susceptible to shedding subsequently to phosphorylation induced by binding of VEGF-A (Rahimi et al., 2009).

The reduced TREM2 FL after activation of TREM2 by antibody ligation might be due to enhanced endocytosis of the full length receptor after ligand binding (see fig. 17). Such a down-regulation of receptor signaling by endocytosis and degradation of receptor-ligand complex is a well established process, known for multiple receptors e.g. insulin receptor, EGF receptor (Sorkin & Duex 2010) and the IL-2 receptor (Legrue et al., 1991). TREM2 FL levels are reduced in HEK293 PS1 DN cells compared to HEK293 PS1 WT. However, activation of TREM2 by antibody ligation don't affect the TREM2 FL levels in HEK293 PS1 DN (see fig. 17 C), suggesting less efficient endocytosis of TREM2 after ligand binding in these cells. One explanation for this observation might be the general impairment of endocytosis upon γ-secretase inhibition (Tamboli et al., 2008). Further endocytosis assays and antibody uptake assays are necessary to assess the contribution of endocytosis in receptor down-regulation.

The ectodomain shedding of TREM2 would be consistent with the presence of soluble variants of TREM1 (sTREM1) in blood serum and plasma of septic shock patients (Gibot et al., 2004; Mahdy et al., 2006) and TREM2 (sTREM2) detected in human CSF as described in the literature (Piccio et al., 2008). The origin of sTREM is discussed controversially, in particular because sTREMs are found with or without association to DAP12. It was postulated that either a splice variant results in sTREM (Gingras et al., 2002) or that it is shed from membrane bound TREMs. sTREM1 levels decrease upon treatment of human monocytes with metalloprotease inhibitors which might suggest shedding (Gomez-Pina et al., 2007). This is further supported by the molecular weight of ~27 kDa determined for sTREM1 (Gibot et al., 2004). Nothing is known about the size of the sTREM2 fragment. However, based on the amino acid sequence, the ectodomain of TREM1 should be larger then the ectodomain of TREM2 (Bouchon et al., 2000). This led to the assumption that the ~15 kDa soluble fragment detected in this study (see fig. 17) represents a sTREM2 variant as described by Piccio and colleagues. Although, little is known about the function of the sTREMs they are suggested to negatively regulate TREM signaling by neutralizing TREM ligands (Bouchon et al., 2001a; Piccio et al., 2007; Piccio et al., 2008)

TREM2/DAP12 complexes could interact *in cis* with plexin-A1 as well as *in trans* with the plexin-A1 ligand semaphorin 6D, forming a higher order multimeric complex and regulating cellular adhesion and motility (Takegahara et al., 2006). Co-IPs with TREM2 and different deletion mutants of plexin-A1 identified the interaction site in the extracellular located TIG domain of

plexin-A1. This, and the interaction of TREM2 with semaphorin 6D *in trans*, suggest an interaction via the TREM2 ectodomain. Thus, a shedding of the TREM2 ectodomain might negatively regulate the interaction with plexin-A1, thereby modulating cellular motility and axon guidance. This might contribute to the migration defects which our lab recently observed in PS1 deficient BV-2 cells (data of Sonia Tosheva, not shown) and which were confirmed by a very recent paper, demonstrating migration deficits in N9 cell after treatment with γ-secretase inhibitors as well as in primary microglia of PS2 $^{-/-}$ mice (Farfara et al., 2010). According to this, it would be interesting to study migration of microglia cells in response to overexpression of different TREM2 variants or after treatment with shedding modulators. Furthermore, TREM2 $^{-/-}$ (Seno et al., 2009) mice could be analyzed for axonal alterations. If they exhibit an axonal phenotype, the contribution of plexin A1 and semaphorin 6D, can be further analyzed in more detail.
It is well established that shed ectodomains serve as ligands for other receptors. sAPP for example can bind to DR-6 inducing axonal pruning and neuronal death (Nikolaev et al., 2009). Additionally, the shed ectodomain of E-cadherin which binds to ErbB receptors promotes their activation (Najy et al., 2008). Thus, the TREM2 ectodomain might also serve as a ligand for another receptor. Further experiments are required to analyze the stability of the ectodomain and to find and identify putative binding partners.

4.1.2 Cleavage of TREM2 CTF by γ-secretase

Ectodomain shedding of type I membrane proteins is required for subsequent cleavage of the membrane-tethered CTF by γ-secretase. Besides γ-secretase, there are four different classes of intramembrane proteases which can catalyze the cleavage reaction within the membrane: The signal peptide peptidases (SPP) (Grigorenko et al., 2002; Ponting et al., 2002; Weihofen et al., 2002), the signal peptide peptidase like proteins (SPPLs) which cleave TNFα (Fluhrer et al., 2006; Friedmann et al., 2006), the site-2 proteases (S2P) (Rawson et al., 1997) known for the cleavage of sterol regulatory element binding proteins (SREBPs) and the rhomboid serine proteases which cleave transmembrane ligand substrates e. g. the EGF ligand Spitz in *Drosophila* (Urban et al., 2001; Freeman 2004). However, all these protein classes have specific requirements for their substrate CTFs. Only γ-secretase cleaves CTFs of type I transmembrane proteins.
Pharmacological inhibition of the γ-secretase complex with the specific inhibitor DAPT (Dovey et al., 2001) and subsequent accumulation of a TREM2 CTF fragment (see chapter. 3.1.2) reveal that TREM2 CTF is a γ-secretase substrate. This is supported by demonstration of TREM2 CTF accumulation after co-expression with PS1 DN (see chapter. 3.1.2). Both methods are well estab-

lished to prove γ-secretase mediated cleavage of the main γ-secretase substrates APP (Steiner et al., 1999; Kim et al., 2001) and Notch (Berezovska et al., 2000; Jack et al., 2001). PS1 DN is an artificial PS mutant of a critical aspartyl residue in the active site which doesn't occur in AD patients. However, there are mutations of PS1 linked to EOAD which cause partial loss of γ-secretase function according to cleavage of APP and Notch (see 1.1.2.2). The accumulation of TREM2 CTF in the tested PS FAD variants L166P and ΔEx9 (see chapter. 3.1.2) indicates that a partial loss of γ-secretase function is sufficient to impair TREM2 processing and suggests contribution of TREM2 cleavage impairment in AD pathology of patients with PS dependent EOAD. According to the age-of-onset of AD, L166P and ΔEx9 are severe mutations. Thus, it would be interesting to check whether weaker PS mutations with a later age-of-onset are also inhibit TREM2 processing.

Although γ-secretase is located in the Golgi, TGN, secretory vesicles, plasma membrane and lysosomes/endosomes, substantial γ-secretase activity is located on the plasma membrane and/or endosomes (Kaether et al., 2006a; Kaether et al., 2006b), implicating that cleavage of substrates occurs at the cell surface. Indeed, TREM2 CTF was found in immunofluorescence experiments to accumulate at the cell surface upon γ-secretase inhibition (see chapter 3.2.1). Moreover, expression of a truncated TREM2 construct (TREM2ΔECD) which lacks the ectodomain of TREM2 and thereby resembles an immediate γ-secretase substrate accumulates at the cell surface as well (see chapter 3.2.1). The surface localization of TREM2 CTF was approved and quantified by surface biotinylation studies (see chapter 3.2.1). The observed plasma membrane localization is consistent with accumulation of APP CTFs at the cell surface that follows γ-secretase inhibition (Kim et al., 2001). The same was shown for Notch, inhibition of γ-secretase either by pharmacological inhibitors or by point mutations in presenilin has been shown to end up in the accumulation of NEXT (Notch extracellular truncation) (Mumm et al., 2000).

Besides APP and Notch, the γ-secretase complex cleaves several type I transmembrane proteins. All of them are expressed on various cell types, but a microglia-specific substrate has not yet been demonstrated. Thus, TREM2 is the first identified microglia-specific γ-secretase substrate.

γ-Secretase cleaves substrate CTFs within the tm-domain, resulting in liberation of extracellular and lumenal parts from cellular membranes. While the physiological functions of extracellular peptides are largely unknown, certain ICDs (see 1.1.5.3) translocate to the nucleus and serve as transcriptional co-factor for gene regulation. This has been demonstrated for Notch, which ICD regulate the transcription of developmental genes (Mumm & Kopan 2000). To shut off the transcriptional regulation, NICD can be degraded via the ubiquitin-proteasome pathway (Gupta-Rossi et al., 2001; Oberg et al., 2001). AICD in contrast is very unstable and degraded rapidly by

the proteasome or IDE (Edbauer et al., 2002a; Buoso et al., 2010). However, some studies suggest a gene regulatory function of AICD most likely after stabilization by adapter proteins like Fe65 (Kimberly et al., 2001; Buoso et al., 2010). Notably, there are several other ICDs (e. g. ICDs of syndecan-2, nectin-1α and p75) which are rapidly degraded after their release by γ-secretase (Kopan & Ilagan 2004).

In all experiments there was no ICD of TREM2 (TICD) detectable, suggesting a fast degradation by either the ubiquitin-proteasome pathway or other proteases for example in the lysosome. To test this, TICD detection in cells treated with either proteasome inhibitors like MG132, or lysosomal inhibitors like NH_4Cl is required.

Overexpression of recombinant TICD-like fragment in HeLa cells doesn't reveal a nuclear localization (fig. 16), indicating that a transcriptional activity of TICD is unlikely. The staining pattern of the TICD-like fragment rather indicated a vesicular localization. However, the identity of these vesicles is unclear. Since lysosomal degradation of the Notch3 ICD (Jia et al., 2009) and the ErbB4 ICD (Zeng et al., 2009) has been already established, the observed vesicular staining might represent lysosomes. Future co-stainings of the TICD-like fragment and different compartment markers could help to identify the observed vesicles.

Based on the above findings, presence of TICD and contribution to nuclear signaling is unlikely, but could not be completely ruled out, because stabilization by an putative adapter protein was not tested. Such an stabilizing effect has been shown for Fe65 on the AICD. It might also be possible that an adaptor protein directly inhibit the TICD degrading enzymes.

As discussed for shedding, γ-secretase cleavage can also be induced by ligand binding. TREM2 CTF levels are slightly elevated in HEK PS1 DN cells upon activation (fig. 15) but not in PS1 WT cells. Thus, an effect of ligand binding on γ-secretase cleavage of TREM2 is unlikely, but the slight increase of CTFs could be indirectly caused by increased shedding after ligand binding. However, the demonstration of constitutive shedding of TREM2 (see fig. 21 G-L) and the unchanged TREM2 ECD levels in HEK PS1 DN cells upon activation (see fig. 17) rather favor a model in which ligand binding stabilizes TREM2 FL.

Taken together, TREM2 undergoes constitutive shedding by ADAMs or MMPs in absence of a ligand, releasing a ~15 kDa ectodomain to the supernatant. The ectodomain release is stimulated by phorbol esters supporting the role of ADAMs. The observed shedding could thereby provide an explanation for the occurrence of sTREM2 in cerebrospinal fluid (Piccio et al., 2008). The remaining CTF is subsequently cleaved by γ-secretase releasing an ICD which is rapidly degraded by the proteasome or in lysosomal compartments. All these findings clearly indicate

that TREM2 undergoes RIP. However, presence of a ligand seems to stabilize TREM2 FL at the cell surface and might induce endocytosis of the TREM2-DAP12-ligand complex.

4.2 γ-secretase dependent interaction of TREM2 and DAP12

4.2.1 Inhibition of γ-secretase cleavage alters interaction of TREM2 with DAP12

Since TICD seems to be rapidly degraded, it is unlikely that the main function of TREM2 RIP is the release of a transcriptional active fragment. Furthermore, a function of RIP in the down-regulation of signaling is unlikely. Thus, the function of TREM2 RIP remains unclear. One putative function of RIP could be the degradation of membrane localized TREM2 in absence of a ligand (see fig. 26, right side). This would coincide with the hypothesis that γ-secretase has a general role in degradation of membrane proteins (Kopan & Ilagan 2004).

Intracellularly, TREM2 is mainly localized in the Golgi complex and in cytoplasmic vesicles with constitutive shuttling to the plasma membrane (Sessa et al., 2004; Prada et al., 2006). Absence of a ligand or an interaction partner like plexin-A1 might therefore result in the accumulation of the full length receptor inside the membrane. Under these conditions, RIP might be the mechanism to remove TREM2 FL from the membrane (see fig. 26, right side). This hypothesis is supported by the vesicular staining seen in TREM2 overexpressing cells without DAPT treatment (see fig. 11). These stainings were achieved with an antibody against the C-terminal myc-tag, which is part of the TICD liberated by γ-secretase from TREM2. Thus, the staining pattern might represent vesicular structures, either containing myc-tagged TICD or uncleaved TREM2 CTFs. This idea is supported by the finding that overexpression of a TICD-like fragment results in a comparable staining pattern (see fig. 16).

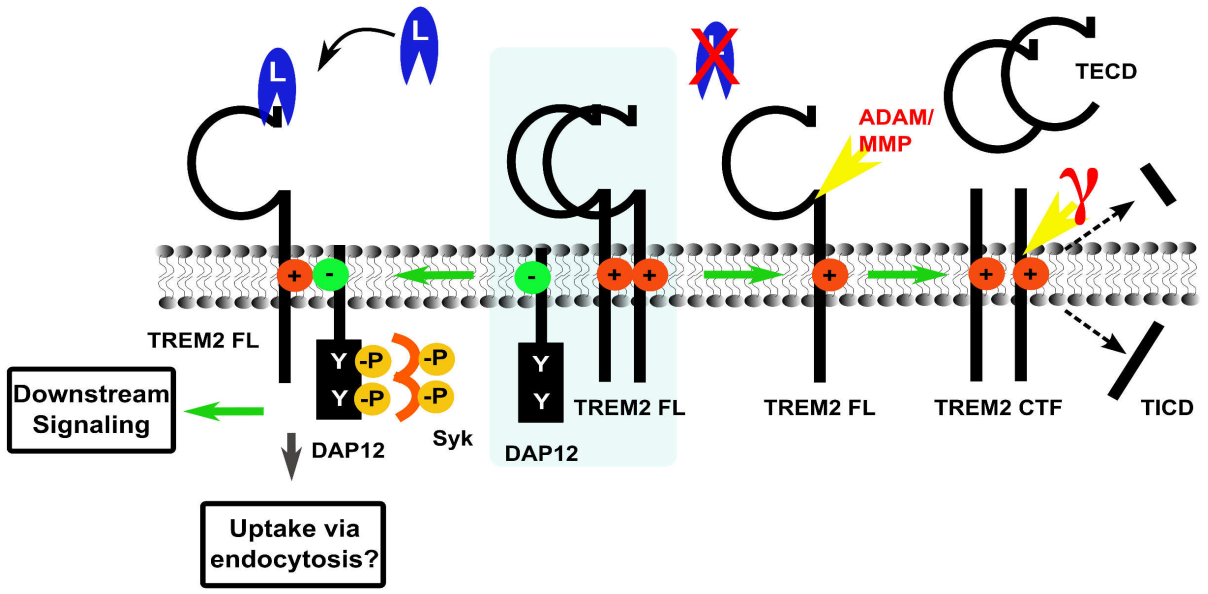

Figure 26: Hypothetical scheme for the sequential processing of TREM2.

In absence of a ligand, ectodomain of membrane-accumulated TREM2 FL (blue box) is first shed by a sheddase of the ADAM or MMP family, leaving the TREM2 CTF inside the membrane. This small stub is then cleaved by γ-secretase into two small fragments which are immediately degraded. In presence of a ligand the full-length receptor is stabilized. Ligand binding further induces dimerization with DAP12, favoring phosphorylation of the ITAM domain by a Src-family kinase. Phosphorylated ITAM recruits Syk, which then activates the downstream signaling cascade. To down-regulate the signaling the TREM2-DAP12-ligand complex is taken up into the cells most likely through endocytosis. TECD, TREM2 extracellular domain; L, ligand; TICD, TREM2 intracellular domain.

Presence and binding of a ligand might protect TREM2 FL against ectodomain shedding. This is supported by decreased levels of TECD in HEK293 PS1 WT cells upon TREM2 activation (see fig. 17). Since ectodomain shedding is an absolute prerequisite for subsequent γ-secretase cleavage, this processing step is also blocked. Hence, TREM2 FL is stabilized at the membrane and can engage with the co-receptor DAP12, stimulating downstream signaling via activation of Syk (see fig. 26, left side). To down-regulate the signaling, the binding of the ligand might further induce endocytosis of the TREM2-DAP12-ligand complex as indicated by the reduced levels of TREM2 FL after activation (see fig. 17). However, the results with increased TREM2 CTFs in HEK PS1 DN cells after activation (fig. 15), don't support this model.

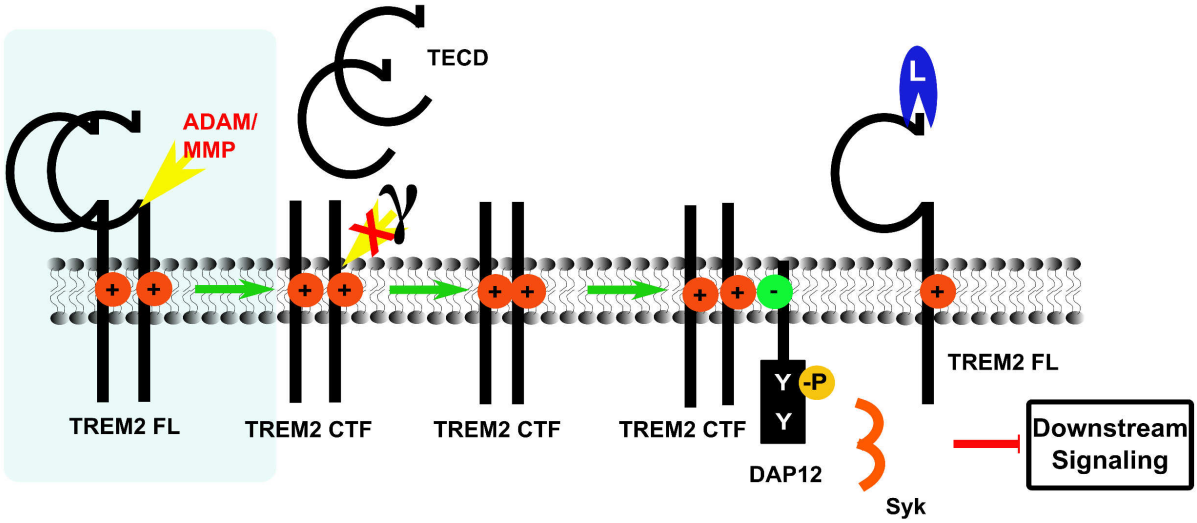

Figure 27: Hypothetical scheme of impaired TREM2 processing upon γ-secretase inhibition.

After ectodomain shedding of the full length TREM2 (blue box), TREM2 CTFs accumulate in the membrane, because subsequent degradation of the CTFs is blocked due to an inactive γ-secretase. Thus, CTFs trap DAP12 thereby preventing interaction with the FL receptor, witch is stabilized by ligand binding. This results in an incomplete phosphorylation of the ITAM domain, failed activation of Syk and impaired downstream signaling. TECD, TREM2 extracellular domain; L, ligand.

Based on the model established above (fig. 26), inhibition of γ-secretase should result in the accumulation of TREM2 CTF at the membrane. Indeed, this was shown in this work (fig. 9-13). Interaction between TREM2 and DAP12 is mediated by the charged lysine residue inside the tm-region (see 1.5 and 1.6). Since the tm-domain is part of the accumulating CTFs these fragments can engage with DAP12. Accordingly, the CTFs might be able to trap DAP12. Thus, the amount of co-receptor available to engage with TREM2 FL, or other DAP12 associated receptors, such as signal regulatory protein-β1 (SIRPβ1) (Tomasello & Vivier 2005; Gaikwad et al., 2009) or complement receptors (Mocsai et al., 2006) would be reduced. This in turn would prevent phosphorylation of DAP12 and blocks activation of the downstream located Syk. In consequence of this, downstream signaling of TREM2/DAP12 or other DAP12 associated receptors would be impaired (see fig. 27). Since TREM2-DAP12 signaling regulates phagocytosis processes, impaired interaction of functional TREM2 FL with DAP12 through γ-secretase inhibition would result in a phagocytosis defect.

4.2.2 Inhibition of γ-secretase impairs DAP12 phosphorylation

The accumulation of TREM2 at the plasma membrane (fig. 12 and 13) and the altered interaction of TREM2 with DAP12 upon γ-secretase inhibition (fig. 22, 23), support the model established in fig. 27. Moreover, the phosphorylation of DAP12 was found to be impaired. Notably, γ-

secretase inhibition doesn't result in full blocking of the DAP12 phosphorylation but in a monophosphorylated ITAM domain (fig. 24).

It was previously shown that dependent on the interacting receptor, DAP12 mediated signaling could either be activatory or inhibitory. For example signaling via DAP12 and MDL-1 (myeloid DAP12-associated lectin 1) results in calcium mobilization and cellular activation (Bakker et al., 1999). In contrast, as mentioned in the introduction (see 1.5.2), activation of DAP12 and TREM2 results in inhibition of TLR responses (Hamerman et al., 2006). To explain this paradox Turnbull & Colonna established a hypothesis in which the phosphorylation state of DAP12 (monophosphorylated or full phosphorylated) directs the downstream signaling either to activatory or inhibitory cell response (Turnbull & Colonna 2007). Based on this hypothesis, high avidity ligands are suggested to lead to a full phosphorylation of the DAP12 ITAM domain, whereas the binding of a low avidity ligand is suggested to activate SH2-domain-containing protein tyrosine phosphatase 1 (SHP1). Thereupon, SHP1 deactivates Src kinases in the signaling complex, preventing full phosphorylation of the DAP12 ITAM motif, thereby stabilizing DAP12 in a monophosphorylated state. This in turn blocks binding and activation of Syk and the downstream located PLCγ (see fig. 28, left side). PLCγ catalyzes the degradation of phosphatidylinositol-4,5-bisphosphate (PtdIns(4,5)P_2) which is necessary to anchor two proteins involved in the TLR signaling cascade, MyD88 (myeloid differentiation primary-response gene 88) and TIRAP (Toll/IL-1-receptor-domain-containing adapter protein). Thus, inhibited PLCγ would stabilize PtdIns(4,5)P_2 in the membrane, allowing binding of MyD88 and TIRAP (Kagan & Medzhitov 2006). Finally, this cascade could stabilize the TLR response (fig. 28, left side). Moreover, the inactive Syk kinase might fail to activate phosphatidylinositol-3 kinase (PI3K) (Vieira et al., 2001; Huang et al., 2006). This inhibits inactivation of AKT which in turn amplifies activation of the mitogen activated protein kinase kinase kinase (MAPKKK; fig. 29, left side) (Turnbull & Colonna 2007; Ivashkiv 2009). Recently, an additional indirect pathway was shown, coupling DAP12 signaling via intergrins to the inhibition of TLRs and to the increased expression of the anti-inflammatory cytokine IL-10 (Wang et al., 2010). This pathway would also be impaired by reduced DAP12 phosphorylation, thereby facilitating TLR response resulting in higher levels of proinflammatory cytokines.

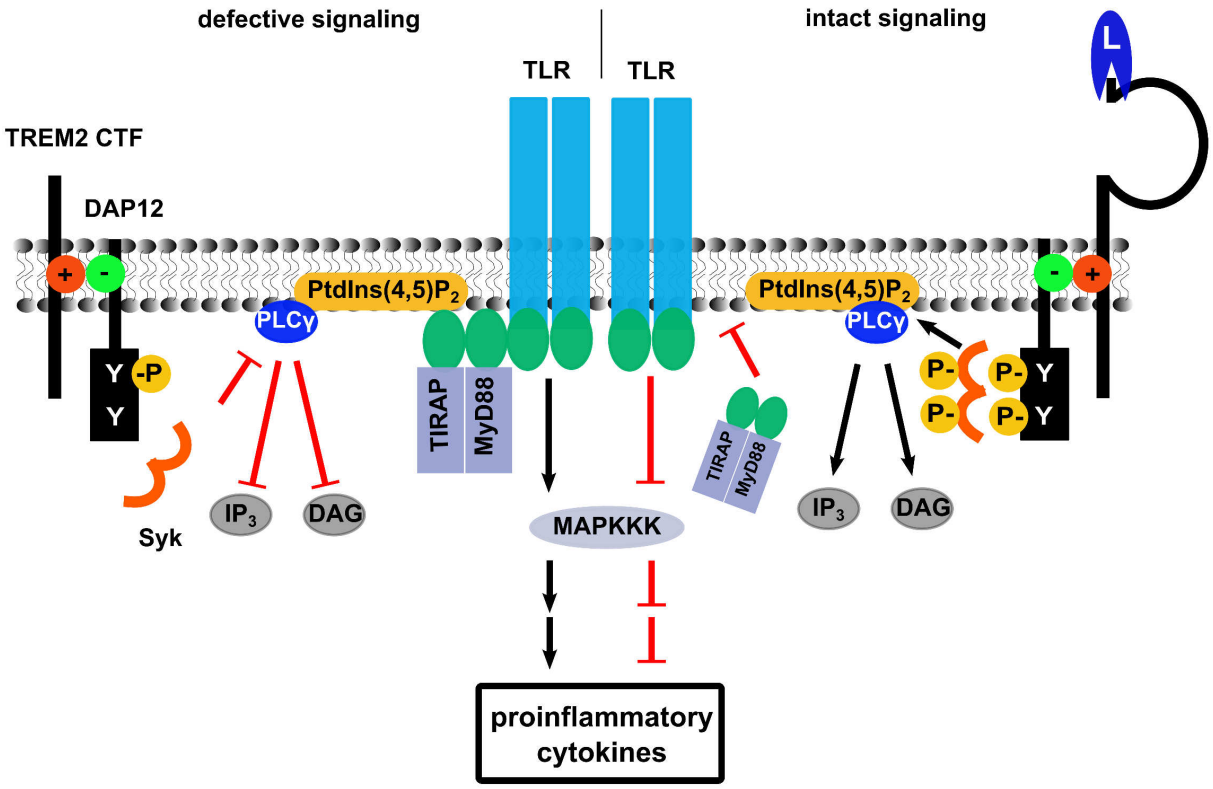

Figure 28: Impaired DAP12 signaling stabilizes TLR response via PLCγ.

In the defective signaling pathway (left side) monophosphorylated DAP12 blocks binding and activation of Syk. Inactive PLCγ stabilizes PtdIns(4,5)P_2 in the membrane. Recruitment of TIRAP and MyD88 facilitate TLR response which results finally in proinflammatory cytokine production. In the intact signaling pathway (right side) Syk is activated by a completely phosphorylated DAP12, thereby stimulating degradation of PtdIns(4,5)P_2 by PLCγ. PtdIns(4,5)P_2 functions as a docking site for TIRAP and it is required for recruitment of MyD88 to the TLR complex. Thus, PtdIns(4,5)P_2 degradation through activated PLCγ impairs TLR signaling. IP_3, inositol triphosphate; DAG, diacylglycerol. Modified from "Activating and inhibitory functions of DAP12" (Turnbull & Colonna 2007).

Inhibition of γ-secretase reduces the phosphorylation state of DAP12 (see chapter 3.3.3), which according to the hypothesis of Turnbull & Colonna could evoke both activatory or inhibitory cell responses. Thus, RIP might enable cells to switch between pro- and anti-inflammatory cell response.

As already discussed, some RIP processes involved in receptor signaling base on the release of an ICD as signal mediating fragment. Thus, RIP of TREM2 demonstrated in this work, is the first RIP dependent signaling cascade in which not the ICD, but the CTF functions as signal mediating fragment.

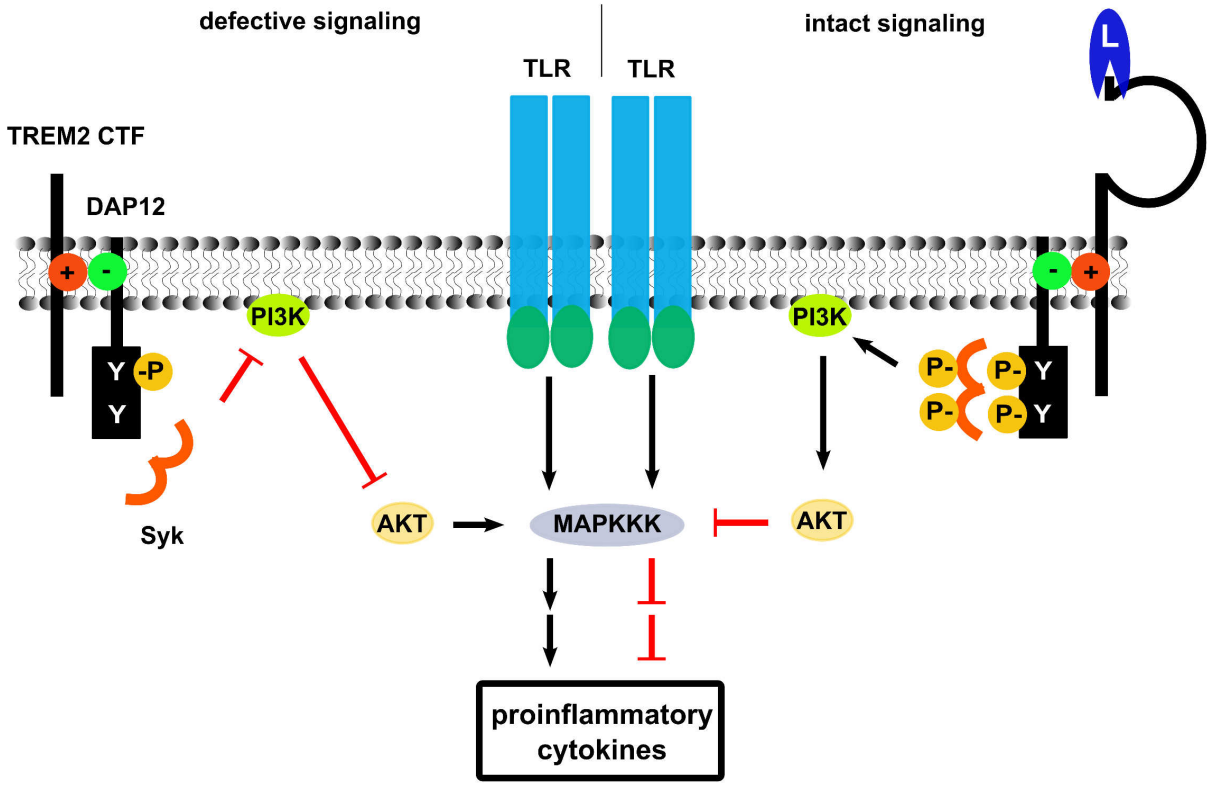

Figure 29: Impaired DAP12 signaling stabilizes TLR response via PI3K.

In the defective signaling cascade (left side) unbound Syk fail to activate PI3K, thereby stabilizing AKT activity. AKT activates MAPKKK a kinase in the downstream signaling of TLR, ending up in proinflammatory cytokine production. In the intact signaling cascade (right side) bound and activated Syk stimulates PI3K which in turn facilitates phosphorylation of AKT. Phosphorylated and thus inactivated AKT fails to phosphorylate MAPKKK. This in the end impairs production of proinflammatory cytokines. Modified from "Activating and inhibitory functions of DAP12" (Turnbull & Colonna 2007)

Notably, c-Src transcription is downregulated in response to reduced ephrin B2 signaling in PS dko MEF cells and upon pharmacological γ-secretase inhibition (Waschbusch et al., 2009). Since it is not clear which kinase of the Src family is responsible for the DAP12 phosphorylation, the reduced c-Src levels upon γ-secretase inhibition might contribute to the impaired ITAM phosphorylation. It was further shown, that the ephrin B2 intracellular domain which is released after γ-secretase cleavage can directly bind Src. This in turn impairs the interaction with the inhibitory kinase Csk, allowing autophosphorylation of Src, thereby facilitating Src activity (Georgakopoulos et al., 2006).

4.3 Potential effects of impaired TREM2/DAP12 signaling on phagocytosis and degradation of Aβ

Many studies have linked TREM2 to phagocytosis but the potential mechanism underlying this effect is unclear. Regulation of PLCγ and PI3K activity by DAP12 signaling (Jiang et al., 2002; Mao et al., 2006; Peng et al., 2010) might be involved. Impaired TREM2 signaling might thereby result in changed turnover of phosphatidylinositols (PtdIns) in the membrane.

PtdIns(4,5)P_2 is an important signaling lipid (~1-2 % of the whole content) of the inner leaflet of the membrane (Tran et al., 1993; Raucher et al., 2000) which is well known to be involved in actin filament reorganization and extension (Takenawa & Itoh 2001). It was also found to play an important role during phagocytosis. While PtdIns(4,5)P_2 accumulates in the forming phagosome at the basement, it has been shown that its deprivation, accompanied with actin disassembling is essential for phagosome sealing (Botelho et al., 2000). Impaired PtdIns(4,5)P_2 metabolism or overexpression of the PtdIns(4,5)P_2 forming enzyme phosphatidylinositol phosphate kinase I prevents actin disassembly, necessary for the completion of phagocytosis (Scott et al., 2005; Cheeseman et al., 2006). Most likely the observed deprivation of PtdIns(4,5)P_2 results from hydrolysis by PLCγ which is recruited to the phagocytic cup through the SH2 domain. Hydrolysis of PtdIns(4,5)P_2 results in the release of IP_3 and DAG. IP_3 as a Ca^{2+}-channel regulator, also plays a crucial role in phagocytosis because the occurrence of Ca^{2+}-transients during phagocytosis is well established (Nunes & Demaurex 2010). The role of DAG is not that clear, but it can induce negative curvatures of lipid membranes due to its small polar head group. Thus, it is suggested to be involved in membrane bulging and fission (Carrasco & Merida 2007). PtdIns(4,5)P_2 serves further as source for phosphatidylinositol 3,4,5-trisphosphate (PtdIns(3,4,5)P_3) another lipid found to be accumulated in the phagocytic cup. It is also established to be responsible for recruitment of myosin X, a motor protein important for pseudopod extension and closure of the phagosome (Cox et al., 2002). Generation of PtdIns(3,4,5)P_3 is catalyzed by PI3K which has to be activated by binding of active Syk to the p85 regulatory subunit. It has been shown that inhibitors of PI3K like Wortmannin affected the phagocytosis of large particles (< 3 μm in diameter), while smaller particles remain unaffected (Yeung & Grinstein 2007).

As discussed above, both PLCγ and PI3K are important for the metabolism of PtdIns during formation and closure of phagosomes. Decreased γ-secretase cleavage and impaired DAP12/TREM2 signaling might therefore alter the activity of PLCγ and PI3K (see fig. 28) and the lipid composition in and around the phagosome. This would be a putative mechanism by which inhibited TREM2 processing can account for the blocked phagocytosis of fAβ in BV-2

cells stably expressing PS1 FAD variants (see fig. 25) or for the phagocytosis defect demonstrated primary microglia of PS deficient mice and in the microglia cell line N9 after downregulation of PS1 (Farfara et al., 2010).

TREM2 mediated phagocytosis is associated with decreased levels of proinflammatory cytokines (Takahashi et al., 2005; Takahashi et al., 2007). Since PLCγ and PI3K regulate TLR signaling by the pathways illustrated in fig. 28 and 29, this would support the involvement of these two proteins in phagocytosis.

In the future, it would be interesting to measure the transition of PtdIns(4,5)P_2 with the help of the PH domain of PLCδ (Raucher et al., 2000) in life cell imaging experiments upon γ-secretase inhibition. Moreover, measurements of cytokine profiles could help to assess the contribution of γ-secretase inhibition to the regulation of pro-inflammatory cytokines. It would be further important to analyze the triggering factor of TREM2 signaling. Two different variants could be suggested which induce an ITAM mediated inflammatory cascade (see fig. 30). TREM2 might be activated either directly through Aβ or might be cross activated through an Aβ binding scavenger receptor. TREM2 has been found to be expressed in microglia surrounding Aβ plaques (Frank et al., 2008; Melchior et al., 2010). Binding studies of TREM2 with different variants of Aβ are necessary to check whether Aβ can serve as TREM2 ligand. *In vivo* phosphorylation assays can then be used to monitor the DAP12 phosphorylation state upon Aβ treatment.

It has been reported that the uptake of fAβ *in vitro* by BV-2 cells was attenuated under proinflammatory conditions (Koenigsknecht-Talboo & Landreth 2005). The authors reported that fAβ activated BV-2 cells which then responded by generating a proinflammatory environment. The inflammatory mediated suppression of fAβ uptake was dependent on NFκB activation, linking Aβ uptake to TLR response. Since ITAM signaling has been linked via the CARD9 directly to NFκB activation (Ivashkiv 2009), the suppression might be regulated by DAP12 or other ITAM containing co-receptors like FcRγ. Interestingly, the phagocytosis upon antibody mediated activation of FcR is unaffected by the proinflammatory milieu. Thus, FcRγ the ITAM-containing co-receptor of FcRs might not be involved in the NFκB activation. The levels of cytokines, chemokines and other proinflammatory molecules are elevated in brains of AD patients as well as in animal disease models (Akiyama et al., 2000). This might explain why Aβ removal from the brain is observed after passive immunization with anti-Aβ antibodies (Bard et al., 2000; Bacskai et al., 2002; Wilcock et al., 2003) as well as active immunization with Aβ (Schenk et al., 1999), while the removal of Aβ without vaccination is inefficient. Hickman and colleagues reported that the

levels of Aβ degrading enzymes like IDE and NEP are reduced in primary microglia from APP-PS1 transgenic mice in an age-dependent manner. This reduction is accompanied by inreased levels of proinflammatory cytokines and a reduction of Aβ scavenger receptors (Hickman et al., 2008).

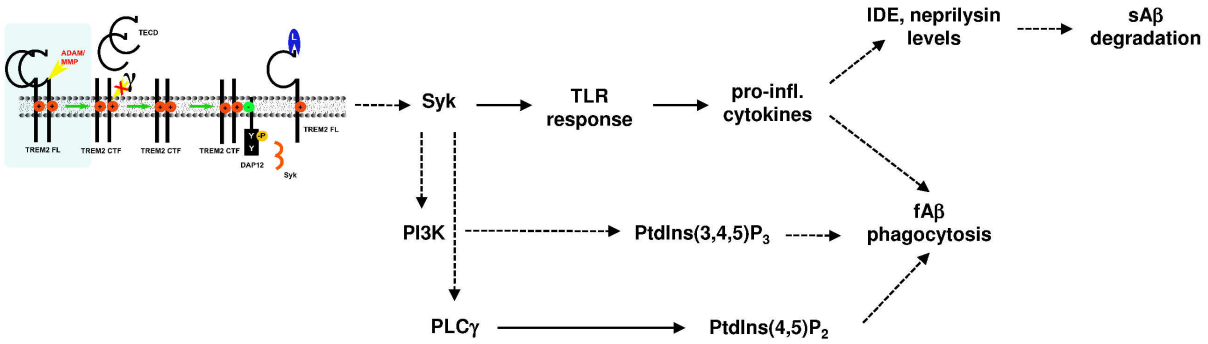

Figure 30: Hypothetical link between impaired TREM2 cleavage and attenuated Aβ phagocytosis and degeneration.

Taken together, the observed impaired γ-secretase cleavage of TREM2 leads to accumulation of TREM2 CTFs in the plasma membrane, trapping DAP12. This in turn might block the interaction with DAP12 associated receptors like TREM2 FL or SIRPβ1 involved in phagocytosis. Moreover, the DAP12 phosphorylation state is impaired due to altered interaction with TREM2 FL preventing activation of Syk. Thus, activation of PLCγ and PI3K might be impaired, resulting in a facilitated TLR response and a stabilization of PtdIns(4,5)P_2 in the microglia membrane. This in combination with the elevated levels of pro-inflammatory cytokines might then finally result in attenuated fAβ uptake and impaired degradation of sAβ by degrading proteases (fig. 30).

This proposed cascade could thereby provide a mechanism by which γ-secretase inhibition can be linked to defective phagocytosis of microglia, observed in PS deficient primary microglia (Farfara et al., 2010). This could further underlie the inefficient clearance of Aβ in brains of PS-linked AD patients.

5 OUTLOOK

So far the inefficient phagocytosis and clearance of Aβ by microglia in AD brains is not understood. However, the impaired TREM2 processing demonstrated in this work, could provide an possible explanation. Future experiments in transgenic mice would be important to test pathophysiological relevance.

TREM2 deficient mice (Colonna et al., 2007) could be crossed with an AD model like APP transgenic mice which produce increased levels of Aβ. These mice could be then compared to control mice concerning the age of plaque appearance.

The present findings indicate an involvement of γ-secretase in TREM2 mediated migration and phagocytosis of microglia. Thus, microglia behavior could be monitored in these mice by *in vivo* microscopy.

Alternatively, it would be feasible to inject different variants of Aβ into the brains of TREM2 deficient mice and to analyze the time-dependent Aβ clearance compared to control mice. The different variants of Aβ would further allow to test whether TREM2 deficiency affects the uptake of both sAβ and fAβ. However, the suggested *in vivo* experiments would only allow to monitor the phagocytosis of Aβ in respect to TREM2 deficiency and not to an impaired TREM2 processing. For this it could be helpful to analyze mice with a conditional PS knockout in microglia. In these mice the TREM2 processing could be proven by a C-terminal TREM2 antibody. Injection of Aβ in these mice would further allow to analyze phagocytosis with respect to accumulation of TREM2 CTFs. Finally, a transgenic mouse could be generated that overexpress the TREM2 CTF construct, used in this study, in microglia.

The cleavage of APP CTFs by γ-secretase is a very important step in the development of AD pathology. Modulation of γ-secretase activity by artificial γ-secretase inhibitors is therefore a frequently proposed therapeutic strategy against AD. However, based on the presented results, γ-sceretase might also regulate microglia activity via TREM2 processing. An inhibition of γ-secretase could have therefore also detrimental effects for the progress of AD. For this reason, it would be necessary to develop γ-secretase modulators which impair γ-sceretase cleavage of APP CTFs, but don't affect the processing of TREM2. Furthermore, it would be possible to develop specific inhibitors for the TREM2 sheddase. Inhibition of the TREM2 sheddase stabilizes the TREM2 FL receptor and would thereby stimulate the TREM2/DAP12 signaling pathway and promote the uptake of Aβ.

Although the known clinical methods to diagnose AD in later stages are very efficient, these

methods fail to identify risk patients. For this purpose biomarkers are of very high interest. sTREM2 has been previously detected in human blood and CSF (Gibot et al., 2004; Mahdy et al., 2006; Piccio et al., 2008). Since the demonstrated TECD seems to be similar with these sTREM2 variants, it should be feasible to detect TECD in CSF of AD patients. A strong increase of TECD in CSF would indicate an accumulation of TREM2 CTFs which could result in impaired Aβ clearance by microglia and might indicate a higher risk to develop AD. The TREM2 Aβ-like fragment has not yet been detected in human CSF or blood. Thus, detection methods for this particular fragment could be developed. Decreased levels of this fragment would then directly indicate impaired γ-secretase activity. Accordingly, cleavage products of TREM2 like TECD and the Aβ-like peptide might be used as biomarkers.

6 ABSTRACT

Alzheimer's disease (AD) is a progressive neurodegenerative disorder, affecting millions of people worldwide. AD is histopathologically characterized by the appearance of neurofibrillary tangles, which are intraneuronal accumulations of hyperphosphorylated tau protein, and extracellular β-amyloid plaques. β-Amyloid plaques arise from progressive accumulation of Aβ, a small hydrophobic peptide, in the brain. Aβ derives from sequential proteolytic processing of the amyloid precursor protein (APP). The final processing step in the generation of Aβ is catalyzed by the γ-secretase complex, consisting of presenilin-1 (PS1), the active subunit, nicastrin, Aph-1 (anterior pharynx defective-1) and PEN-2 (presenilin enhancer element-2). Besides APP, the γ-secretase has several other substrates and is also involved in the endocytosis of membrane bound lipoprotein receptors.

In addition to neurofibrillary tangles and amyloid plaques, activation of microglia and inflammatory processes are also fundamental characteristics in the brain of AD patients. Activated microglia appear to play a dual role in AD. On one hand they produce pro-inflammatory cytokines, reactive oxygen species and nitric oxide, augmenting inflammatory processes and oxidative stress which might promote neuronal damage. On the other hand microglia can phagocytose Aβ, thereby contributing to its clearance from the brain. However, the accumulation of Aβ in AD brains indicates an insufficient clearance of Aβ in AD pathogenesis which is not yet understood. Since γ-secretase was previously linked to endocytosis, it might also be implicated in phagocytic processes by microglia and clearance of Aβ.

Here it is shown by biochemical experiments in cell culture models, that the triggering receptor expressed on myeloid cells-2 (TREM2) represents a novel substrate for γ-secretase in microglia. Pharmacological inhibition of γ-secretase resulted in accumulation of a TREM2 C-terminal fragment. This fragment also accumulated upon expression of a dominant negative variant of PS1. Immunofluorescence and biotinylation experiments further indicated that the processing of TREM2 occurs at the plasma membrane. In addition, cell biological experiments demonstrated shedding of the TREM2 ectodomain. Thus, TREM2 follows the canonical proteolytic processing pathway of γ-secretase substrates which consists of an initial cleavage within the ectodomain followed by intramembranous cleavage of the resulting membrane-tethered CTF by γ-secretase. The usage of selective protease inhibitors also indicated the involvement of a metalloprotease, likely of the ADAM family, in TREM2 ectodomain shedding. TREM2 dependent signaling required the interaction with its co-receptor DAP12. Interestingly, co-immunoprecipitations revealed impaired

interaction of TREM2 and DAP12 upon γ-secretase inhibition Moreover, the impaired interaction resulted in decreased phosphorylation of DAP12. Expression of different PS1 FAD mutants, led to decreased phagocytosis of Aβ. Thus, a partial loss of γ-secretase activity might decrease the capacity of microglia to clear Aβ.

Taken together, these results indicate a critical function of γ-secretase in microglia and might help to understand molecular mechanisms underlying impaired Aβ clearance in the pathogenesis of AD.

7 REFERENCES

Acquati, F., M. Accarino, et al. (2000). "The gene encoding DRAP (BACE2), a glycosylated transmembrane protein of the aspartic protease family, maps to the down critical region." FEBS Lett **468**(1): 59-64.

Ahmad, M., T. Takino, et al. (2006). "Cleavage of amyloid-beta precursor protein (APP) by membrane-type matrix metalloproteinases." J Biochem **139**(3): 517-526.

Ahmed, R. R., C. J. Holler, et al. (2010). "BACE1 and BACE2 enzymatic activities in Alzheimer's disease." J Neurochem **112**(4): 1045-1053.

Akiyama, H., S. Barger, et al. (2000). "Inflammation and Alzheimer's disease." Neurobiol Aging **21**(3): 383-421.

Akomolafe, A., A. Beiser, et al. (2006). "Diabetes mellitus and risk of developing Alzheimer disease: results from the Framingham Study." Arch Neurol **63**(11): 1551-1555.

Alonso, A., T. Zaidi, et al. (2001). "Hyperphosphorylation induces self-assembly of tau into tangles of paired helical filaments/straight filaments." Proc Natl Acad Sci U S A **98**(12): 6923-6928.

Alves da Costa, C., C. Sunyach, et al. (2006). "Presenilin-dependent gamma-secretase-mediated control of p53-associated cell death in Alzheimer's disease." J Neurosci **26**(23): 6377-6385.

Andersen, K., L. J. Launer, et al. (1995). "Do nonsteroidal anti-inflammatory drugs decrease the risk for Alzheimer's disease? The Rotterdam Study." Neurology **45**(8): 1441-1445.

Annaert, W. G., L. Levesque, et al. (1999). "Presenilin 1 controls gamma-secretase processing of amyloid precursor protein in pre-golgi compartments of hippocampal neurons." J Cell Biol **147**(2): 277-294.

Aoki, N., A. Zganiacz, et al. (2004). "Differential regulation of DAP12 and molecules associated with DAP12 during host responses to mycobacterial infection." Infect Immun **72**(5): 2477-2483.

Apelt, J., M. Bigl, et al. (2004). "Aging-related increase in oxidative stress correlates with developmental pattern of beta-secretase activity and beta-amyloid plaque formation in transgenic Tg2576 mice with Alzheimer-like pathology." Int J Dev Neurosci **22**(7): 475-484.

Bacskai, B. J., S. T. Kajdasz, et al. (2002). "Non-Fc-mediated mechanisms are involved in clearance of amyloid-beta in vivo by immunotherapy." J Neurosci **22**(18): 7873-7878.

Bakker, A. B., E. Baker, et al. (1999). "Myeloid DAP12-associating lectin (MDL)-1 is a cell surface receptor involved in the activation of myeloid cells." Proc Natl Acad Sci U S A **96**(17): 9792-9796.

Ballatore, C., V. M. Lee, et al. (2007). "Tau-mediated neurodegeneration in Alzheimer's disease and related disorders." Nat Rev Neurosci **8**(9): 663-672.

Bamberger, M. E., M. E. Harris, et al. (2003). "A cell surface receptor complex for fibrillar beta-amyloid mediates microglial activation." J Neurosci **23**(7): 2665-2674.

Barbiero, L., L. Benussi, et al. (2003). "BACE-2 is overexpressed in Down's syndrome." Exp Neurol **182**(2): 335-345.

Bard, F., C. Cannon, et al. (2000). "Peripherally administered antibodies against amyloid beta-peptide enter the central nervous system and reduce pathology in a mouse model of Alzheimer disease." Nat Med **6**(8): 916-919.

Barrow, C. J. and M. G. Zagorski (1991). "Solution structures of beta peptide and its constituent fragments: relation to amyloid deposition." Science **253**(5016): 179-182.

Bayer, T. A., R. Cappai, et al. (1999). "It all sticks together--the APP-related family of proteins and Alzheimer's disease." Mol Psychiatry **4**(6): 524-528.

Bell, R. D., A. P. Sagare, et al. (2007). "Transport pathways for clearance of human Alzheimer's amyloid beta-peptide and apolipoproteins E and J in the mouse central nervous system." J Cereb Blood Flow Metab **27**(5): 909-918.

Benjannet, S., A. Elagoz, et al. (2001). "Post-translational processing of beta-secretase (beta-amyloid-converting enzyme) and its ectodomain shedding. The pro- and transmembrane/cytosolic domains affect its cellular activity and amyloid-beta production." J Biol Chem **276**(14): 10879-10887.

Bennett, B. D., S. Babu-Khan, et al. (2000a). "Expression analysis of BACE2 in brain and peripheral tissues." J Biol Chem **275**(27): 20647-20651.

Bennett, B. D., P. Denis, et al. (2000b). "A furin-like convertase mediates propeptide cleavage of BACE, the Alzheimer's beta -secretase." J Biol Chem **275**(48): 37712-37717.

Bentahir, M., O. Nyabi, et al. (2006). "Presenilin clinical mutations can affect gamma-secretase activity by different mechanisms." J Neurochem **96**(3): 732-742.

Berezovska, O., C. Jack, et al. (2000). "Rapid Notch1 nuclear translocation after ligand binding depends on presenilin-associated gamma-secretase activity." Ann N Y Acad Sci **920**: 223-226.

Bertram, L. and R. E. Tanzi (2008). "Thirty years of Alzheimer's disease genetics: the implications of systematic meta-analyses." Nat Rev Neurosci **9**(10): 768-778.

Betancor, L., F. Schelotto, et al. (2005). "An attenuated Salmonella Enteritidis strain derivative of the main

genotype circulating in Uruguay is an effective vaccine for chickens." Vet Microbiol **107**(1-2): 81-89.
Beutner, C., K. Roy, et al. (2010). "Generation of microglial cells from mouse embryonic stem cells." Nat Protoc **5**(9): 1481-1494.
Bickel, H. (2010). "Das Wichtigste 1 - Die Epidemiologie der Demenz." Deutsche Alzheimer Gesellschaft e.V.
Birnboim, H. C. and J. Doly (1979). "A rapid alkaline extraction procedure for screening recombinant plasmid DNA." Nucleic Acids Res **7**(6): 1513-1523.
Bleharski, J. R., V. Kiessler, et al. (2003). "A role for triggering receptor expressed on myeloid cells-1 in host defense during the early-induced and adaptive phases of the immune response." J Immunol **170**(7): 3812-3818.
Blumberg, P. M. (1988). "Protein kinase C as the receptor for the phorbol ester tumor promoters: sixth Rhoads memorial award lecture." Cancer Res **48**(1): 1-8.
Bolmont, T., F. Haiss, et al. (2008). "Dynamics of the microglial/amyloid interaction indicate a role in plaque maintenance." J Neurosci **28**(16): 4283-4292.
Bondareff, W., C. Harrington, et al. (1994). "Immunohistochemical staging of neurofibrillary degeneration in Alzheimer's disease." J Neuropathol Exp Neurol **53**(2): 158-164.
Bonifacino, J. S. (2004). "The GGA proteins: adaptors on the move." Nat Rev Mol Cell Biol **5**(1): 23-32.
Borchelt, D. R., G. Thinakaran, et al. (1996). "Familial Alzheimer's disease-linked presenilin 1 variants elevate Abeta1-42/1-40 ratio in vitro and in vivo." Neuron **17**(5): 1005-1013.
Botelho, R. J., M. Teruel, et al. (2000). "Localized biphasic changes in phosphatidylinositol-4,5-bisphosphate at sites of phagocytosis." J Cell Biol **151**(7): 1353-1368.
Bouchon, A., J. Dietrich, et al. (2000). "Cutting edge: inflammatory responses can be triggered by TREM-1, a novel receptor expressed on neutrophils and monocytes." J Immunol **164**(10): 4991-4995.
Bouchon, A., F. Facchetti, et al. (2001a). "TREM-1 amplifies inflammation and is a crucial mediator of septic shock." Nature **410**(6832): 1103-1107.
Bouchon, A., C. Hernandez-Munain, et al. (2001b). "A DAP12-mediated pathway regulates expression of CC chemokine receptor 7 and maturation of human dendritic cells." J Exp Med **194**(8): 1111-1122.
Bozkulak, E. C. and G. Weinmaster (2009). "Selective use of ADAM10 and ADAM17 in activation of Notch1 signaling." Mol Cell Biol **29**(21): 5679-5695.
Braak, H. and E. Braak (1991). "Neuropathological stageing of Alzheimer-related changes." Acta Neuropathol **82**(4): 239-259.
Braak, H. and E. Braak (1996). "Evolution of the neuropathology of Alzheimer's disease." Acta Neurol Scand Suppl **165**: 3-12.
Bradford, M. M. (1976). "A rapid and sensitive method for the quantitation of microgram quantities of protein utilizing the principle of protein-dye binding." Anal Biochem **72**: 248-254.
Brandt, R., J. Leger, et al. (1995). "Interaction of tau with the neural plasma membrane mediated by tau's amino-terminal projection domain." J Cell Biol **131**(5): 1327-1340.
Breitner, J. C., K. A. Welsh, et al. (1995). "Delayed onset of Alzheimer's disease with nonsteroidal anti-inflammatory and histamine H2 blocking drugs." Neurobiol Aging **16**(4): 523-530.
Bu, G. (2009). "Apolipoprotein E and its receptors in Alzheimer's disease: pathways, pathogenesis and therapy." Nat Rev Neurosci **10**(5): 333-344.
Bulloj, A., M. C. Leal, et al. (2010). "Insulin-degrading enzyme sorting in exosomes: a secretory pathway for a key brain amyloid-beta degrading protease." J Alzheimers Dis **19**(1): 79-95.
Buoso, E., C. Lanni, et al. (2010). "beta-Amyloid precursor protein metabolism: focus on the functions and degradation of its intracellular domain." Pharmacol Res **62**(4): 308-317.
Butovsky, O., Y. Ziv, et al. (2006). "Microglia activated by IL-4 or IFN-gamma differentially induce neurogenesis and oligodendrogenesis from adult stem/progenitor cells." Mol Cell Neurosci **31**(1): 149-160.
Buxbaum, J. D., K. N. Liu, et al. (1998). "Evidence that tumor necrosis factor alpha converting enzyme is involved in regulated alpha-secretase cleavage of the Alzheimer amyloid protein precursor." J Biol Chem **273**(43): 27765-27767.
Cai, X. D., T. E. Golde, et al. (1993). "Release of excess amyloid beta protein from a mutant amyloid beta protein precursor." Science **259**(5094): 514-516.
Cameron, B. and G. E. Landreth (2010). "Inflammation, microglia, and Alzheimer's disease." Neurobiol Dis **37**(3): 503-509.
Cao, X. and T. C. Sudhof (2001). "A transcriptionally [correction of transcriptively] active complex of APP with Fe65 and histone acetyltransferase Tip60." Science **293**(5527): 115-120.
Capell, A., J. Grunberg, et al. (1998). "The proteolytic fragments of the Alzheimer's disease-associated presenilin-1 form heterodimers and occur as a 100-150-kDa molecular mass complex." J Biol Chem **273**(6): 3205-3211.
Capell, A., H. Steiner, et al. (2000). "Maturation and pro-peptide cleavage of beta-secretase." J Biol Chem **275**(40): 30849-30854.
Cardona, A. E., E. P. Pioro, et al. (2006). "Control of microglial neurotoxicity by the fractalkine receptor." Nat

Neurosci **9**(7): 917-924.
Carrasco, S. and I. Merida (2007). "Diacylglycerol, when simplicity becomes complex." Trends Biochem Sci **32**(1): 27-36.
Cheeseman, K. L., T. Ueyama, et al. (2006). "Targeting of protein kinase C-epsilon during Fcgamma receptor-dependent phagocytosis requires the epsilonC1B domain and phospholipase C-gamma1." Mol Biol Cell **17**(2): 799-813.
Chen, F., H. Hasegawa, et al. (2006). "TMP21 is a presenilin complex component that modulates gamma-secretase but not epsilon-secretase activity." Nature **440**(7088): 1208-1212.
Choi, S. H., K. Veeraraghavalu, et al. (2008). "Non-cell-autonomous effects of presenilin 1 variants on enrichment-mediated hippocampal progenitor cell proliferation and differentiation." Neuron **59**(4): 568-580.
Chouery, E., V. Delague, et al. (2008). "Mutations in TREM2 lead to pure early-onset dementia without bone cysts." Hum Mutat **29**(9): E194-204.
Chung, D. H., W. E. Seaman, et al. (2002). "Characterization of TREM-3, an activating receptor on mouse macrophages: definition of a family of single Ig domain receptors on mouse chromosome 17." Eur J Immunol **32**(1): 59-66.
Chung, H., M. I. Brazil, et al. (1999). "Uptake, degradation, and release of fibrillar and soluble forms of Alzheimer's amyloid beta-peptide by microglial cells." J Biol Chem **274**(45): 32301-32308.
Chung, S. H. (2009). "Aberrant phosphorylation in the pathogenesis of Alzheimer's disease." BMB Rep **42**(8): 467-474.
Chyung, J. H. and D. J. Selkoe (2003). "Inhibition of receptor-mediated endocytosis demonstrates generation of amyloid beta-protein at the cell surface." J Biol Chem **278**(51): 51035-51043.
Cirrito, J. R., R. Deane, et al. (2005). "P-glycoprotein deficiency at the blood-brain barrier increases amyloid-beta deposition in an Alzheimer disease mouse model." J Clin Invest **115**(11): 3285-3290.
Citron, M., T. S. Diehl, et al. (1996). "Evidence that the 42- and 40-amino acid forms of amyloid beta protein are generated from the beta-amyloid precursor protein by different protease activities." Proc Natl Acad Sci U S A **93**(23): 13170-13175.
Citron, M., T. Oltersdorf, et al. (1992). "Mutation of the beta-amyloid precursor protein in familial Alzheimer's disease increases beta-protein production." Nature **360**(6405): 672-674.
Cleary, J. P., D. M. Walsh, et al. (2005). "Natural oligomers of the amyloid-beta protein specifically disrupt cognitive function." Nat Neurosci **8**(1): 79-84.
Codony-Servat, J., J. Albanell, et al. (1999). "Cleavage of the HER2 ectodomain is a pervanadate-activable process that is inhibited by the tissue inhibitor of metalloproteases-1 in breast cancer cells." Cancer Res **59**(6): 1196-1201.
Colonna, M. and F. Facchetti (2003). "TREM-1 (triggering receptor expressed on myeloid cells): a new player in acute inflammatory responses." J Infect Dis **187 Suppl 2**: S397-401.
Colonna, M., I. Turnbull, et al. (2007). "The enigmatic function of TREM-2 in osteoclastogenesis." Adv Exp Med Biol **602**: 97-105.
Corder, E. H., A. M. Saunders, et al. (1993). "Gene dose of apolipoprotein E type 4 allele and the risk of Alzheimer's disease in late onset families." Science **261**(5123): 921-923.
Corneveaux, J. J., A. J. Myers, et al. (2010). "Association of CR1, CLU and PICALM with Alzheimer's disease in a cohort of clinically characterized and neuropathologically verified individuals." Hum Mol Genet **19**(16): 3295-3301.
Cox, D., J. S. Berg, et al. (2002). "Myosin X is a downstream effector of PI(3)K during phagocytosis." Nat Cell Biol **4**(7): 469-477.
Creemers, J. W., D. Ines Dominguez, et al. (2001). "Processing of beta-secretase by furin and other members of the proprotein convertase family." J Biol Chem **276**(6): 4211-4217.
Daigle, I. and C. Li (1993). "apl-1, a Caenorhabditis elegans gene encoding a protein related to the human beta-amyloid protein precursor." Proc Natl Acad Sci U S A **90**(24): 12045-12049.
Davalos, D., J. Grutzendler, et al. (2005). "ATP mediates rapid microglial response to local brain injury in vivo." Nat Neurosci **8**(6): 752-758.
Daws, M. R., L. L. Lanier, et al. (2001). "Cloning and characterization of a novel mouse myeloid DAP12-associated receptor family." Eur J Immunol **31**(3): 783-791.
Daws, M. R., P. M. Sullam, et al. (2003). "Pattern recognition by TREM-2: binding of anionic ligands." J Immunol **171**(2): 594-599.
De Felice, F. G., M. N. Vieira, et al. (2009). "Protection of synapses against Alzheimer's-linked toxins: insulin signaling prevents the pathogenic binding of Abeta oligomers." Proc Natl Acad Sci U S A **106**(6): 1971-1976.
De Strooper, B. (2007). "Loss-of-function presenilin mutations in Alzheimer disease. Talking Point on the role of presenilin mutations in Alzheimer disease." EMBO Rep **8**(2): 141-146.

De Strooper, B., W. Annaert, et al. (1999). "A presenilin-1-dependent gamma-secretase-like protease mediates release of Notch intracellular domain." Nature **398**(6727): 518-522.
Deane, R., R. D. Bell, et al. (2009). "Clearance of amyloid-beta peptide across the blood-brain barrier: implication for therapies in Alzheimer's disease." CNS Neurol Disord Drug Targets **8**(1): 16-30.
Deane, R., A. Sagare, et al. (2008a). "apoE isoform-specific disruption of amyloid beta peptide clearance from mouse brain." J Clin Invest **118**(12): 4002-4013.
Deane, R., A. Sagare, et al. (2008b). "The role of the cell surface LRP and soluble LRP in blood-brain barrier Abeta clearance in Alzheimer's disease." Curr Pharm Des **14**(16): 1601-1605.
Deane, R., Z. Wu, et al. (2004). "LRP/amyloid beta-peptide interaction mediates differential brain efflux of Abeta isoforms." Neuron **43**(3): 333-344.
DeMattos, R. B., J. R. Cirrito, et al. (2004). "ApoE and clusterin cooperatively suppress Abeta levels and deposition: evidence that ApoE regulates extracellular Abeta metabolism in vivo." Neuron **41**(2): 193-202.
Dickson, D. W. (2009). "Neuropathology of non-Alzheimer degenerative disorders." Int J Clin Exp Pathol **3**(1): 1-23.
Diehlmann, A., N. Ida, et al. (1999). "Analysis of presenilin 1 and presenilin 2 expression and processing by newly developed monoclonal antibodies." J Neurosci Res **56**(4): 405-419.
Dominguez, D., J. Tournoy, et al. (2005). "Phenotypic and biochemical analyses of BACE1- and BACE2-deficient mice." J Biol Chem **280**(35): 30797-30806.
Dovey, H. F., V. John, et al. (2001). "Functional gamma-secretase inhibitors reduce beta-amyloid peptide levels in brain." J Neurochem **76**(1): 173-181.
Drewes, G., B. Trinczek, et al. (1995). "Microtubule-associated protein/microtubule affinity-regulating kinase (p110mark). A novel protein kinase that regulates tau-microtubule interactions and dynamic instability by phosphorylation at the Alzheimer-specific site serine 262." J Biol Chem **270**(13): 7679-7688.
Dries, D. R. and G. Yu (2008). "Assembly, maturation, and trafficking of the gamma-secretase complex in Alzheimer's disease." Curr Alzheimer Res **5**(2): 132-146.
Duce, J. A., A. Tsatsanis, et al. (2010). "Iron-export ferroxidase activity of beta-amyloid precursor protein is inhibited by zinc in Alzheimer's disease." Cell **142**(6): 857-867.
Duyckaerts, C., M. C. Potier, et al. (2008). "Alzheimer disease models and human neuropathology: similarities and differences." Acta Neuropathol **115**(1): 5-38.
Edbauer, D., M. Willem, et al. (2002a). "Insulin-degrading enzyme rapidly removes the beta-amyloid precursor protein intracellular domain (AICD)." J Biol Chem **277**(16): 13389-13393.
Edbauer, D., E. Winkler, et al. (2002b). "Presenilin and nicastrin regulate each other and determine amyloid beta-peptide production via complex formation." Proc Natl Acad Sci U S A **99**(13): 8666-8671.
Edwards, D. R., M. M. Handsley, et al. (2008). "The ADAM metalloproteinases." Mol Aspects Med **29**(5): 258-289.
Ekdahl, C. T., J. H. Claasen, et al. (2003). "Inflammation is detrimental for neurogenesis in adult brain." Proc Natl Acad Sci U S A **100**(23): 13632-13637.
El Khoury, J., M. Toft, et al. (2007). "Ccr2 deficiency impairs microglial accumulation and accelerates progression of Alzheimer-like disease." Nat Med **13**(4): 432-438.
Esch, F. S., P. S. Keim, et al. (1990). "Cleavage of amyloid beta peptide during constitutive processing of its precursor." Science **248**(4959): 1122-1124.
Etcheberrigaray, R., M. Tan, et al. (2004). "Therapeutic effects of PKC activators in Alzheimer's disease transgenic mice." Proc Natl Acad Sci U S A **101**(30): 11141-11146.
Farfara, D., D. Trudler, et al. (2010). "gamma-Secretase component presenilin is important for microglia beta-amyloid clearance." Ann Neurol.
Farris, W., S. Mansourian, et al. (2003). "Insulin-degrading enzyme regulates the levels of insulin, amyloid beta-protein, and the beta-amyloid precursor protein intracellular domain in vivo." Proc Natl Acad Sci U S A **100**(7): 4162-4167.
Farzan, M., C. E. Schnitzler, et al. (2000). "BACE2, a beta -secretase homolog, cleaves at the beta site and within the amyloid-beta region of the amyloid-beta precursor protein." Proc Natl Acad Sci U S A **97**(17): 9712-9717.
Feng, S. M., C. I. Sartor, et al. (2007). "The HER4 cytoplasmic domain, but not its C terminus, inhibits mammary cell proliferation." Mol Endocrinol **21**(8): 1861-1876.
Fluhrer, R., A. Capell, et al. (2002). "A non-amyloidogenic function of BACE-2 in the secretory pathway." J Neurochem **81**(5): 1011-1020.
Fluhrer, R., G. Grammer, et al. (2006). "A gamma-secretase-like intramembrane cleavage of TNFalpha by the GxGD aspartyl protease SPPL2b." Nat Cell Biol **8**(8): 894-896.
Ford, J. W. and D. W. McVicar (2009). "TREM and TREM-like receptors in inflammation and disease." Curr Opin Immunol **21**(1): 38-46.
Forstl, H. and A. Kurz (1999). "Clinical features of Alzheimer's disease." Eur Arch Psychiatry Clin Neurosci

249(6): 288-290.
Francis, R., G. McGrath, et al. (2002). "aph-1 and pen-2 are required for Notch pathway signaling, gamma-secretase cleavage of betaAPP, and presenilin protein accumulation." Dev Cell **3**(1): 85-97.
Frank, S., G. J. Burbach, et al. (2008). "TREM2 is upregulated in amyloid plaque-associated microglia in aged APP23 transgenic mice." Glia **56**(13): 1438-1447.
Frautschy, S. A., F. Yang, et al. (1998). "Microglial response to amyloid plaques in APPsw transgenic mice." Am J Pathol **152**(1): 307-317.
Freeman, M. (2004). "Proteolysis within the membrane: rhomboids revealed." Nat Rev Mol Cell Biol **5**(3): 188-197.
Friedhoff, P., M. von Bergen, et al. (2000). "Structure of tau protein and assembly into paired helical filaments." Biochim Biophys Acta **1502**(1): 122-132.
Friedmann, E., E. Hauben, et al. (2006). "SPPL2a and SPPL2b promote intramembrane proteolysis of TNFalpha in activated dendritic cells to trigger IL-12 production." Nat Cell Biol **8**(8): 843-848.
Fulga, T. A., I. Elson-Schwab, et al. (2007). "Abnormal bundling and accumulation of F-actin mediates tau-induced neuronal degeneration in vivo." Nat Cell Biol **9**(2): 139-148.
Gaikwad, S., S. Larionov, et al. (2009). "Signal regulatory protein-beta1: a microglial modulator of phagocytosis in Alzheimer's disease." Am J Pathol **175**(6): 2528-2539.
Georgakopoulos, A., C. Litterst, et al. (2006). "Metalloproteinase/Presenilin1 processing of ephrinB regulates EphB-induced Src phosphorylation and signaling." EMBO J **25**(6): 1242-1252.
Giaccone, G., F. Tagliavini, et al. (1989). "Down patients: extracellular preamyloid deposits precede neuritic degeneration and senile plaques." Neurosci Lett **97**(1-2): 232-238.
Gibot, S., M. N. Kolopp-Sarda, et al. (2004). "A soluble form of the triggering receptor expressed on myeloid cells-1 modulates the inflammatory response in murine sepsis." J Exp Med **200**(11): 1419-1426.
Gingras, M. C., H. Lapillonne, et al. (2002). "TREM-1, MDL-1, and DAP12 expression is associated with a mature stage of myeloid development." Mol Immunol **38**(11): 817-824.
Goate, A., M. C. Chartier-Harlin, et al. (1991). "Segregation of a missense mutation in the amyloid precursor protein gene with familial Alzheimer's disease." Nature **349**(6311): 704-706.
Goedert, M., C. M. Wischik, et al. (1988). "Cloning and sequencing of the cDNA encoding a core protein of the paired helical filament of Alzheimer disease: identification as the microtubule-associated protein tau." Proc Natl Acad Sci U S A **85**(11): 4051-4055.
Goldgaber, D., M. I. Lerman, et al. (1987). "Characterization and chromosomal localization of a cDNA encoding brain amyloid of Alzheimer's disease." Science **235**(4791): 877-880.
Gomez-Pina, V., A. Soares-Schanoski, et al. (2007). "Metalloproteinases shed TREM-1 ectodomain from lipopolysaccharide-stimulated human monocytes." J Immunol **179**(6): 4065-4073.
Gong, C. X., I. Grundke-Iqbal, et al. (1994). "Dephosphorylation of Alzheimer's disease abnormally phosphorylated tau by protein phosphatase-2A." Neuroscience **61**(4): 765-772.
Goutte, C., M. Tsunozaki, et al. (2002). "APH-1 is a multipass membrane protein essential for the Notch signaling pathway in Caenorhabditis elegans embryos." Proc Natl Acad Sci U S A **99**(2): 775-779.
Grathwohl, S. A., R. E. Kalin, et al. (2009). "Formation and maintenance of Alzheimer's disease beta-amyloid plaques in the absence of microglia." Nat Neurosci **12**(11): 1361-1363.
Grigorenko, A. P., Y. K. Moliaka, et al. (2002). "Novel class of polytopic proteins with domains associated with putative protease activity." Biochemistry (Mosc) **67**(7): 826-835.
Grundke-Iqbal, I., K. Iqbal, et al. (1986a). "Microtubule-associated protein tau. A component of Alzheimer paired helical filaments." J Biol Chem **261**(13): 6084-6089.
Grundke-Iqbal, I., K. Iqbal, et al. (1986b). "Abnormal phosphorylation of the microtubule-associated protein tau (tau) in Alzheimer cytoskeletal pathology." Proc Natl Acad Sci U S A **83**(13): 4913-4917.
Gupta-Rossi, N., O. Le Bail, et al. (2001). "Functional interaction between SEL-10, an F-box protein, and the nuclear form of activated Notch1 receptor." J Biol Chem **276**(37): 34371-34378.
Gutwein, P., S. Mechtersheimer, et al. (2003). "ADAM10-mediated cleavage of L1 adhesion molecule at the cell surface and in released membrane vesicles." FASEB J **17**(2): 292-294.
Haass, C., A. Y. Hung, et al. (1993). "beta-Amyloid peptide and a 3-kDa fragment are derived by distinct cellular mechanisms." J Biol Chem **268**(5): 3021-3024.
Haass, C., E. H. Koo, et al. (1992a). "Targeting of cell-surface beta-amyloid precursor protein to lysosomes: alternative processing into amyloid-bearing fragments." Nature **357**(6378): 500-503.
Haass, C., C. A. Lemere, et al. (1995). "The Swedish mutation causes early-onset Alzheimer's disease by beta-secretase cleavage within the secretory pathway." Nat Med **1**(12): 1291-1296.
Haass, C., M. G. Schlossmacher, et al. (1992b). "Amyloid beta-peptide is produced by cultured cells during normal metabolism." Nature **359**(6393): 322-325.
Haass, C. and D. J. Selkoe (1993). "Cellular processing of beta-amyloid precursor protein and the genesis of amyloid beta-peptide." Cell **75**(6): 1039-1042.
Haass, C. and H. Steiner (2002). "Alzheimer disease gamma-secretase: a complex story of GxGD-type presenilin

proteases." Trends Cell Biol **12**(12): 556-562.
Hamerman, J. A., J. R. Jarjoura, et al. (2006). "Cutting edge: inhibition of TLR and FcR responses in macrophages by triggering receptor expressed on myeloid cells (TREM)-2 and DAP12." J Immunol **177**(4): 2051-2055.
Hamerman, J. A., M. Ni, et al. (2009). "The expanding roles of ITAM adapters FcRgamma and DAP12 in myeloid cells." Immunol Rev **232**(1): 42-58.
Hamerman, J. A., N. K. Tchao, et al. (2005). "Enhanced Toll-like receptor responses in the absence of signaling adaptor DAP12." Nat Immunol **6**(6): 579-586.
Hanisch, U. K. and H. Kettenmann (2007). "Microglia: active sensor and versatile effector cells in the normal and pathologic brain." Nat Neurosci **10**(11): 1387-1394.
Hanisch, U. K., M. Prinz, et al. (2001). "The protein tyrosine kinase inhibitor AG126 prevents the massive microglial cytokine induction by pneumococcal cell walls." Eur J Immunol **31**(7): 2104-2115.
Hardy, J. and D. J. Selkoe (2002). "The amyloid hypothesis of Alzheimer's disease: progress and problems on the road to therapeutics." Science **297**(5580): 353-356.
Harold, D., R. Abraham, et al. (2009). "Genome-wide association study identifies variants at CLU and PICALM associated with Alzheimer's disease." Nat Genet **41**(10): 1088-1093.
Hartmann, D., B. de Strooper, et al. (2002). "The disintegrin/metalloprotease ADAM 10 is essential for Notch signalling but not for alpha-secretase activity in fibroblasts." Hum Mol Genet **11**(21): 2615-2624.
Hass, M. R. and B. A. Yankner (2005). "A {gamma}-secretase-independent mechanism of signal transduction by the amyloid precursor protein." J Biol Chem **280**(44): 36895-36904.
Hausler, K. G., M. Prinz, et al. (2002). "Interferon-gamma differentially modulates the release of cytokines and chemokines in lipopolysaccharide- and pneumococcal cell wall-stimulated mouse microglia and macrophages." Eur J Neurosci **16**(11): 2113-2122.
Haynes, S. E., G. Hollopeter, et al. (2006). "The P2Y12 receptor regulates microglial activation by extracellular nucleotides." Nat Neurosci **9**(12): 1512-1519.
He, G., W. Luo, et al. (2010). "Gamma-secretase activating protein is a therapeutic target for Alzheimer's disease." Nature **467**(7311): 95-98.
He, X., W. P. Chang, et al. (2002). "Memapsin 2 (beta-secretase) cytosolic domain binds to the VHS domains of GGA1 and GGA2: implications on the endocytosis mechanism of memapsin 2." FEBS Lett **524**(1-3): 183-187.
Heber, S., J. Herms, et al. (2000). "Mice with combined gene knock-outs reveal essential and partially redundant functions of amyloid precursor protein family members." J Neurosci **20**(21): 7951-7963.
Hebert, S. S., L. Serneels, et al. (2006). "Regulated intramembrane proteolysis of amyloid precursor protein and regulation of expression of putative target genes." EMBO Rep **7**(7): 739-745.
Helming, L., E. Tomasello, et al. (2008). "Essential role of DAP12 signaling in macrophage programming into a fusion-competent state." Sci Signal **1**(43): ra11.
Hemming, M. L., J. E. Elias, et al. (2008). "Proteomic profiling of gamma-secretase substrates and mapping of substrate requirements." PLoS Biol **6**(10): e257.
Herz, J. and H. H. Bock (2002). "Lipoprotein receptors in the nervous system." Annu Rev Biochem **71**: 405-434.
Herz, J. and Y. Chen (2006). "Reelin, lipoprotein receptors and synaptic plasticity." Nat Rev Neurosci **7**(11): 850-859.
Hickman, S. E., E. K. Allison, et al. (2008). "Microglial dysfunction and defective beta-amyloid clearance pathways in aging Alzheimer's disease mice." J Neurosci **28**(33): 8354-8360.
Higashi, S. and K. Miyazaki (2003). "Novel processing of beta-amyloid precursor protein catalyzed by membrane type 1 matrix metalloproteinase releases a fragment lacking the inhibitor domain against gelatinase A." Biochemistry **42**(21): 6514-6526.
Hjorth, E., D. Frenkel, et al. (2010). "Effects of immunomodulatory substances on phagocytosis of abeta(1-42) by human microglia." Int J Alzheimers Dis **2010**.
Hoek, R. M., S. R. Ruuls, et al. (2000). "Down-regulation of the macrophage lineage through interaction with OX2 (CD200)." Science **290**(5497): 1768-1771.
Hooper, C., R. Killick, et al. (2008). "The GSK3 hypothesis of Alzheimer's disease." J Neurochem **104**(6): 1433-1439.
Horuk, R. and J. L. Gross (1990). "Protein kinase C-linked inactivation of the interleukin-1 receptor in a human transformed B-cell line." Biochim Biophys Acta **1052**(1): 173-178.
Hsieh, C. L., M. Koike, et al. (2009). "A role for TREM2 ligands in the phagocytosis of apoptotic neuronal cells by microglia." J Neurochem **109**(4): 1144-1156.
Hu, X., W. He, et al. (2008). "Genetic deletion of BACE1 in mice affects remyelination of sciatic nerves." FASEB J **22**(8): 2970-2980.
Hu, X., C. W. Hicks, et al. (2006). "Bace1 modulates myelination in the central and peripheral nervous system." Nat Neurosci **9**(12): 1520-1525.

Hu, Y. and M. E. Fortini (2003). "Different cofactor activities in gamma-secretase assembly: evidence for a nicastrin-Aph-1 subcomplex." J Cell Biol **161**(4): 685-690.
Huang, Z. Y., D. R. Barreda, et al. (2006). "Differential kinase requirements in human and mouse Fc-gamma receptor phagocytosis and endocytosis." J Leukoc Biol **80**(6): 1553-1562.
Hung, A. Y. and D. J. Selkoe (1994). "Selective ectodomain phosphorylation and regulated cleavage of beta-amyloid precursor protein." EMBO J **13**(3): 534-542.
Huse, J. T., D. S. Pijak, et al. (2000). "Maturation and endosomal targeting of beta-site amyloid precursor protein-cleaving enzyme. The Alzheimer's disease beta-secretase." J Biol Chem **275**(43): 33729-33737.
Hussain, I., G. Christie, et al. (2001). "Prodomain processing of Asp1 (BACE2) is autocatalytic." J Biol Chem **276**(26): 23322-23328.
Hussain, I., D. Powell, et al. (1999). "Identification of a novel aspartic protease (Asp 2) as beta-secretase." Mol Cell Neurosci **14**(6): 419-427.
Hussain, I., D. J. Powell, et al. (2000). "ASP1 (BACE2) cleaves the amyloid precursor protein at the beta-secretase site." Mol Cell Neurosci **16**(5): 609-619.
Ishiguro, K., A. Shiratsuchi, et al. (1993). "Glycogen synthase kinase 3 beta is identical to tau protein kinase I generating several epitopes of paired helical filaments." FEBS Lett **325**(3): 167-172.
Ittner, L. M., Y. D. Ke, et al. (2010). "Dendritic function of tau mediates amyloid-beta toxicity in Alzheimer's disease mouse models." Cell **142**(3): 387-397.
Ivashkiv, L. B. (2009). "Cross-regulation of signaling by ITAM-associated receptors." Nat Immunol **10**(4): 340-347.
Iwata, N., S. Tsubuki, et al. (2001). "Metabolic regulation of brain Abeta by neprilysin." Science **292**(5521): 1550-1552.
Iwata, N., S. Tsubuki, et al. (2000). "Identification of the major Abeta1-42-degrading catabolic pathway in brain parenchyma: suppression leads to biochemical and pathological deposition." Nat Med **6**(2): 143-150.
Jack, C., O. Berezovska, et al. (2001). "Effect of PS1 deficiency and an APP gamma-secretase inhibitor on Notch1 signaling in primary mammalian neurons." Brain Res Mol Brain Res **87**(2): 166-174.
Jacobsen, K. T., L. Adlerz, et al. (2010). "Insulin-like growth factor-1 (IGF-1)-induced processing of amyloid-beta precursor protein (APP) and APP-like protein 2 is mediated by different metalloproteinases." J Biol Chem **285**(14): 10223-10231.
Jalbert, J. J., L. A. Daiello, et al. (2008). "Dementia of the Alzheimer type." Epidemiol Rev **30**: 15-34.
Jarrett, J. T., E. P. Berger, et al. (1993). "The carboxy terminus of the beta amyloid protein is critical for the seeding of amyloid formation: implications for the pathogenesis of Alzheimer's disease." Biochemistry **32**(18): 4693-4697.
Jefferies, W. A., M. R. Food, et al. (1996). "Reactive microglia specifically associated with amyloid plaques in Alzheimer's disease brain tissue express melanotransferrin." Brain Res **712**(1): 122-126.
Jia, L., G. Yu, et al. (2009). "Lysosome-dependent degradation of Notch3." Int J Biochem Cell Biol **41**(12): 2594-2598.
Jiang, K., B. Zhong, et al. (2002). "Syk regulation of phosphoinositide 3-kinase-dependent NK cell function." J Immunol **168**(7): 3155-3164.
Jiang, Q., C. Y. Lee, et al. (2008). "ApoE promotes the proteolytic degradation of Abeta." Neuron **58**(5): 681-693.
Joachim, C. L. and D. J. Selkoe (1992). "The seminal role of beta-amyloid in the pathogenesis of Alzheimer disease." Alzheimer Dis Assoc Disord **6**(1): 7-34.
Jolly-Tornetta, C. and B. A. Wolf (2000). "Protein kinase C regulation of intracellular and cell surface amyloid precursor protein (APP) cleavage in CHO695 cells." Biochemistry **39**(49): 15282-15290.
Kaether, C., C. Haass, et al. (2006a). "Assembly, trafficking and function of gamma-secretase." Neurodegener Dis **3**(4-5): 275-283.
Kaether, C., S. Schmitt, et al. (2006b). "Amyloid precursor protein and Notch intracellular domains are generated after transport of their precursors to the cell surface." Traffic **7**(4): 408-415.
Kagan, J. C. and R. Medzhitov (2006). "Phosphoinositide-mediated adaptor recruitment controls Toll-like receptor signaling." Cell **125**(5): 943-955.
Kamboh, M. I., R. L. Minster, et al. (2010). "Association of CLU and PICALM variants with Alzheimer's disease." Neurobiol Aging.
Kern, A., B. Roempp, et al. (2006). "Down-regulation of endogenous amyloid precursor protein processing due to cellular aging." J Biol Chem **281**(5): 2405-2413.
Kim, J., J. M. Basak, et al. (2009). "The role of apolipoprotein E in Alzheimer's disease." Neuron **63**(3): 287-303.
Kim, S. H., J. Y. Leem, et al. (2001). "Multiple effects of aspartate mutant presenilin 1 on the processing and trafficking of amyloid precursor protein." J Biol Chem **276**(46): 43343-43350.
Kimberly, W. T., W. Xia, et al. (2000). "The transmembrane aspartates in presenilin 1 and 2 are obligatory for gamma-secretase activity and amyloid beta-protein generation." J Biol Chem **275**(5): 3173-3178.
Kimberly, W. T., J. B. Zheng, et al. (2001). "The intracellular domain of the beta-amyloid precursor protein is stabilized by Fe65 and translocates to the nucleus in a notch-like manner." J Biol Chem **276**(43): 40288-

40292.
Kitajima, I., M. Kuriyama, et al. (1989). "Nasu-Hakola disease (membranous lipodystrophy). Clinical, histopathological and biochemical studies of three cases." J Neurol Sci **91**(1-2): 35-52.
Kitazume, S., Y. Tachida, et al. (2003). "Characterization of alpha 2,6-sialyltransferase cleavage by Alzheimer's beta -secretase (BACE1)." J Biol Chem **278**(17): 14865-14871.
Klesney-Tait, J., I. R. Turnbull, et al. (2006). "The TREM receptor family and signal integration." Nat Immunol **7**(12): 1266-1273.
Koenigsknecht-Talboo, J. and G. E. Landreth (2005). "Microglial phagocytosis induced by fibrillar beta-amyloid and IgGs are differentially regulated by proinflammatory cytokines." J Neurosci **25**(36): 8240-8249.
Koenigsknecht, J. and G. Landreth (2004). "Microglial phagocytosis of fibrillar beta-amyloid through a beta1 integrin-dependent mechanism." J Neurosci **24**(44): 9838-9846.
Koh, Y. H., C. A. von Arnim, et al. (2005). "BACE is degraded via the lysosomal pathway." J Biol Chem **280**(37): 32499-32504.
Kohutek, Z. A., C. G. diPierro, et al. (2009). "ADAM-10-mediated N-cadherin cleavage is protein kinase C-alpha dependent and promotes glioblastoma cell migration." J Neurosci **29**(14): 4605-4615.
Koike, H., S. Tomioka, et al. (1999). "Membrane-anchored metalloprotease MDC9 has an alpha-secretase activity responsible for processing the amyloid precursor protein." Biochem J **343 Pt 2**: 371-375.
Koizumi, S., Y. Shigemoto-Mogami, et al. (2007). "UDP acting at P2Y6 receptors is a mediator of microglial phagocytosis." Nature **446**(7139): 1091-1095.
Kojro, E. and F. Fahrenholz (1995). "Ligand-induced cleavage of the V2 vasopressin receptor by a plasma membrane metalloproteinase." J Biol Chem **270**(12): 6476-6481.
Koo, E. H. (2002). "The beta-amyloid precursor protein (APP) and Alzheimer's disease: does the tail wag the dog?" Traffic **3**(11): 763-770.
Kopan, R. and A. Goate (2002). "Aph-2/Nicastrin: an essential component of gamma-secretase and regulator of Notch signaling and Presenilin localization." Neuron **33**(3): 321-324.
Kopan, R. and M. X. Ilagan (2004). "Gamma-secretase: proteasome of the membrane?" Nat Rev Mol Cell Biol **5**(6): 499-504.
Kuhn, P. H., H. Wang, et al. (2010). "ADAM10 is the physiologically relevant, constitutive alpha-secretase of the amyloid precursor protein in primary neurons." EMBO J **29**(17): 3020-3032.
Kuhnke, D., G. Jedlitschky, et al. (2007). "MDR1-P-Glycoprotein (ABCB1) Mediates Transport of Alzheimer's amyloid-beta peptides--implications for the mechanisms of Abeta clearance at the blood-brain barrier." Brain Pathol **17**(4): 347-353.
LaDu, M. J., M. T. Falduto, et al. (1994). "Isoform-specific binding of apolipoprotein E to beta-amyloid." J Biol Chem **269**(38): 23403-23406.
LaFerla, F. M. and S. Oddo (2005). "Alzheimer's disease: Abeta, tau and synaptic dysfunction." Trends Mol Med **11**(4): 170-176.
Lai, E. C. (2002). "Notch cleavage: Nicastrin helps Presenilin make the final cut." Curr Biol **12**(6): R200-202.
Lam, F. C., R. Liu, et al. (2001). "beta-Amyloid efflux mediated by p-glycoprotein." J Neurochem **76**(4): 1121-1128.
Lambert, M. P., A. K. Barlow, et al. (1998). "Diffusible, nonfibrillar ligands derived from Abeta1-42 are potent central nervous system neurotoxins." Proc Natl Acad Sci U S A **95**(11): 6448-6453.
Lammich, S., E. Kojro, et al. (1999). "Constitutive and regulated alpha-secretase cleavage of Alzheimer's amyloid precursor protein by a disintegrin metalloprotease." Proc Natl Acad Sci U S A **96**(7): 3922-3927.
Lammich, S., M. Okochi, et al. (2002). "Presenilin-dependent intramembrane proteolysis of CD44 leads to the liberation of its intracellular domain and the secretion of an Abeta-like peptide." J Biol Chem **277**(47): 44754-44759.
Lanier, L. L. (2009). "DAP10- and DAP12-associated receptors in innate immunity." Immunol Rev **227**(1): 150-160.
Lanier, L. L., B. C. Corliss, et al. (1998). "Immunoreceptor DAP12 bearing a tyrosine-based activation motif is involved in activating NK cells." Nature **391**(6668): 703-707.
Lazarov, O., J. Robinson, et al. (2005). "Environmental enrichment reduces Abeta levels and amyloid deposition in transgenic mice." Cell **120**(5): 701-713.
Lee, H. K., P. Kumar, et al. (2009). "The insulin/Akt signaling pathway is targeted by intracellular beta-amyloid." Mol Biol Cell **20**(5): 1533-1544.
Lee, S. F., S. Shah, et al. (2002). "Mammalian APH-1 interacts with presenilin and nicastrin and is required for intramembrane proteolysis of amyloid-beta precursor protein and Notch." J Biol Chem **277**(47): 45013-45019.
Legrue, S. J., T. L. Sheu, et al. (1991). "The role of receptor-ligand endocytosis and degradation in interleukin-2 signaling and T-lymphocyte proliferation." Lymphokine Cytokine Res **10**(6): 431-436.
Leissring, M. A., W. Farris, et al. (2003). "Enhanced proteolysis of beta-amyloid in APP transgenic mice prevents plaque formation, secondary pathology, and premature death." Neuron **40**(6): 1087-1093.

Lesne, S., M. T. Koh, et al. (2006). "A specific amyloid-beta protein assembly in the brain impairs memory." Nature **440**(7082): 352-357.
Levy-Lahad, E., E. M. Wijsman, et al. (1995). "A familial Alzheimer's disease locus on chromosome 1." Science **269**(5226): 970-973.
Li, Q. and T. C. Sudhof (2004). "Cleavage of amyloid-beta precursor protein and amyloid-beta precursor-like protein by BACE 1." J Biol Chem **279**(11): 10542-10550.
Li, T., C. Hawkes, et al. (2006). "Cyclin-dependent protein kinase 5 primes microtubule-associated protein tau site-specifically for glycogen synthase kinase 3beta." Biochemistry **45**(10): 3134-3145.
Li, T. and H. K. Paudel (2006). "Glycogen synthase kinase 3beta phosphorylates Alzheimer's disease-specific Ser396 of microtubule-associated protein tau by a sequential mechanism." Biochemistry **45**(10): 3125-3133.
Lichtenthaler, S. F., D. I. Dominguez, et al. (2003). "The cell adhesion protein P-selectin glycoprotein ligand-1 is a substrate for the aspartyl protease BACE1." J Biol Chem **278**(49): 48713-48719.
Lin, X., G. Koelsch, et al. (2000). "Human aspartic protease memapsin 2 cleaves the beta-secretase site of beta-amyloid precursor protein." Proc Natl Acad Sci U S A **97**(4): 1456-1460.
Liu, Y., W. Hao, et al. (2006). "Suppression of microglial inflammatory activity by myelin phagocytosis: role of p47-PHOX-mediated generation of reactive oxygen species." J Neurosci **26**(50): 12904-12913.
Liu, Y., I. Soto, et al. (2005). "SIRPbeta1 is expressed as a disulfide-linked homodimer in leukocytes and positively regulates neutrophil transepithelial migration." J Biol Chem **280**(43): 36132-36140.
Luo, L. Q., L. E. Martin-Morris, et al. (1990). "Identification, secretion, and neural expression of APPL, a Drosophila protein similar to human amyloid protein precursor." J Neurosci **10**(12): 3849-3861.
Luo, W. J., H. Wang, et al. (2003). "PEN-2 and APH-1 coordinately regulate proteolytic processing of presenilin 1." J Biol Chem **278**(10): 7850-7854.
Maas, T., J. Eidenmuller, et al. (2000). "Interaction of tau with the neural membrane cortex is regulated by phosphorylation at sites that are modified in paired helical filaments." J Biol Chem **275**(21): 15733-15740.
Magdesian, M. H., M. M. Carvalho, et al. (2008). "Amyloid-beta binds to the extracellular cysteine-rich domain of Frizzled and inhibits Wnt/beta-catenin signaling." J Biol Chem **283**(14): 9359-9368.
Magnus, T., A. Chan, et al. (2001). "Microglial phagocytosis of apoptotic inflammatory T cells leads to down-regulation of microglial immune activation." J Immunol **167**(9): 5004-5010.
Mahdy, A. M., D. A. Lowes, et al. (2006). "Production of soluble triggering receptor expressed on myeloid cells by lipopolysaccharide-stimulated human neutrophils involves de novo protein synthesis." Clin Vaccine Immunol **13**(4): 492-495.
Mahley, R. W. (1988). "Apolipoprotein E: cholesterol transport protein with expanding role in cell biology." Science **240**(4852): 622-630.
Majumdar, A., D. Cruz, et al. (2007). "Activation of microglia acidifies lysosomes and leads to degradation of Alzheimer amyloid fibrils." Mol Biol Cell **18**(4): 1490-1496.
Malito, E., R. E. Hulse, et al. (2008). "Amyloid beta-degrading cryptidases: insulin degrading enzyme, presequence peptidase, and neprilysin." Cell Mol Life Sci **65**(16): 2574-2585.
Mandelkow, E. M. and E. Mandelkow (1998). "Tau in Alzheimer's disease." Trends Cell Biol **8**(11): 425-427.
Mandrekar, S., Q. Jiang, et al. (2009). "Microglia mediate the clearance of soluble Abeta through fluid phase macropinocytosis." J Neurosci **29**(13): 4252-4262.
Mantovani, A., A. Sica, et al. (2004). "The chemokine system in diverse forms of macrophage activation and polarization." Trends Immunol **25**(12): 677-686.
Mao, D., H. Epple, et al. (2006). "PLCgamma2 regulates osteoclastogenesis via its interaction with ITAM proteins and GAB2." J Clin Invest **116**(11): 2869-2879.
Marambaud, P., J. Shioi, et al. (2002). "A presenilin-1/gamma-secretase cleavage releases the E-cadherin intracellular domain and regulates disassembly of adherens junctions." EMBO J **21**(8): 1948-1956.
Marzolo, M. P., R. von Bernhardi, et al. (2000). "Expression of alpha(2)-macroglobulin receptor/low density lipoprotein receptor-related protein (LRP) in rat microglial cells." J Neurosci Res **60**(3): 401-411.
Matsuda, S., Y. Matsuda, et al. (2009). "Maturation of BRI2 generates a specific inhibitor that reduces APP processing at the plasma membrane and in endocytic vesicles." Neurobiol Aging.
Mattiace, L. A., P. Davies, et al. (1990). "Microglia in cerebellar plaques in Alzheimer's disease." Acta Neuropathol **80**(5): 493-498.
May, P., Y. K. Reddy, et al. (2002). "Proteolytic processing of low density lipoprotein receptor-related protein mediates regulated release of its intracellular domain." J Biol Chem **277**(21): 18736-18743.
McKercher, S. R., B. E. Torbett, et al. (1996). "Targeted disruption of the PU.1 gene results in multiple hematopoietic abnormalities." EMBO J **15**(20): 5647-5658.
McVicar, D. W., L. S. Taylor, et al. (1998). "DAP12-mediated signal transduction in natural killer cells. A dominant role for the Syk protein-tyrosine kinase." J Biol Chem **273**(49): 32934-32942.
Melchior, B., A. E. Garcia, et al. (2010). "Dual induction of TREM2 and tolerance-related transcript, Tmem176b, in amyloid transgenic mice: implications for vaccine-based therapies for Alzheimer's disease." ASN Neuro

2(3): e00037.
Meyer-Luehmann, M., T. L. Spires-Jones, et al. (2008). "Rapid appearance and local toxicity of amyloid-beta plaques in a mouse model of Alzheimer's disease." Nature **451**(7179): 720-724.
Milward, E. A., R. Papadopoulos, et al. (1992). "The amyloid protein precursor of Alzheimer's disease is a mediator of the effects of nerve growth factor on neurite outgrowth." Neuron **9**(1): 129-137.
Miners, J. S., S. Baig, et al. (2008). "Abeta-degrading enzymes in Alzheimer's disease." Brain Pathol **18**(2): 240-252.
Mocsai, A., C. L. Abram, et al. (2006). "Integrin signaling in neutrophils and macrophages uses adaptors containing immunoreceptor tyrosine-based activation motifs." Nat Immunol **7**(12): 1326-1333.
Mocsai, A., J. Ruland, et al. (2010). "The SYK tyrosine kinase: a crucial player in diverse biological functions." Nat Rev Immunol **10**(6): 387-402.
Monje, M. L., H. Toda, et al. (2003). "Inflammatory blockade restores adult hippocampal neurogenesis." Science **302**(5651): 1760-1765.
Morris, H. R., M. N. Khan, et al. (2001). "The genetic and pathological classification of familial frontotemporal dementia." Arch Neurol **58**(11): 1813-1816.
Motonaga, K., M. Itoh, et al. (2002). "Elevated expression of beta-site amyloid precursor protein cleaving enzyme 2 in brains of patients with Down syndrome." Neurosci Lett **326**(1): 64-66.
Mukherjee, A. and L. B. Hersh (2002). "Regulation of amyloid beta-peptide levels by enzymatic degradation." J Alzheimers Dis **4**(5): 341-348.
Mullan, M., F. Crawford, et al. (1992). "A pathogenic mutation for probable Alzheimer's disease in the APP gene at the N-terminus of beta-amyloid." Nat Genet **1**(5): 345-347.
Mumm, J. S. and R. Kopan (2000). "Notch signaling: from the outside in." Dev Biol **228**(2): 151-165.
Mumm, J. S., E. H. Schroeter, et al. (2000). "A ligand-induced extracellular cleavage regulates gamma-secretase-like proteolytic activation of Notch1." Mol Cell **5**(2): 197-206.
Murakami, D., I. Okamoto, et al. (2003). "Presenilin-dependent gamma-secretase activity mediates the intramembranous cleavage of CD44." Oncogene **22**(10): 1511-1516.
N'Diaye, E. N., C. S. Branda, et al. (2009). "TREM-2 (triggering receptor expressed on myeloid cells 2) is a phagocytic receptor for bacteria." J Cell Biol **184**(2): 215-223.
Nadler, Y., A. Alexandrovich, et al. (2008). "Increased expression of the gamma-secretase components presenilin-1 and nicastrin in activated astrocytes and microglia following traumatic brain injury." Glia **56**(5): 552-567.
Nagano, T., S. H. Kimura, et al. (2010). "Prostaglandin E2 reduces amyloid beta-induced phagocytosis in cultured rat microglia." Brain Res **1323**: 11-17.
Najy, A. J., K. C. Day, et al. (2008). "The ectodomain shedding of E-cadherin by ADAM15 supports ErbB receptor activation." J Biol Chem **283**(26): 18393-18401.
Napoli, I., K. Kierdorf, et al. (2009). "Microglial precursors derived from mouse embryonic stem cells." Glia **57**(15): 1660-1671.
Narita, M., D. M. Holtzman, et al. (1997). "Alpha2-macroglobulin complexes with and mediates the endocytosis of beta-amyloid peptide via cell surface low-density lipoprotein receptor-related protein." J Neurochem **69**(5): 1904-1911.
Naruse, S., G. Thinakaran, et al. (1998). "Effects of PS1 deficiency on membrane protein trafficking in neurons." Neuron **21**(5): 1213-1221.
Neumann, H. and K. Takahashi (2007). "Essential role of the microglial triggering receptor expressed on myeloid cells-2 (TREM2) for central nervous tissue immune homeostasis." J Neuroimmunol **184**(1-2): 92-99.
Nikolaev, A., T. McLaughlin, et al. (2009). "APP binds DR6 to trigger axon pruning and neuron death via distinct caspases." Nature **457**(7232): 981-989.
Nimmerjahn, A., F. Kirchhoff, et al. (2005). "Resting microglial cells are highly dynamic surveillants of brain parenchyma in vivo." Science **308**(5726): 1314-1318.
Nishimoto, I., T. Okamoto, et al. (1993). "Alzheimer amyloid protein precursor complexes with brain GTP-binding protein G(o)." Nature **362**(6415): 75-79.
Nunes, P. and N. Demaurex (2010). "The role of calcium signaling in phagocytosis." J Leukoc Biol **88**(1): 57-68.
Oberg, C., J. Li, et al. (2001). "The Notch intracellular domain is ubiquitinated and negatively regulated by the mammalian Sel-10 homolog." J Biol Chem **276**(38): 35847-35853.
Oddo, S., A. Caccamo, et al. (2003a). "Amyloid deposition precedes tangle formation in a triple transgenic model of Alzheimer's disease." Neurobiol Aging **24**(8): 1063-1070.
Oddo, S., A. Caccamo, et al. (2003b). "Triple-transgenic model of Alzheimer's disease with plaques and tangles: intracellular Abeta and synaptic dysfunction." Neuron **39**(3): 409-421.
Okamoto, I., Y. Kawano, et al. (2001). "Proteolytic release of CD44 intracellular domain and its role in the CD44 signaling pathway." J Cell Biol **155**(5): 755-762.
Oltersdorf, T., P. J. Ward, et al. (1990). "The Alzheimer amyloid precursor protein. Identification of a stable intermediate in the biosynthetic/degradative pathway." J Biol Chem **265**(8): 4492-4497.
Paloneva, J., M. Kestila, et al. (2000). "Loss-of-function mutations in TYROBP (DAP12) result in a presenile

dementia with bone cysts." Nat Genet **25**(3): 357-361.
Paloneva, J., J. Mandelin, et al. (2003). "DAP12/TREM2 deficiency results in impaired osteoclast differentiation and osteoporotic features." J Exp Med **198**(4): 669-675.
Paloneva, J., T. Manninen, et al. (2002). "Mutations in two genes encoding different subunits of a receptor signaling complex result in an identical disease phenotype." Am J Hum Genet **71**(3): 656-662.
Pardossi-Piquard, R., C. Bohm, et al. (2009). "TMP21 transmembrane domain regulates gamma-secretase cleavage." J Biol Chem **284**(42): 28634-28641.
Paresce, D. M., H. Chung, et al. (1997). "Slow degradation of aggregates of the Alzheimer's disease amyloid beta-protein by microglial cells." J Biol Chem **272**(46): 29390-29397.
Paresce, D. M., R. N. Ghosh, et al. (1996). "Microglial cells internalize aggregates of the Alzheimer's disease amyloid beta-protein via a scavenger receptor." Neuron **17**(3): 553-565.
Pastorino, L., A. F. Ikin, et al. (2002). "The carboxyl-terminus of BACE contains a sorting signal that regulates BACE trafficking but not the formation of total A(beta)." Mol Cell Neurosci **19**(2): 175-185.
Peng, Q., S. Malhotra, et al. (2010). "TREM2- and DAP12-dependent activation of PI3K requires DAP10 and is inhibited by SHIP1." Sci Signal **3**(122): ra38.
Perlmutter, L. S., E. Barron, et al. (1990). "Morphologic association between microglia and senile plaque amyloid in Alzheimer's disease." Neurosci Lett **119**(1): 32-36.
Perry, V. H., J. A. Nicoll, et al. (2010). "Microglia in neurodegenerative disease." Nat Rev Neurol **6**(4): 193-201.
Peschon, J. J., J. L. Slack, et al. (1998). "An essential role for ectodomain shedding in mammalian development." Science **282**(5392): 1281-1284.
Piccio, L., C. Buonsanti, et al. (2008). "Identification of soluble TREM-2 in the cerebrospinal fluid and its association with multiple sclerosis and CNS inflammation." Brain **131**(Pt 11): 3081-3091.
Piccio, L., C. Buonsanti, et al. (2007). "Blockade of TREM-2 exacerbates experimental autoimmune encephalomyelitis." Eur J Immunol **37**(5): 1290-1301.
Pike, C. J., B. J. Cummings, et al. (1994). "Beta-amyloid-induced changes in cultured astrocytes parallel reactive astrocytosis associated with senile plaques in Alzheimer's disease." Neuroscience **63**(2): 517-531.
Pitas, R. E., J. K. Boyles, et al. (1987). "Astrocytes synthesize apolipoprotein E and metabolize apolipoprotein E-containing lipoproteins." Biochim Biophys Acta **917**(1): 148-161.
Ponting, C. P., M. Hutton, et al. (2002). "Identification of a novel family of presenilin homologues." Hum Mol Genet **11**(9): 1037-1044.
Postina, R., A. Schroeder, et al. (2004). "A disintegrin-metalloproteinase prevents amyloid plaque formation and hippocampal defects in an Alzheimer disease mouse model." J Clin Invest **113**(10): 1456-1464.
Prada, I., G. N. Ongania, et al. (2006). "Triggering receptor expressed in myeloid cells 2 (TREM2) trafficking in microglial cells: continuous shuttling to and from the plasma membrane regulated by cell stimulation." Neuroscience **140**(4): 1139-1148.
Prager, K., L. Wang-Eckhardt, et al. (2007). "A structural switch of presenilin 1 by glycogen synthase kinase 3beta-mediated phosphorylation regulates the interaction with beta-catenin and its nuclear signaling." J Biol Chem **282**(19): 14083-14093.
Prince, M. and J. Jackson (2009). "World Alzheimer Report 2009." Alzheimer's Disease International.
Prokop, S., K. Shirotani, et al. (2004). "Requirement of PEN-2 for stabilization of the presenilin N-/C-terminal fragment heterodimer within the gamma-secretase complex." J Biol Chem **279**(22): 23255-23261.
Pul, R., T. Kopadze, et al. (2009). "Polyclonal immunoglobulins (IVIg) induce expression of MMP-9 in microglia." J Neuroimmunol **217**(1-2): 46-50.
Qi-Takahara, Y., M. Morishima-Kawashima, et al. (2005). "Longer forms of amyloid beta protein: implications for the mechanism of intramembrane cleavage by gamma-secretase." J Neurosci **25**(2): 436-445.
Qiu, Z., D. K. Strickland, et al. (1999). "Alpha2-macroglobulin enhances the clearance of endogenous soluble beta-amyloid peptide via low-density lipoprotein receptor-related protein in cortical neurons." J Neurochem **73**(4): 1393-1398.
Rahimi, N., T. E. Golde, et al. (2009). "Identification of ligand-induced proteolytic cleavage and ectodomain shedding of VEGFR-1/FLT1 in leukemic cancer cells." Cancer Res **69**(6): 2607-2614.
Ransohoff, R. M. and V. H. Perry (2009). "Microglial physiology: unique stimuli, specialized responses." Annu Rev Immunol **27**: 119-145.
Ratovitski, T., H. H. Slunt, et al. (1997). "Endoproteolytic processing and stabilization of wild-type and mutant presenilin." J Biol Chem **272**(39): 24536-24541.
Raucher, D., T. Stauffer, et al. (2000). "Phosphatidylinositol 4,5-bisphosphate functions as a second messenger that regulates cytoskeleton-plasma membrane adhesion." Cell **100**(2): 221-228.
Rawson, R. B., N. G. Zelenski, et al. (1997). "Complementation cloning of S2P, a gene encoding a putative metalloprotease required for intramembrane cleavage of SREBPs." Mol Cell **1**(1): 47-57.
Reed-Geaghan, E. G., J. C. Savage, et al. (2009). "CD14 and toll-like receptors 2 and 4 are required for fibrillar A{beta}-stimulated microglial activation." J Neurosci **29**(38): 11982-11992.

Reth, M. (1989). "Antigen receptor tail clue." Nature **338**(6214): 383-384.
Roberson, E. D., K. Scearce-Levie, et al. (2007). "Reducing endogenous tau ameliorates amyloid beta-induced deficits in an Alzheimer's disease mouse model." Science **316**(5825): 750-754.
Robinson, M. S. (2004). "Adaptable adaptors for coated vesicles." Trends Cell Biol **14**(4): 167-174.
Rogers, J., N. R. Cooper, et al. (1992). "Complement activation by beta-amyloid in Alzheimer disease." Proc Natl Acad Sci U S A **89**(21): 10016-10020.
Rosen, D. R., L. Martin-Morris, et al. (1989). "A Drosophila gene encoding a protein resembling the human beta-amyloid protein precursor." Proc Natl Acad Sci U S A **86**(7): 2478-2482.
Sastre, M., H. Steiner, et al. (2001). "Presenilin-dependent gamma-secretase processing of beta-amyloid precursor protein at a site corresponding to the S3 cleavage of Notch." EMBO Rep **2**(9): 835-841.
Sato, T., T. S. Diehl, et al. (2007). "Active gamma-secretase complexes contain only one of each component." J Biol Chem **282**(47): 33985-33993.
Satoh, J. and Y. Kuroda (2000). "Amyloid precursor protein beta-secretase (BACE) mRNA expression in human neural cell lines following induction of neuronal differentiation and exposure to cytokines and growth factors." Neuropathology **20**(4): 289-296.
Saxena, M. T., E. H. Schroeter, et al. (2001). "Murine notch homologs (N1-4) undergo presenilin-dependent proteolysis." J Biol Chem **276**(43): 40268-40273.
Scaffidi, P., T. Misteli, et al. (2002). "Release of chromatin protein HMGB1 by necrotic cells triggers inflammation." Nature **418**(6894): 191-195.
Schenk, D., R. Barbour, et al. (1999). "Immunization with amyloid-beta attenuates Alzheimer-disease-like pathology in the PDAPP mouse." Nature **400**(6740): 173-177.
Schmid, C. D., L. N. Sautkulis, et al. (2002). "Heterogeneous expression of the triggering receptor expressed on myeloid cells-2 on adult murine microglia." J Neurochem **83**(6): 1309-1320.
Schroeter, E. H., J. A. Kisslinger, et al. (1998). "Notch-1 signalling requires ligand-induced proteolytic release of intracellular domain." Nature **393**(6683): 382-386.
Schweizer, A., S. Kornfeld, et al. (1996). "Cysteine34 of the cytoplasmic tail of the cation-dependent mannose 6-phosphate receptor is reversibly palmitoylated and required for normal trafficking and lysosomal enzyme sorting." J Cell Biol **132**(4): 577-584.
Scott, C. C., W. Dobson, et al. (2005). "Phosphatidylinositol-4,5-bisphosphate hydrolysis directs actin remodeling during phagocytosis." J Cell Biol **169**(1): 139-149.
Seals, D. F. and S. A. Courtneidge (2003). "The ADAMs family of metalloproteases: multidomain proteins with multiple functions." Genes Dev **17**(1): 7-30.
Selkoe, D. J. (2001). "Alzheimer's disease: genes, proteins, and therapy." Physiol Rev **81**(2): 741-766.
Seno, H., H. Miyoshi, et al. (2009). "Efficient colonic mucosal wound repair requires Trem2 signaling." Proc Natl Acad Sci U S A **106**(1): 256-261.
Sessa, G., P. Podini, et al. (2004). "Distribution and signaling of TREM2/DAP12, the receptor system mutated in human polycystic lipomembraneous osteodysplasia with sclerosing leukoencephalopathy dementia." Eur J Neurosci **20**(10): 2617-2628.
Seubert, P., T. Oltersdorf, et al. (1993). "Secretion of beta-amyloid precursor protein cleaved at the amino terminus of the beta-amyloid peptide." Nature **361**(6409): 260-263.
Shah, S., S. F. Lee, et al. (2005). "Nicastrin functions as a gamma-secretase-substrate receptor." Cell **122**(3): 435-447.
Shankar, G. M., S. Li, et al. (2008). "Amyloid-beta protein dimers isolated directly from Alzheimer's brains impair synaptic plasticity and memory." Nat Med **14**(8): 837-842.
Shen, J., R. T. Bronson, et al. (1997). "Skeletal and CNS defects in Presenilin-1-deficient mice." Cell **89**(4): 629-639.
Sherrington, R., E. I. Rogaev, et al. (1995). "Cloning of a gene bearing missense mutations in early-onset familial Alzheimer's disease." Nature **375**(6534): 754-760.
Shiba, T., S. Kametaka, et al. (2004). "Insights into the phosphoregulation of beta-secretase sorting signal by the VHS domain of GGA1." Traffic **5**(6): 437-448.
Shibata, M., S. Yamada, et al. (2000). "Clearance of Alzheimer's amyloid-ss(1-40) peptide from brain by LDL receptor-related protein-1 at the blood-brain barrier." J Clin Invest **106**(12): 1489-1499.
Shoji, M., T. E. Golde, et al. (1992). "Production of the Alzheimer amyloid beta protein by normal proteolytic processing." Science **258**(5079): 126-129.
Sinha, S., J. P. Anderson, et al. (1999). "Purification and cloning of amyloid precursor protein beta-secretase from human brain." Nature **402**(6761): 537-540.
Sisodia, S. S. (1992). "Beta-amyloid precursor protein cleavage by a membrane-bound protease." Proc Natl Acad Sci U S A **89**(13): 6075-6079.
Sisodia, S. S. (1999). "Alzheimer's disease: perspectives for the new millennium." J Clin Invest **104**(9): 1169-1170.
Sisodia, S. S., E. H. Koo, et al. (1990). "Evidence that beta-amyloid protein in Alzheimer's disease is not derived

by normal processing." Science **248**(4954): 492-495.
Skovronsky, D. M., D. B. Moore, et al. (2000). "Protein kinase C-dependent alpha-secretase competes with beta-secretase for cleavage of amyloid-beta precursor protein in the trans-golgi network." J Biol Chem **275**(4): 2568-2575.
Slack, B. E., L. K. Ma, et al. (2001). "Constitutive shedding of the amyloid precursor protein ectodomain is up-regulated by tumour necrosis factor-alpha converting enzyme." Biochem J **357**(Pt 3): 787-794.
Small, S. A. and K. Duff (2008). "Linking Abeta and tau in late-onset Alzheimer's disease: a dual pathway hypothesis." Neuron **60**(4): 534-542.
Smith, A. M., H. M. Gibbons, et al. (2010). "Valproic acid enhances microglial phagocytosis of amyloid-beta(1-42)." Neuroscience **169**(1): 505-515.
Smith, P. K., R. I. Krohn, et al. (1985). "Measurement of protein using bicinchoninic acid." Anal Biochem **150**(1): 76-85.
Soba, P., S. Eggert, et al. (2005). "Homo- and heterodimerization of APP family members promotes intercellular adhesion." EMBO J **24**(20): 3624-3634.
Solans, A., X. Estivill, et al. (2000). "A new aspartyl protease on 21q22.3, BACE2, is highly similar to Alzheimer's amyloid precursor protein beta-secretase." Cytogenet Cell Genet **89**(3-4): 177-184.
Song, W., P. Nadeau, et al. (1999). "Proteolytic release and nuclear translocation of Notch-1 are induced by presenilin-1 and impaired by pathogenic presenilin-1 mutations." Proc Natl Acad Sci U S A **96**(12): 6959-6963.
Sorensen, E. B. and S. D. Conner (2010). "gamma-secretase-dependent cleavage initiates notch signaling from the plasma membrane." Traffic **11**(9): 1234-1245.
Sorkin, A. and J. E. Duex (2010). "Quantitative analysis of endocytosis and turnover of epidermal growth factor (EGF) and EGF receptor." Curr Protoc Cell Biol **Chapter 15**: Unit 15 14.
Spasic, D., A. Tolia, et al. (2006). "Presenilin-1 maintains a nine-transmembrane topology throughout the secretory pathway." J Biol Chem **281**(36): 26569-26577.
Stalder, M., A. Phinney, et al. (1999). "Association of microglia with amyloid plaques in brains of APP23 transgenic mice." Am J Pathol **154**(6): 1673-1684.
Stefano, L., G. Racchetti, et al. (2009). "The surface-exposed chaperone, Hsp60, is an agonist of the microglial TREM2 receptor." J Neurochem **110**(1): 284-294.
Steiner, H., H. Romig, et al. (1999). "Amyloidogenic function of the Alzheimer's disease-associated presenilin 1 in the absence of endoproteolysis." Biochemistry **38**(44): 14600-14605.
Steiner, H., E. Winkler, et al. (2002). "PEN-2 is an integral component of the gamma-secretase complex required for coordinated expression of presenilin and nicastrin." J Biol Chem **277**(42): 39062-39065.
Stewart, C. R., L. M. Stuart, et al. (2010). "CD36 ligands promote sterile inflammation through assembly of a Toll-like receptor 4 and 6 heterodimer." Nat Immunol **11**(2): 155-161.
Stockley, J. H., R. Ravid, et al. (2006). "Altered beta-secretase enzyme kinetics and levels of both BACE1 and BACE2 in the Alzheimer's disease brain." FEBS Lett **580**(28-29): 6550-6560.
Strittmatter, W. J., A. M. Saunders, et al. (1993). "Apolipoprotein E: high-avidity binding to beta-amyloid and increased frequency of type 4 allele in late-onset familial Alzheimer disease." Proc Natl Acad Sci U S A **90**(5): 1977-1981.
Tagliavini, F., G. Giaccone, et al. (1988). "Preamyloid deposits in the cerebral cortex of patients with Alzheimer's disease and nondemented individuals." Neurosci Lett **93**(2-3): 191-196.
Takahashi, K., M. Prinz, et al. (2007). "TREM2-transduced myeloid precursors mediate nervous tissue debris clearance and facilitate recovery in an animal model of multiple sclerosis." PLoS Med **4**(4): e124.
Takahashi, K., C. D. Rochford, et al. (2005). "Clearance of apoptotic neurons without inflammation by microglial triggering receptor expressed on myeloid cells-2." J Exp Med **201**(4): 647-657.
Takaki, R., S. R. Watson, et al. (2006). "DAP12: an adapter protein with dual functionality." Immunol Rev **214**: 118-129.
Takasugi, N., T. Tomita, et al. (2003). "The role of presenilin cofactors in the gamma-secretase complex." Nature **422**(6930): 438-441.
Takata, K., Y. Kitamura, et al. (2003). "Heat shock protein-90-induced microglial clearance of exogenous amyloid-beta1-42 in rat hippocampus in vivo." Neurosci Lett **344**(2): 87-90.
Takegahara, N., H. Takamatsu, et al. (2006). "Plexin-A1 and its interaction with DAP12 in immune responses and bone homeostasis." Nat Cell Biol **8**(6): 615-622.
Takenawa, T. and T. Itoh (2001). "Phosphoinositides, key molecules for regulation of actin cytoskeletal organization and membrane traffic from the plasma membrane." Biochim Biophys Acta **1533**(3): 190-206.
Talamagas, A. A., S. Efthimiopoulos, et al. (2007). "Abeta(1-40)-induced secretion of matrix metalloproteinase-9 results in sAPPalpha release by association with cell surface APP." Neurobiol Dis **28**(3): 304-315.
Tamboli, I. Y., E. Barth, et al. (2010). "Statins promote the degradation of extracellular amyloid {beta}-peptide by microglia via stimulation of exosome-associated IDE secretion." J Biol Chem.

Tamboli, I. Y., K. Prager, et al. (2008). "Loss of gamma-secretase function impairs endocytosis of lipoprotein particles and membrane cholesterol homeostasis." J Neurosci **28**(46): 12097-12106.

Tan, Z. S., S. Seshadri, et al. (2003). "Plasma total cholesterol level as a risk factor for Alzheimer disease: the Framingham Study." Arch Intern Med **163**(9): 1053-1057.

Tanaka, J. (2000). "Nasu-Hakola disease: a review of its leukoencephalopathic and membranolipodystrophic features." Neuropathology **20 Suppl**: S25-29.

Tatsch, M. F., C. M. Bottino, et al. (2006). "Neuropsychiatric symptoms in Alzheimer disease and cognitively impaired, nondemented elderly from a community-based sample in Brazil: prevalence and relationship with dementia severity." Am J Geriatr Psychiatry **14**(5): 438-445.

Thinakaran, G., D. B. Teplow, et al. (1996). "Metabolism of the "Swedish" amyloid precursor protein variant in neuro2a (N2a) cells. Evidence that cleavage at the "beta-secretase" site occurs in the golgi apparatus." J Biol Chem **271**(16): 9390-9397.

Tian, Q. and J. Wang (2002). "Role of serine/threonine protein phosphatase in Alzheimer's disease." Neurosignals **11**(5): 262-269.

Tomasello, E. and E. Vivier (2005). "KARAP/DAP12/TYROBP: three names and a multiplicity of biological functions." Eur J Immunol **35**(6): 1670-1677.

Tomita, S., Y. Kirino, et al. (1998). "Cleavage of Alzheimer's amyloid precursor protein (APP) by secretases occurs after O-glycosylation of APP in the protein secretory pathway. Identification of intracellular compartments in which APP cleavage occurs without using toxic agents that interfere with protein metabolism." J Biol Chem **273**(11): 6277-6284.

Tran, D., P. Gascard, et al. (1993). "Cellular distribution of polyphosphoinositides in rat hepatocytes." Cell Signal **5**(5): 565-581.

Turnbull, I. R. and M. Colonna (2007). "Activating and inhibitory functions of DAP12." Nat Rev Immunol **7**(2): 155-161.

Turnbull, I. R., S. Gilfillan, et al. (2006). "Cutting edge: TREM-2 attenuates macrophage activation." J Immunol **177**(6): 3520-3524.

Tyler, S. J., D. Dawbarn, et al. (2002). "alpha- and beta-secretase: profound changes in Alzheimer's disease." Biochem Biophys Res Commun **299**(3): 373-376.

Uchihara, T., C. Duyckaerts, et al. (1995). "ApoE immunoreactivity and microglial cells in Alzheimer's disease brain." Neurosci Lett **195**(1): 5-8.

Urban, S., J. R. Lee, et al. (2001). "Drosophila rhomboid-1 defines a family of putative intramembrane serine proteases." Cell **107**(2): 173-182.

Vassar, R., B. D. Bennett, et al. (1999). "Beta-secretase cleavage of Alzheimer's amyloid precursor protein by the transmembrane aspartic protease BACE." Science **286**(5440): 735-741.

Vassar, R. and M. Citron (2000). "Abeta-generating enzymes: recent advances in beta- and gamma-secretase research." Neuron **27**(3): 419-422.

Veeraraghavalu, K., S. H. Choi, et al. (2010). "Expression of familial Alzheimer's disease-linked human presenilin 1 variants impair enrichment-induced adult hippocampal neurogenesis." Neurodegener Dis **7**(1-3): 46-49.

Verloes, A., P. Maquet, et al. (1997). "Nasu-Hakola syndrome: polycystic lipomembranous osteodysplasia with sclerosing leucoencephalopathy and presenile dementia." J Med Genet **34**(9): 753-757.

Vernon-Wilson, E. F., W. J. Kee, et al. (2000). "CD47 is a ligand for rat macrophage membrane signal regulatory protein SIRP (OX41) and human SIRPalpha 1." Eur J Immunol **30**(8): 2130-2137.

Vetrivel, K. S., X. Meckler, et al. (2009). "Alzheimer disease Abeta production in the absence of S-palmitoylation-dependent targeting of BACE1 to lipid rafts." J Biol Chem **284**(6): 3793-3803.

Vieira, O. V., R. J. Botelho, et al. (2001). "Distinct roles of class I and class III phosphatidylinositol 3-kinases in phagosome formation and maturation." J Cell Biol **155**(1): 19-25.

Voehringer, D., D. B. Rosen, et al. (2004). "CD200 receptor family members represent novel DAP12-associated activating receptors on basophils and mast cells." J Biol Chem **279**(52): 54117-54123.

von Arnim, C. A., A. Kinoshita, et al. (2005). "The low density lipoprotein receptor-related protein (LRP) is a novel beta-secretase (BACE1) substrate." J Biol Chem **280**(18): 17777-17785.

von Koch, C. S., H. Zheng, et al. (1997). "Generation of APLP2 KO mice and early postnatal lethality in APLP2/APP double KO mice." Neurobiol Aging **18**(6): 661-669.

Vossel, K. A., K. Zhang, et al. (2010). "Tau reduction prevents Abeta-induced defects in axonal transport." Science **330**(6001): 198.

Wahle, T., K. Prager, et al. (2005). "GGA proteins regulate retrograde transport of BACE1 from endosomes to the trans-Golgi network." Mol Cell Neurosci **29**(3): 453-461.

Walsh, D. M., J. V. Fadeeva, et al. (2003). "gamma-Secretase cleavage and binding to FE65 regulate the nuclear translocation of the intracellular C-terminal domain (ICD) of the APP family of proteins." Biochemistry **42**(22): 6664-6673.

Walsh, D. M., I. Klyubin, et al. (2002). "Naturally secreted oligomers of amyloid beta protein potently inhibit

hippocampal long-term potentiation in vivo." Nature **416**(6880): 535-539.
Walter, J., A. Capell, et al. (1997). "Ectodomain phosphorylation of beta-amyloid precursor protein at two distinct cellular locations." J Biol Chem **272**(3): 1896-1903.
Walter, J., R. Fluhrer, et al. (2001a). "Phosphorylation regulates intracellular trafficking of beta-secretase." J Biol Chem **276**(18): 14634-14641.
Walter, J., J. Grunberg, et al. (1998). "Proteolytic fragments of the Alzheimer's disease associated presenilins-1 and -2 are phosphorylated in vivo by distinct cellular mechanisms." Biochemistry **37**(17): 5961-5967.
Walter, J., C. Kaether, et al. (2001b). "The cell biology of Alzheimer's disease: uncovering the secrets of secretases." Curr Opin Neurobiol **11**(5): 585-590.
Walter, J., A. Schindzielorz, et al. (2000). "Phosphorylation of the beta-amyloid precursor protein at the cell surface by ectocasein kinases 1 and 2." J Biol Chem **275**(31): 23523-23529.
Wang, D. S., D. W. Dickson, et al. (2006). "beta-Amyloid degradation and Alzheimer's disease." J Biomed Biotechnol **2006**(3): 58406.
Wang, L., R. A. Gordon, et al. (2010). "Indirect inhibition of Toll-like receptor and type I interferon responses by ITAM-coupled receptors and integrins." Immunity **32**(4): 518-530.
Waschbusch, D., S. Born, et al. (2009). "Presenilin 1 affects focal adhesion site formation and cell force generation via c-Src transcriptional and posttranslational regulation." J Biol Chem **284**(15): 10138-10149.
Webster, S., B. Bradt, et al. (1997a). "Aggregation state-dependent activation of the classical complement pathway by the amyloid beta peptide." J Neurochem **69**(1): 388-398.
Webster, S., L. F. Lue, et al. (1997b). "Molecular and cellular characterization of the membrane attack complex, C5b-9, in Alzheimer's disease." Neurobiol Aging **18**(4): 415-421.
Weggen, S., A. Diehlmann, et al. (1998). "Prominent expression of presenilin-1 in senile plaques and reactive astrocytes in Alzheimer's disease brain." Neuroreport **9**(14): 3279-3283.
Weggen, S., J. L. Eriksen, et al. (2001). "A subset of NSAIDs lower amyloidogenic Abeta42 independently of cyclooxygenase activity." Nature **414**(6860): 212-216.
Weidemann, A., G. Konig, et al. (1989). "Identification, biogenesis, and localization of precursors of Alzheimer's disease A4 amyloid protein." Cell **57**(1): 115-126.
Weihofen, A., K. Binns, et al. (2002). "Identification of signal peptide peptidase, a presenilin-type aspartic protease." Science **296**(5576): 2215-2218.
Weldon, D. T., S. D. Rogers, et al. (1998). "Fibrillar beta-amyloid induces microglial phagocytosis, expression of inducible nitric oxide synthase, and loss of a select population of neurons in the rat CNS in vivo." J Neurosci **18**(6): 2161-2173.
Wenk, G. L. (2003). "Neuropathologic changes in Alzheimer's disease." J Clin Psychiatry **64 Suppl 9**: 7-10.
Wertkin, A. M., R. S. Turner, et al. (1993). "Human neurons derived from a teratocarcinoma cell line express solely the 695-amino acid amyloid precursor protein and produce intracellular beta-amyloid or A4 peptides." Proc Natl Acad Sci U S A **90**(20): 9513-9517.
Wilcock, D. M., G. DiCarlo, et al. (2003). "Intracranially administered anti-Abeta antibodies reduce beta-amyloid deposition by mechanisms both independent of and associated with microglial activation." J Neurosci **23**(9): 3745-3751.
Willem, M., A. N. Garratt, et al. (2006). "Control of peripheral nerve myelination by the beta-secretase BACE1." Science **314**(5799): 664-666.
Wiltfang, J., H. Esselmann, et al. (2002). "Highly conserved and disease-specific patterns of carboxyterminally truncated Abeta peptides 1-37/38/39 in addition to 1-40/42 in Alzheimer's disease and in patients with chronic neuroinflammation." J Neurochem **81**(3): 481-496.
Wimo, A. and M. Prince (2010). "World Alzheimer Report 2010: The global economic impact of dementia." Alzheimer's Disease International.
Winkler, E., S. Hobson, et al. (2009). "Purification, pharmacological modulation, and biochemical characterization of interactors of endogenous human gamma-secretase." Biochemistry **48**(6): 1183-1197.
Wolfe, M. S. (2007). "When loss is gain: reduced presenilin proteolytic function leads to increased Abeta42/Abeta40. Talking Point on the role of presenilin mutations in Alzheimer disease." EMBO Rep **8**(2): 136-140.
Wolfe, M. S., J. De Los Angeles, et al. (1999a). "Are presenilins intramembrane-cleaving proteases? Implications for the molecular mechanism of Alzheimer's disease." Biochemistry **38**(35): 11223-11230.
Wolfe, M. S., W. Xia, et al. (1999b). "Two transmembrane aspartates in presenilin-1 required for presenilin endoproteolysis and gamma-secretase activity." Nature **398**(6727): 513-517.
Wong, P. C., H. Cai, et al. (2002). "Genetically engineered mouse models of neurodegenerative diseases." Nat Neurosci **5**(7): 633-639.
Woo, M. S., J. S. Park, et al. (2008). "Inhibition of MMP-3 or -9 suppresses lipopolysaccharide-induced expression of proinflammatory cytokines and iNOS in microglia." J Neurochem **106**(2): 770-780.
Wright, G. J., M. J. Puklavec, et al. (2000). "Lymphoid/neuronal cell surface OX2 glycoprotein recognizes a novel

receptor on macrophages implicated in the control of their function." Immunity **13**(2): 233-242.
Wyss-Coray, T. and L. Mucke (2002). "Inflammation in neurodegenerative disease--a double-edged sword." Neuron **35**(3): 419-432.
Xu, H., P. Greengard, et al. (1995). "Regulated formation of Golgi secretory vesicles containing Alzheimer beta-amyloid precursor protein." J Biol Chem **270**(40): 23243-23245.
Yamaguchi, H., S. Hirai, et al. (1988). "Diffuse type of senile plaques in the brains of Alzheimer-type dementia." Acta Neuropathol **77**(2): 113-119.
Yamaguchi, H., S. Hirai, et al. (1989). "Diffuse type of senile plaques in the cerebellum of Alzheimer-type dementia demonstrated by beta protein immunostain." Acta Neuropathol **77**(3): 314-319.
Yan, P., A. W. Bero, et al. (2009). "Characterizing the appearance and growth of amyloid plaques in APP/PS1 mice." J Neurosci **29**(34): 10706-10714.
Yan, R., M. J. Bienkowski, et al. (1999). "Membrane-anchored aspartyl protease with Alzheimer's disease beta-secretase activity." Nature **402**(6761): 533-537.
Yan, R., J. B. Munzner, et al. (2001). "BACE2 functions as an alternative alpha-secretase in cells." J Biol Chem **276**(36): 34019-34027.
Yan, S. D., X. Chen, et al. (1996). "RAGE and amyloid-beta peptide neurotoxicity in Alzheimer's disease." Nature **382**(6593): 685-691.
Yang, H. Q., J. Pan, et al. (2007). "New protein kinase C activator regulates amyloid precursor protein processing in vitro by increasing alpha-secretase activity." Eur J Neurosci **26**(2): 381-391.
Yeung, T. and S. Grinstein (2007). "Lipid signaling and the modulation of surface charge during phagocytosis." Immunol Rev **219**: 17-36.
Yin, K. J., J. R. Cirrito, et al. (2006). "Matrix metalloproteinases expressed by astrocytes mediate extracellular amyloid-beta peptide catabolism." J Neurosci **26**(43): 10939-10948.
Yu, G., M. Nishimura, et al. (2000). "Nicastrin modulates presenilin-mediated notch/glp-1 signal transduction and betaAPP processing." Nature **407**(6800): 48-54.
Zeng, F., J. Xu, et al. (2009). "Nedd4 mediates ErbB4 JM-a/CYT-1 ICD ubiquitination and degradation in MDCK II cells." FASEB J **23**(6): 1935-1945.
Zhang, Y., R. Guan, et al. (2001). "Growth hormone (GH)-induced dimerization inhibits phorbol ester-stimulated GH receptor proteolysis." J Biol Chem **276**(27): 24565-24573.
Zheng, H., M. Jiang, et al. (1995). "beta-Amyloid precursor protein-deficient mice show reactive gliosis and decreased locomotor activity." Cell **81**(4): 525-531.
Zheng, H. and E. H. Koo (2006). "The amyloid precursor protein: beyond amyloid." Mol Neurodegener **1**: 5.
Zhou, S., H. Zhou, et al. (2005). "CD147 is a regulatory subunit of the gamma-secretase complex in Alzheimer's disease amyloid beta-peptide production." Proc Natl Acad Sci U S A **102**(21): 7499-7504.
Zlokovic, B. V. (2008). "The blood-brain barrier in health and chronic neurodegenerative disorders." Neuron **57**(2): 178-201.

8 ACKNOWLEDGMENT

I express my deep gratitude to my supervisor Prof. Dr. Jochen Walter for giving me the opportunity to carry out this study in his lab. His encouragement, continued guidance and perpetual support from the initial to the final level made this thesis possible.

I am grateful to Prof. Dr. Sven Burgdorf that he kindly agreed to act as the second referee for this dissertation. I am also thankful to Prof. Dr. Thorsten Lang and Prof. Dr. Harald Neumann for their valuable time.

I thank Prof. Harald Neumann for his support. The meetings with him brought up always new ideas. Furthermore; I thank him and his colleagues for providing me the ES derived microglia cells as well as the initial TREM2 and DAP12 constructs which serve as basis for all constructs cloned during this thesis. I thank Dr. Markus Kummer for helping me to carry out the Aβ phagocytosis assay.

I deeply appreciate the help of all my former and present lab colleagues Dr. Kai Prager, Dr. Natasa Kukoc, Dr. Tina Wahle, Dr. Martin Siepmann, Dr. Irfan Tamboli, Dr. Sathish Kumar, Dr. Konstantin Glebov, Jessica, Heike, Esther, Sonia, Manish, Tien, Sebastian, Leonie and Mareike and the members of the neurobiology lab. I sincerely thank all of you for the discussions, advice, critical comments, friendship and time and for offering a very conducive environment in the lab. I enjoyed all the fun, laughs and lab events we had together.

I thank all people, who critically read this thesis and gave constructive comments. I also thank all my friends for understanding me and giving a helping hand whenever needed.

Last but not least, I owe my deepest gratitude to my family. Without your support and believe in me, I would have never reach this milestone.

In no words I can express my gratitude to Heike. Your everlasting encouragement and understanding, faith in me and love, gave me the energy to overcome all adversities.

9 CURRICULUM VITAE

PATRICK WUNDERLICH

PUBLIKATIONEN

Tamboli IY, Barth E, Christian L, Siepmann M, Kumar S, Singh S, Tolksdorf K, Heneka MT, Lütjohann D, Wunderlich P, Walter J (2010): Statins promote the degradation of extracellular amyloid {beta}-peptide by microglia via stimulation of exosome-associated insulin-degrading enzyme (IDE) secretion. **J Biol Chem. 2010 Nov 26;285(48):37405-14**

Stirnberg M, Maurer E, Horstmeyer A, Kolp S, Frank S, Bald T, Arenz K, Janzer A, Prager K, Wunderlich P, Walter J, Gütschow M (2010): Proteolytic processing of the serine protease matriptase-2: identification of the cleavage sites required for its autocatalytic release from the cell surface. **Biochem J. 2010 Aug 15;430(1):87-95**

Apelt J, Bigl M, Wunderlich P, Schliebs R (2004): Aging-related increase in oxidative stress correlates with developmental pattern of beta-secretase activity and beta-amyloid plaque formation in transgenic Tg2576 mice with Alzheimer-like pathology. **Int J Dev Neurosci. 2004 Nov;22(7):475-84**